UNIVERSITY OF OKLAHOMA

GRADUATE COLLEGE

RESPONSES OF SOIL MICROBIAL COMMUNITIES TO CLIMATE WARMING

A DISSERTATION

SUBMITTED TO THE GRADUATE FACULTY

in partial fulfillment of the requirements for the

Degree of

DOCTOR OF PHILOSOPHY

By

MENGTING YUAN
Norman, Oklahoma
2017

RESPONSES OF SOIL MICROBIAL COMMUNITIES TO CLIMATE WARMING

A DISSERTATION APPROVED FOR THE
DEPARTMENT OF MICROBIOLOGY AND PLANT BIOLOGY

BY

_____
Dr. Boris Wawrik, Chair

_____
Dr. Michael Kaspari

_____
Dr. Heather McCarthy

_____
Dr. Yiqi Luo

_____
Dr. Jizhong Zhou

Dedication

To Jason

My companion, friend, and supporter,

with whom besides me, cheerfulness doubled and melancholy halved

To Andrew

A source of unlimited happiness and energy,

without whom my work time could have doubled but efficiency could have halved

Acknowledgement

This journey of pursuing a doctoral degree in a country far away from home is truly a challenging, yet rich and wonderful experience, in terms of both the exploration of science and the experience of life. Along the way, for countless times, I received kind help and inspiring support, without which it would not be possible for me to approach the finish line of this journey. I am grateful to all who brought me here, for being part of my life in the past six years, during the process of this work.

First of all, I would like to express my great thanks to my advisor, Dr. Jizhong Zhou, for granting me the chance to start this unique journey of life at the first place and financially support me throughout my Ph.D. research. I thank you for your patience on advising me through the numerous scientific questions I have encountered, for your detailed and repeated comments and corrections when teaching me how to write, for your reassuring encouragements when things did not work so well for me, and for your continuous pushes for progress, which I once felt annoyed, but then realized how they had helped me successfully completed seminars, gained chances of presentations, and published papers. Your intriguing advice will last throughout my career.

Also, I would like to convey my deep appreciation to my advisory committee members, who have always been supportive, and leading me towards the pursuit of better science and a better life. I would like to thank my advisory committee chair, Dr. Boris Wawrik, on providing wise suggestions and help on almost everything I asked, from SIP experimental design, lab operation protocol, to the preparation of all kinds of paperwork, organization of committee meetings, enrollment, and even on family-work balance issue I once had. Discussions with you were never long, but genuinely

encouraging. I thank Dr. Yiqi Luo, for teaching me to think in a systematic way, just as a well-structured ecosystem model does, which helped me to notice the links among seemingly unrelated data. Thank you for willing to spend the time to give me instructions even if you were very busy. Both your course and your discussions in project meetings were good learning experiences to me. I also thank Dr. Heather McCarthy, for your expertise in plant biology, a field I was not familiar but still managed to explore in my general exam proposal, with the many constructive comments that brought me confidence. Your optimism influenced me a lot. Last but not least, I would like to thank Dr. Michael Kaspari, for introducing me to the concepts in ecology for the first time, for guiding me on how to discover good scientific questions and formulate meaningful hypotheses, and for the rigorous scientific reasoning you taught me, through commenting both my work and other articles. Thank you for giving me these important training that a scientist should have.

Then, I would like to sincerely thank many of my colleagues at the Institute of Environmental Genomics, who taught me experiments and data analysis, discussed and solved problems with me, collaborated and fought side by side with me. Without you, this work, or tasks in every single project I worked on, could not be finished. I especially thank Dr. Kai Xue for patiently teaching me how to work on basically everything from the beginning.

I also must thank my collaborators from other institutes, including Dr. James Tiedje (MSU), Dr. James Cole (MSU), Dr. Ted Schuur (NAU), Dr. Kostas Konstantinidis (GATech), and Dr. Ryan Penton (ASU), for insightful communications on the project I

worked on, and for their time and efforts in providing samples, analytical tools and feedbacks on my manuscripts.

Finally, I give my deepest gratitude to my dear parents, Xin Yuan and Gang Shi, who are physically far away from me during the years that this work was being done, but whose trust and support always encouraged me to move forward. Whenever needed, they have a hand for me. The completion of this work is never possible without them.

Table of contents

List of Tables

List of Figures

Abstract

Strong scientific evidence supports that anthropogenic activities since industrialization have caused instability in earth's climate, featured by increasing global surface temperature, increasing greenhouse gas concentration in the atmosphere. Climate change has then caused a series of changes in the earth's ecosystems, which can have significant impacts on the biosphere and our human being. Although huge efforts have been put into the research in climate science since the past century, due to the complexity of the climate system and its broad and long-lasting influence, there are still countless question marks and uncertainties in our understanding of climate change and its influence on earth and human society. Microorganisms are among the tiniest groups of life, but play important roles in the cycling of carbon and other nutrient elements in the biosphere. However, their response and feedback to climate warming in different ecosystems is still difficult to predict, limited by the lack of mechanistic understanding of the complex microbial community, their functions, their interactions among themselves and under warming perturbation. With the fast advance of high-throughput metagenomic technologies and the development of environmental microbiology, deep and detailed characterization of microbial diversity and functions became available, which provided great chances in promoting our insights into the mechanisms by which microbial communities mediate the carbon balance in a warmer world. This dissertation applied several metagenomic technologies to probe the soil microbial community responses to warming and permafrost thaw based on field observations and experiments in two ecosystems, a permafrost underlain Alaska tundra, and a temperate tall grass prairie in Oklahoma. Microbial decomposition of soil carbon in high latitude tundra

underlain with permafrost is one of the most important, but poorly understood, potential positive feedbacks of greenhouse gas emissions from terrestrial ecosystems into the atmosphere in a warmer world. On the other hand, temperate grassland provided a contrast to the cold weather and huge soil carbon storage in the tundra, allowing the comparison of different ecosystems in terms of their sensitivity and vulnerability to warming.

In the beginning of this work, we sought answers to the question that how microbial functional diversity was affected by regional warming induced long-term permafrost thaw. Soil columns were collected from a tundra site where three locations with different lengths of permafrost degradation history were on record. A functional gene array (i.e. GeoChip 4.2) was used to analyze the functional capacities of soil microbial communities in these samples. Compared with the minimally thawed site, the number of detected functional gene probes across the 15-65 cm depth profile at the moderately and extensively thawed sites decreased by 25 % and 5 %, while the community functional gene β-diversity increased by 34% and 45%, respectively, revealing decreased functional gene richness but increased community heterogeneity along the thaw progression. Particularly, the moderately thawed site contained microbial communities with the highest abundances of many genes involved in prokaryotic C degradation, ammonification, and nitrification processes, but lower abundances of fungal C decomposition and anaerobic-related genes. Significant correlations were observed between functional gene abundance and vascular plant primary productivity, suggesting that plant growth and species composition could be co-evolving traits together with microbial community composition. This study reveals the complex responses of

microbial functional potentials to thaw related soil and plant changes, and provides information on potential microbially mediated biogeochemical cycles in tundra ecosystems.

Next, a field warming experiment was set up to increase the winter soil temperature in tundra by snow cover coupled with spring snow removal. Using integrated metagenomic technologies, we showed that the microbial functional community structure in the active layer of tundra soil was significantly altered after only 1.5 years of warming, a rapid response demonstrating the high sensitivity of this ecosystem to warming. The abundance of microbial functional genes involved in both aerobic and anaerobic C decomposition was also markedly increased by this short-term warming. Consistent with this, ecosystem respiration (R_{eco}) increased up to 38%. In addition, warming enhanced genes involved in nutrient cycling, which likely contributed to an observed increase (30%) in gross primary productivity (GPP). However, the GPP increase did not offset the extra R_{eco}, resulting in significantly more net C loss in warmed plots compared to control plots. Altogether, our results demonstrate the vulnerability of active layer soil C in this permafrost-based tundra ecosystem to climate warming and the importance of microbial communities in mediating such vulnerability.

Then, we conducted quantitative comparisons of the responses of soil microbial communities to warming at tundra and the prairie ecosystems. Climate warming has been differentially increasing the global surface temperature, with the greatest temperature elevation observed in the northern high-latitude regions. Although tundra and underlain permafrost in those areas were predicted vulnerable to climate warming, few quantitative comparisons were reported between tundra and other grassland

ecosystems, especially of the composition and structure of soil microbial communities and their functional diversity. We compared the early responses of soil microbial composition and functional gene abundance to experimental warming between a tundra site and a temperate tall grass prairie using several metagenomic technologies, including functional gene microarray, amplicon sequencing, and metagenomic shotgun sequencing. Despite distinct species and functional gene pools in soils from the two ecosystems, genes involved in carbon and nitrogen cycling showed positive responses to warming at both sites, but with 36% more significantly responding genes and a greater magnitude of response for 10 genes at the tundra site. The functional gene compositions were correlated with temperature, moisture, ecosystem respiration and gross primary production at the tundra sites, but mostly with substrate related variables, plant biomass and nitrate concentration, at the prairie, implying different limiting factors in microbial growth and functions. These results revealed the higher sensitivity of tundra soil microbial communities to warming, compared with those from temperature prairie, and provided field evidence in supporting that northern high-latitude regions might be more vulnerable to climate warming.

At last, we extended our exploration of the warming influence on the microbial community to the interaction of microorganism in the community by constructing co-occurrence networks for a time series sample set from the temperate prairie. Although intensive reports have shown that warming can influence the soil microbial community composition and structure, little is clear about how the microbial interactions among themselves would be influenced. Here, soil microbial co-occurrence networks were constructed using 16S rRNA gene amplicon sequences extracted from monthly samples

collected in a long-term field warming experiment on a Central Oklahoma grassland. We observed substantially larger and more connected networks for warmed communities compared with control, despite huge variation in network structures along season. The increase in network complexity under warming was concurrent to decreased phylogenetic diversity, reflecting environmental filtering and increased functional association in altered soil and vegetation conditions. A portion of identified keystone taxa, which play important roles in network topology, reoccur in different networks, representing a preserved prominent group in grassland soils across the season and under warming. The structure of microbial networks introduced a dimension beyond species abundance, which revealed more complicated responses of microbial communities to climate warming.

Overall, this work provided valuable field evidence on microbial community's response to climate warming, revealed different sensitivities of these responses in tundra and prairie, and captured the seasonal dynamics of soil microbial interactions under warming influence. Many of these findings represent novel insights into our understanding of the microbial-mediated carbon cycle in a warmer world, from which new hypothesis could be formulated, tested, and generate knowledge essential for including the microbial contributions to earth system models, eventually a better prediction of the future climate.

Keywords: climate warming, soil microbial community, metagenomics, tundra, permafrost, temperate grassland, diversity, ecosystem function, microbial interaction, microarray, GeoChip, high-throughput sequencing

Chapter 1: Introduction

1.1 Global warming and its impact on the Earth system

The increasing earth surface mean temperature of 0.2 °C per decade in the past 30 years (Hansen et al 2010), and the reoccurrence of historically warmest years on record since the beginning of this century (NOAA National Centers for Environmental Information 2017) directly evidenced accelerating recent global warming. Other observations, including rising sea level, thawing permafrost, retreating glacier, melting arctic ice, and increasing oceanic heat content, are together consolidating the fact that the climate of the Earth system is undergoing potentially unprecedented changes (Stocker 2014). Despite the huge natural variability in the Earth climate system (Wigley and Raper 1990), these recent changes are considered unusual based on estimates of historical climate changes, and cannot be explained by natural factors alone, such as external forcing of the solar radiation (IPCC 2007). Current explanation agreed that recent global warming is a result of a small positive energy imbalance in the radiative budget of the Earth system, and the anthropogenic emission of greenhouse gases (e.g. carbon dioxide, CO_2) has been the dominant cause of the imbalance (IPCC 2007). The main plausible explanation is that greenhouse gases are capable of absorbing and emitting infrared radiation, and the Earth's atmosphere has been trapping more heat due to the substantial increase in the atmospheric concentrations of the greenhouse gases stemmed from human activities since the Industrial Revolution, as early as the 1830s (Abram et al 2016). This notion was also backed by the unequivocal evidence from ice core studies, which showed that the atmospheric concentrations of CO_2 and methane (CH_4)

were much lower during the past 420,000 years than current (Blasing and Smith 2006, Petit et al 1999).

The recent global warming can have tremendous impacts on natural systems and human society on the planet (IPCC 2007, Stocker 2014). These impacts included changes in precipitation, melting ice and retreating glacier, alteration in hydrological system, permafrost thawing, and changes in the frequency or strength of extremes events, such as droughts, floods, hurricanes, and wildfires. Meanwhile, impacts on biosphere are also broad and vast, including shifts in ecosystems, changes in activities and interactions of biological species, biodiversity loss, species extinction, reductions in crop yields, and alteration in pathogen distribution and disease spreading. Based on a wide range of studies assessing these impacts, as summarized in a few reviews (McMichael 2003, Patz et al 2005, Pecl et al 2017), direct and indirect negative impacts on human society were overwhelmingly predicted. If not curbed successfully, climate change may further lead to more severe stresses in drinking water quality, food security, public health and socioeconomic inequality.

1.2 Responses of terrestrial carbon cycling to climate warming

Due to deep and especially negative impacts of global warming on natural systems and human society, huge international efforts have been seeking to predict the trend of climate warming in the past few decades (IPCC 2007, Stocker 2014). Since the cause of the warming is closely related to atmospheric concentrations of greenhouse gases, especially CO_2, understanding the response of the Earth system carbon cycling to continuing climate warming is vital for making predictions, because the increasing

temperature will affect major aspects of the carbon processes (e.g. photosynthesis and respiration) that contribute to determining the atmospheric concentrations of CO_2. Terrestrial, oceanic and atmospheric carbon reservoirs are in dynamic equilibriums (Stocker 2014). The terrestrial carbon reservoir, the second largest carbon reservoir of the Earth, exchanges carbon mostly with the atmosphere, and mainly through photosynthesis and respiration in natural systems. In a warmer world, both the carbon uptake by photosynthesis and the carbon loss through respiration are likely to be enhanced, but unlikely equally, thus force the balance of the carbon equilibrium to a new state. Generally, two scenarios could happen. If respiration increase more than photosynthesis and a net carbon loss from the land occurs, more greenhouse gases will intensify the warming condition and there will be a positive feedback of terrestrial ecosystem to warming. On the other hand, if more carbon can be fixed from the atmosphere through photosynthetic activity than respiration releases, a negative feedback will happen (Luo 2007, Zhou et al 2012). Contradictory experimental results, as well as model predictions, were reported, debating on whether the terrestrial-atmospheric carbon exchange was positive or negative feedback to warming (Luo 2007). For example, climate warming could trigger abrupt changes in ecosystems in the northern high-latitude regions of the northern hemisphere, where the temperature has increased at rates twice the global average (Comiso et al 2008, Hansen et al 2006, Kortsch et al 2012), and enhance the positive feedbacks to warming (Dufresne et al 2002, Friedlingstein et al 2001, Kirschbaum 2004, Scheffer et al 2006, Walter et al 2006). Many ecosystems in these regions are predicted as tipping elements in the Earth's climate system (Duarte et al 2012, Lenton et al 2008). However, other

ecosystems, such as temperate grasslands and forests, were much less reported to respond similarly in terms of the feedback type and the magnitude of responses to warming (Lenton et al 2008). And whether the acclimation of soil respiration, reported in some studies (Chen et al 2003, Luo et al 2001, Tucker et al 2013), in the long run could mitigate the carbon loss from those ecosystems remains unclear. Currently, the debates on the responses of global carbon cycling are still ongoing, therefore leave one central question in climate warming studies open: will the continuing warming cause more carbon to be trapped by the terrestrial carbon reservoir or more carbon from the reservoir to be released the atmosphere (Luo 2007)?

Answer this central question requires quantifying the size of carbon pools and modeling the processes that transfer the carbon among pools. While the mechanism of photosynthesis and respiration related to plant physiology and their control factors are well understood (Bardgett et al 2008), and the plant community composition and succession are relatively easy to survey, belowground processes mediated by microbial communities are difficult to characterize and disentangle. Therefore, current ecosystem models simplify the microbial decomposition to a temperature and moisture regulated first-order equation or its variants but do not include microbial physiology. The efforts of modeling microbial enzymatic processes were often oversimplified for field application. The first-order decomposition model can accurately predict heterotrophic respiration in laboratory microcosms in many cases, but is limited in capturing the acclimation of microbial respirations, including the changes in the temperature sensitivity (Q_{10}, the rate of change of respiration for every 10 °C temperature increase) and substrate depletion in field settings without intensive data parameterization for each

study site. In fact, the changes in Q_{10} under environmental perturbations reflected the overall effect of very detailed and complicated responses of each species in the microbial community. Without unraveling the black box of microbial community composition, structure, functional potential and responses to environmental changes, it is difficult to explain the wide range, and sometimes contradictory observations on Q_{10} even if accounted for methodological issues and biome differences (Boone et al 1998, Chen and Tian 2005, Davidson et al 2006, Janssens and Pilegaard 2003, Zhou et al 2009), the coarse estimate of microbial adaptation. Hence, it is important to integrate microbial responses to model the carbon cycle and future climate conditions, in which detailed and mechanistic understanding of the soil microbial community upon warming should be the first step.

1.3 Microbial communities influenced by climate warming

In the entire biosphere, microbial communities carry out integral and unique roles in mediating many biogeochemical and ecological processes. The decomposition of organic materials and the cycling of nutrient elements represent fundamental processes that microorganisms play and influence the global carbon cycle in different ecosystems (Bardgett et al 2008). Understanding how soil microbial communities perform under diverse types of disturbance related to climate change is a critical component of climate change biology. With the development of high-throughput metagenomic technologies, our understanding of microbial diversity in the environment has been greatly improved. Rich literatures have reported and discussed the compositional, structural and functional change of soil microbial communities in response to warming (Bradford 2013, Deng et al 2015, Hartley et al 2007, Jassey et al 2013, Nie et al 2013, Pailler et al 2014,

Peltoniemi et al 2015, Rousk et al 2013, Semenova et al 2015, Streit et al 2014, Tucker et al 2013, Wang et al 2014, Yoshitake et al 2015, Zhang et al 2013, Zhang et al 2005, Ziegler et al 2013). The responses depend on ecosystem and climate regime under study, and the interaction of warming with a wide range of other factors (Castro et al 2010, Cavaleri et al 2015, Docherty et al 2012, Walter et al 2013), such as precipitation (Liu et al 2016, Zhang et al 2013), moisture (A'Bear et al 2014, Rousk et al 2013), nutrition level (Hines et al 2014, Melle et al 2015), and the intensity of disturbances like clipping or grazing (Crowther et al 2015, Steven et al 2015, Walter et al 2013, Zhang et al 2005). These studies provided valuable insights into our understanding of soil microbial communities under warming.

However, the massive reports still left knowledge gaps in this complex, and large-scale question. First, although northern high-latitude regions were referred to climate change's hot spot (Schuur et al 2008), the field characterization of microbial communities in those remote areas, and their changes upon warming, are still very limited. Second, very few reports compared the warming influence across different ecosystems and evaluated the relative importance of different ecosystems in contributing to the future carbon cycle. Third, compared with the abundant information on the taxonomic composition of the studied soil microbial communities, much less can be inferred about their function, or functional potentials, which are critical for climate change studies. Fourth, as the importance of microbial interactions in performing ecosystem functions were emphasized in more and more studies (Fuhrman 2009), the influence of warming on these interactions has never been characterized. Thus, the ongoing and future researches are still urgent and necessary in this cross section of

climate change biology and microbial ecology, as our understanding of the microbial system are yet basic compared with that of macro-ecological systems.

1.4 High latitude regions under climate warming

Northern permafrost regions are often considered “hot spot” in the changing climate (Lenton et al 2008, Schuur et al 2008). Their responses to the climate warming are extremely important and have been received extra attention. One reason is that these regions stored an enormous size of carbon, which accounts for nearly 50% of the global soil organic carbon, although they cover only 16% of the global terrestrial area (Schuur et al 2008). A second reason is that the high latitude regions were warmed the most intensely, with an increase in surface temperature twice of global average (Hansen et al 2010), causing the already vulnerable ecosystems becoming more fragile. Climate warming has caused substantial regional permafrost thaw (Jorgenson et al 2010, Lawrence and Slater 2005, Osterkamp 2007, Romanovsky et al 2010), which could promote the frozen soil become biologically active. With microbial decomposition resulting in massive ecosystem carbon loss, the permafrost under the warming will potentially be a vast carbon source to the rise of atmospheric concentrations of greenhouse gases, and aggravate the climate warming (Abbott et al 2016, Schuur et al 2013, Schuur et al 2015).

As soil microorganisms are pivotal mediators of the carbon cycle, monitoring their responses to thaw is crucial for predicting carbon sequestration in permafrost regions. There are a few laboratory incubations (Coolen and Orsi 2015, Mackelprang et al 2011), and field studies (Lipson et al 2015, Taş et al 2014) reported the permafrost region microbial response to thaw, fire, and redox potential changes caused by

hydrology reformation. However, field warming experiments are limited and long-term observations on the microbial responses to permafrost thaw are unclear.

1.5 Scope and objectives of this work

This dissertation aimed at addressing how soil microbial communities respond to climate warming, and what environmental factors influence their assemblage and functions in a warmer world. Samples from field observations and field experiments were collected and combined with the most state-of-the-art high throughput metagenomic technologies to characterize the composition and structure of microbial communities in terms of their taxonomy, functional potential, and interactions. Two ecosystems were studied, the northern high-latitude tundra, one of the most vulnerable ecosystems upon climate warming, and the temperate tall grass prairie, a less understood but important component of the North America landscape. The following summarized the research focus of each chapter.

Chapter 2 focused on evaluating the microbial responses to regional warming induced permafrost thaw and related ecosystem changes at a naturally degrading permafrost site. Field observations were carried out at a moist acidic tundra site, the Eight Mile Lake (EML), where permafrost degradation was recorded for several years to several decades. Soil fractions from the active layer and top permafrost layers sampled across the thawing gradient were analyzed using GeoChip 4.2, a comprehensive functional gene microarray. With a focus on detecting and analyzing the functional gene abundances in these soils, the following questions were addressed: 1) How do natural permafrost thaw and varying thaw histories impact microbial community functional gene composition and abundance? 2) what are the environmental factors influencing

these compositional and abundance-based changes? The study in this chapter targeted to provide detailed microbial functional gene responses due to the influence of long-term and naturally occurring permafrost thaw, leading towards a mechanistic understanding of the future carbon balance of tussock tundra.

Based on knowledge gained from observations of the natural system, field experiments were designed and carried out, as presented in Chapters 3 to 5, to manipulate temperature increase to mimic climate warming conditions. Chapter 3 aimed at revealing the vulnerability of the active layer tundra soil, and the high sensitivity of microbial communities, to experimental warming. The Carbon in Permafrost Experimental Heating Research (CiPEHR) experiment, a nearby tundra site to EML, used snow piles as an insulator to warm soils in winter. It was the first field warming experiment to degrade surface permafrost without delaying spring snow melt. Since soil physical-chemical properties and plant communities were both influenced by warming treatment after only 1.5 years, we predicted that short-term warming would result in selective microbial growth, which would be detected as a shift in the active layer microbial community structure and accompanying gene content, especially in those populations and traits important to both aerobic and anaerobic carbon decomposition and nutrient cycling. To test our hypothesis, soils were collected after two winters of treatment for geochemical and microbial analyses. Several high-throughput metagenomic technologies were used, including microarray, amplicon sequencing and shotgun sequencing of the metagenome. The study presented in this chapter represented one of the earliest comprehensive field studies to demonstrate the early responses of the permafrost microbial communities to climate warming.

The emphasis of Chapter 4 laid in the comparison of the tundra and the prairie ecosystems in terms of their soil microbial responses to experimental warming. Since climate warming has increased the temperature more at high-latitudes, and the carbon storage in permafrost was estimated as twice as the current atmospheric amount, tundra and underlain permafrost were predicted more vulnerable to climate warming. However, few quantitative comparisons were reported between tundra and other grassland ecosystems, especially of the composition and structure of soil microbial communities and their functional diversity. Thus, we analyzed soils samples from a temperate prairie field warming experiment, where a similar degree of temperature increase and time frame of treatment operation were implemented as the tundra experiment presented in Chapter 3. We hypothesized that the microbial community in tundra soils is more sensitive to warming, and imposes greater responses than the prairie communities. To test this hypothesis, species recovered from functional gene array, amplicon sequencing, and shotgun sequencing were analyzed and compared between the two ecosystems in terms of their direction and magnitude of response under warming treatment. This study provided field evidence in supporting that the tundra ecosystem in northern high-latitude region harbored more responsive soil microbial communities than temperate prairie did to short-term climate warming. It also implied the importance of considering the ecosystem type when discussing climate impact on the soil and the carbon cycle.

Chapter 5 extended our current knowledge on the warming influence on soil microbial community beyond the perspective of composition and structure. This chapter tackled the question of how the interactions among microbial species would be influenced by

warming. Microorganisms interact intensively with each other to survive in the environment and perform functions that we observe, including those critical in carbon and nutrient cycling. Despite rich literature reporting the influence of warming on microbial community composition, structure, and functions, whether and how warming would change the interactions among microorganisms remain unclear. In this chapter, soil microbial co-occurrence networks were constructed using 16S rRNA gene amplicon sequences extracted from monthly samples collected in a long-term field warming experiment on a Central Oklahoma grassland to infer the quantity, form, and structures of microbial interactions from network topological structures. Seasonal dynamics of these networks were also captured to compare warming effect on microbial interactions in different time of a year. The networks were analyzed and compared to address the following questions: 1) Are soil microbial networks differ along season alternation? 2) Does warming have an impact on the network structure? 3) Are there potential keystone taxa that are particularly important in network topology? If yes, do they change along the season or by warming? 4) How do the environmental conditions relate to the network structure? The results captured the change of microbial network complexity across the season, and discovered that warming facilitated the interconnection of microbial communities in grassland soils.

The summary chapter highlighted the major results and conclusions from each study presented, illustrated their significance in filling our current knowledge gaps, indicated their implications for future research and contributions to our society. Overall, the exploration in this dissertation provided field evidence on microbial community's response to climate warming, from which many hypotheses could be formulated for

testing towards a mechanistic understanding of these responses, and from which better projections of future climate conditions could be made by implementing the discoveries in this work.

Chapter 2: Microbial functional diversity covaries with permafrost thaw-induced environmental heterogeneity in tundra soil

2.1 Abstract

Permafrost soil in high latitude tundra is one of the largest terrestrial carbon stocks and is highly sensitive to climate warming. Understanding microbial responses to warming induced environmental changes are critical to evaluating their influences on soil biogeochemical cycles. In this study, a functional gene array (i.e. GeoChip 4.2) was used to analyze the functional capacities of soil microbial communities collected from a naturally degrading permafrost region in Central Alaska. Varied thaw history was reported to be the main driver of soil and plant differences across a gradient of minimally, moderately and extensively thawed sites. Compared with the minimally thawed site, the number of detected functional gene probes across the 15-65 cm depth profile at the moderately and extensively thawed sites decreased by 25 % and 5 %, while the community functional gene β-diversity increased by 34% and 45%, respectively, revealing decreased functional gene richness but increased community heterogeneity along the thaw progression. Particularly, the moderately thawed site contained microbial communities with the highest abundances of many genes involved in prokaryotic carbon degradation, ammonification, and nitrification processes, but lower abundances of fungal carbon decomposition and anaerobic-related genes. Significant correlations were observed between functional gene abundance and vascular plant primary productivity, suggesting that plant growth and species composition could be co-evolving traits together with microbial community composition. Altogether, this study reveals the complex responses of microbial functional potentials to thaw related

soil and plant changes and provides information on potential microbially mediated biogeochemical cycles in tundra ecosystems.

1.1 Introduction

Northern permafrost regions have accumulated approximately 1,700 Pg carbon, representing about 50 % of global belowground carbon (Ciais et al 2013, Tarnocai et al 2009). Most of this carbon has been preserved frozen for thousands of years (Schuur et al 2008). Nonetheless, climate warming has caused substantial regional permafrost thaw (Jorgenson et al 2001, Lawrence and Slater 2005, Osterkamp 2007, Romanovsky et al 2010), thickened the seasonally melted active layer and created more unfrozen taliks in recent decades (Chapin et al 2005, Euskirchen et al 2006, Natali et al 2011). Thus, this permafrost carbon pool can potentially be converted into a significant carbon source to the atmosphere by the end of this century through the release of large amounts of greenhouse gases, primarily CO_2 and CH_4, that serve as a positive feedback to climate warming (Abbott et al 2016, Schuur et al 2013, Schuur et al 2015).

As soil microorganisms are pivotal mediators of the carbon cycle in terrestrial ecosystems, monitoring microbial responses to thaw is crucial for predicting carbon sequestration in permafrost regions. They play a fundamental role in soil organic carbon decomposition and impact plant carbon fixation through nutrient exchange with aboveground ecosystems (Van Der Heijden et al 2008). Recently, a few studies have provided evidence of tundra microbial functional potential shifts in response to warming or fire (Taş et al 2014, Xue et al 2016a), which may alter carbon allocation and cycling. Lipson et al (2015) showed that soil redox conditions were the dominant force in shaping microbial communities in a polygonised tundra landscape, and that higher redox potentials allowed for greater microbial diversity. Two independent studies by Mackelprang et al (2011) and (Coolen and Orsi 2015) both incubated

permafrost soil and discovered rapid shifts in microbial functional genes and transcriptomes within two weeks upon thaw. Thus, temperature and redox conditions both play a role in tundra soil dynamics, and may be critical in shaping microbial community composition, function and ultimately, tundra carbon cycling upon permafrost thaw. Yet observations matching the time scale of long-term and naturally occurring permafrost thaw is still lacking, coupled with a limited understanding of detailed influences of such environmental perturbation on microbial functional genes (Mackelprang et al 2016).

In the past two decades, a series of studies have characterized an acidic tundra study site near Eight Mile Lake (EML) in Healy, Alaska. Three locations in this site were identified as minimal (Mi), moderate (Mo) and extensive (Ex) thaw based on both historical records and environmental observations (Osterkamp and Romanovsky 1999, Osterkamp 2007, Schuur et al 2009). The Mi site represents the early stage of permafrost degradation in tussock tundra. The Mo site has documented thawing and ground subsidence since 1985. Thawing at the Ex site, where substantial ground subsidence and periodical thermokarst formation was observed, is estimated to have started in the 1950s (Schuur et al 2009). The differences of thaw extent among the three sites are caused by spatially randomized positive feedbacks between temperature alteration, ground subsidence, hydrological movements, and further thawing. Thus, the divergence in plant communities and soil properties observed presently are mainly due to permafrost thaw (Schuur et al 2009). This site provided a unique opportunity to study the effects of decadal-long permafrost thaw on the ecosystem. Plant community succession in response to thaw exhibited larger plant biomass and aboveground net

primary productivity (ANPP), as well as the replacement of dominant graminoid species with increased abundances of deciduous and evergreen shrubs (Schuur et al 2007). Despite the greater carbon fixation by plants, radiocarbon analysis suggested that this area was transformed to a carbon source from a historical carbon sink, due to recent warming-induced increases in respiration (Hicks Pries et al 2012, Hicks Pries et al 2013a, Schuur et al 2009). Although the carbon storage was similar among sites, the Ex thaw site showed a 2-3 fold increase of old carbon loss, and old carbon comprised 8% more of the ecosystem respiration, compared with that of the Mi thaw site (Schuur et al 2009).

Recently, amplicon sequencing of the 16S rRNA genes and *nifH* genes revealed that the microbial phylogeny as well as the *nifH* harboring communities in the EML site soils were distinct along soil depth profiles, and responded to thaw differently in varied layers corresponding to thaw depth and water table (Deng et al 2015, Penton et al 2016). Here, we specifically focused on detecting and analyzing functional gene abundances in these soils using a functional gene array, GeoChip 4.2, to address the following questions: 1) How do natural permafrost thaw and varying thaw histories impact microbial community functional gene composition and abundance? 2) what are the environmental factors influencing these compositional and abundance-based changes? This study provides detailed microbial functional gene responses due to the influence of long-term and naturally occurring permafrost thaw, which serve as a reference for a mechanistic understanding of the future carbon balance of tussock tundra.

2.2 Materials and methods

2.2.1 Site and sample description

The thaw gradient sites are located on a moist acidic tundra in the discontinuous permafrost region (63^{o} 52’42”N, 149^{o} 15’12”W, 660-700 m elevation) (Lee et al 2010, Schuur et al 2009, Trucco et al 2012, Vogel et al 2009). Distances between Ex and Mo, Mo and Mi, and Ex and Mi sites were about 150 m, 380 m, and 530 m, respectively. The thaw depth, or the thickness of unfrozen surface soil, was measured every 1 to 10 days from May to September 2004, (corresponding to the year when microbial samples were taken), and at the time of soil sampling. A metal rod was inserted into the ground until the frozen layer was reached, and the length of insertion was recorded as thaw depth. The active layer depth, referring to the length from the deepest thawed soil in the summer time to the ground surface, was the largest thaw depth recorded during the growing season (Schuur et al 2009). Soil temperature was recorded every 2 hours at depths of 10 cm, 20 cm, 30 cm and 40 cm by a copper/constantan thermocouple (Schuur et al 2009). The ground surface microtopography for each site was estimated as the standard deviation of local scale elevation measurements, with the effect of overall hillslope statistically removed. The microtopography is a measure of ground surface unevenness caused by thermokarst depressions, a topological sign of permafrost thaw that reforms the tundra landscape (Osterkamp et al 2009).

Replicate sampling cores in each site were located within 50 m of one another. Soil sampling for physiochemical and microbial analyses was described previously (Hicks Pries et al 2012). Briefly, 6 soil cores were collected at each of the 3 thawing sites at the beginning of the growing season (May 2004). Half of the 18 cores reached permafrost,

which ranged in depth from 50-130 cm below surface. All cores avoided tussocks. Layers of each soil column were separated by depth using the following 7 categories; 0-15 cm, 15-25 cm, 25-35 cm, 35-45 cm, 45- 55 cm, 55-65 cm, and below 65 cm. In some cases, cores did not extend into the full profile. Altogether, 107 samples were obtained, 32 from Mi, 26 from Mo, and 39 from Ex sites. Among them, 93 samples were from active layers and 14 from permafrost layers. The number of samples acquired for each depth was shown in Table S1. At the time of sampling (spring), 23 fractions were already seasonally thawed while 84 remained frozen. Samples were transferred frozen from the field to the laboratory where they were stored at -20 °C until further processing. Soil moisture was calculated as the percentage weight loss after drying the samples at 60 °C. The bulk density was determined by the ratio of soil dry weight and bulk volume determined at the time of sampling (Hicks Pries et al 2012). Dried samples were used to analyze soil nitrogen, carbon content, and $\delta^{15}N$ and $\delta^{13}C$ ratios on a Costech (ECS4010) Elemental Analyzer coupled with an isotope ratio mass spectrometer (Hicks Pries et al 2012).

2.2.2 DNA extraction

Genomic DNA was extracted and purified from 5 g of soil for each sample using a PowerMax Soil DNA Isolation Kit (MO BIO Laboratories, Inc., Carlsbad, CA, USA). The concentration of DNA was quantified using Quant-iT PicoGreen dsDNA Assay Kit (Thermo Fisher Scientific, Waltham, MA, USA) on an FLUOstar OPTIMA fluorescence plate reader (BMG LabTech, Jena, Germany). DNA quality was checked on a NanoDrop ND-1000 Spectrophotometer (NanoDrop Technologies Inc., now NanoDrop Products by Thermo Fisher Scientific). The spectrometry absorbance ratios

at 260/280 nm were between 1.7 and 2.2, and the 260/230 nm ratios were greater than 1.8.

2.2.3 Labeling and GeoChip hybridization

GeoChip version 4.2 is a NimbleGen format comprehensive gene array containing 107,950 different 50-mer probes and covering 790 microbial functional genes that encode enzymes for biochemical reactions, including carbon, nitrogen, phosphorus, sulfur cycling and seven other major categories (Tu et al 2014). From each sample, 1 μg DNA was fluorescently labeled for hybridization. The labeling, hybridization, and scanning were processed following the protocols previously described (Xue et al 2016a).

2.2.4 GeoChip data pre-processing

Data normalization was completed on a web-based pipeline (http://ieg.ou.edu/microarray/) as follows. First, the raw probe signals, calculated based on the average pixel intensity of each probe, were adjusted based on control dye intensity and sample set total intensity. Second, signals were filtered by removing the spots with a signal to noise ratio less than 2, and the spots with signal intensity less than 2 times background. Third, probes that generated positive signals in less than 10 % of the samples from a given thaw site (all replicates from within each field site and along the depth profile) were considered low abundance genes and removed from that site for downstream analyses. We identified low abundance genes on a site basis instead of globally to retain functional gene probes unique to one site. Fourth, the probe signals were then normalized to represent relative abundance of genes in each sample. Unless otherwise specified, all gene abundance data reported in this manuscript represent

relative abundance estimations based on the normalized signal intensities of probes targeting said gene. A subset of 70 samples, 23 from Mi, 24 from Mo, and 23 from Ex sites, from depth ranges of 15-65 cm that exhibited a greater variation between sites in regard to functional genes detected with GeoChip were the most responsive to thaw. Detailed analyses on these layers were performed separately where indicated. The raw and normalized data can be accessed through the series accession number GSE97107 in the Gene Expression Omnibus (GEO) database.

2.2.5 Statistical analysis

Normalized GeoChip signals, as well as soil and plant data, were used in the following analyses. (i) Microbial functional gene α-diversity was estimated using positive probe numbers and Shannon-Weiner, Simpson and Piedou's evenness (J) were calculated (Hill 1973). The β-diversities of functional genes among sites were compared using the multivariate homogeneity of group dispersion (Anderson et al 2006), based on the Sørensen index. The relationship between β-diversity and site surface microtopography was determined using Pearson's product moment correlation. (ii) Welsh permutational t-tests were used to compare the diversity indices between each pair of two sites. P values were adjusted based on false discovery rate for the three comparisons. (iii) One-way ANOVAs followed by Fisher's LSD tests were used to test the difference of means among sites for the soil physical-chemical variables, DNA yields, and gene abundances. P values of F tests on gene abundance were corrected among all the detected genes based on false discovery rates, and P values from the LSD test for each individual gene were adjusted using Holm's method. (iv) Repeated measures ANOVAs were carried out to compare soil temperatures among sites. (v) Non-parametric multivariate statistical

analyses, including Multi-response Permutation Procedures (MRPP) (Van Sickle 1997), Analysis of Similarity (ANOSIM) (Clarke 1993), and Permutational Multivariate Analysis of Variance Using Distance Matrices (Adonis) (Anderson 2001), were used to determine the dissimilarity of microbial functional gene profiles among sites and/or depth profiles. Pairwise distances among samples were calculated based on Bray-Curtis indices. When applicable, observations are permuted within the strata of hybridization slide (11-12 samples per slide) to eliminate potential slide effects; (vi) Mantel tests and canonical correspondence analyses (CCA) (Legendre and Legendre 2012) were performed to test correlations between microbial functional composition and soil and plant variables. One set of plant properties was used for each site when performing correlation analysis, which sufficed given the low within site plant variability compared to variability among sites. Samples containing missing soil data were removed from Mantel tests or CCA model construction. The soil and plant variable set in the CCA model was determined by forward selection. All statistical analyses were performed with R program version 3.0.1 (Team 2014) using the packages vegan (Oksanen et al 2013) and agricolae (De Mendiburu 2014).

2.3 Results

2.3.1 Impacts of thaw on microbial functional gene composition and structure

The highest DNA yield originated from 25-35 cm while the lowest was isolated from the top 15 cm and below 65 cm. No significant differences in DNA yield among sites were observed (**Figure S 1**). Microbial functional gene composition was distinct among sites, specifically in the active layer ($P = 0.001$), but only marginally significant ($p < 0.1$) with depth (**Table S 1**). Comparing the communities among sites within depth fractions

resulted in detectable differences only in the middle layers (15-65 cm) rather than surface and deep soils (**Table S 1**). Notably, this middle fraction of soil represents depths that were frozen at the time of sampling, but which are still portions of the active layer (**Figure S 2**).

Table 2.1 Non-parametric multivariate dissimilarity tests of functional gene profiles among the three sites, and between any two sites. Distinct functional gene profiles were detected in the three sites. MRPP, multi-response permutation procedures; Adonis, permutational multivariate analysis of variance using distance matrices; ANOSIM, analysis of similarity. Results presented are based on distance matrices calculated with Bray-Curtis index. Horn, Euclidean, and binomial distances were also used, and generated similar outcomes (all tests significant), thus results not shown. P values <0.05 are in bold.

	MRPP		Adonis		ANOSIM	
	δ	p	F	p	R	p
Among three sites	0.250	**0.001**	11.136	**0.001**	0.234	**0.001**
Mi vs Mo	0.234	**0.001**	24.750	**0.001**	0.452	**0.001**
Mi vs Ex	0.244	**0.005**	5.837	**0.006**	0.109	**0.006**
Mo vs Ex	0.273	**0.002**	5.195	**0.003**	0.117	**0.008**

Functional gene composition from the 70 subsurface samples significantly ($p<0.05$) differed among sites (**Table 2.1**), indicating a substantial impact of thaw on these communities. More unique probes in the Mi site (7.07%, 3298 probes) were detected than in the Ex site (1.50%, 697 probes) and the Mo site (0.11%, 52 probes, **Figure 2.1**a), rendering the functional gene α-diversity the highest in the Mi site, followed by the Ex site, and lowest at Mo ($p<0.05$, **Table S 2**). Evenness exhibited an opposite trend, highest in Mo and lowest in Mi ($p<0.05$, **Table S 2**). The site-unique functional gene probes were analyzed by the functional categories they belonged to, and compared with the portion of probes designed on GeoChip (**Figure 2.1**b). The functional category composition for these site-unique probes was similar in Mi and Ex sites, but different from the Mo site. A smaller portion (4%) of the Mo site unique probes belonged to the

carbon cycling category, compared with Mi (12%) and Ex (12%) sites. Larger portions of Mo site unique probes belonged to nitrogen (17%) and sulfur (8%) categories, compared with the other two sites (both 9% for nitrogen, and 5% and 3% for sulfur in Mi and Ex sites).

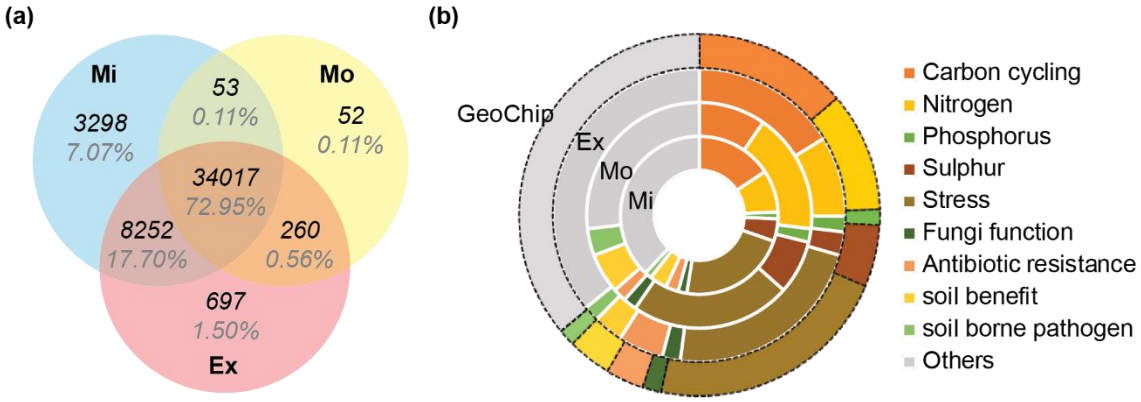

Figure 2.1 (a) Unique and shared probe number detected in the three thawing sites and (b) the categories those unique probes belonged to. Category "others" includes genes gyrB, and those of energy processes, bacteria phages, bioleaching, metal resistance, organic remediation and virulence categories.

Despite the similar physical distances among replicate cores within site and similar sampling depth profiles, the functional gene β-diversity increased at both the Mo and Ex sites, in contrast with the Mi site (**Figure 2.2**a, $p<0.05$), as indicated by the larger average distance from samples to each of their group centroids. The sparseness of microbial functional community composition was strongly correlated ($R^2=0.98$, $P=0.14$, n=3 sites, **Figure 2.2**b) with the surface microtopography of the tundra. Together, both the α- and β-diversity of the soil microbial functional genes were affected by thaw extent.

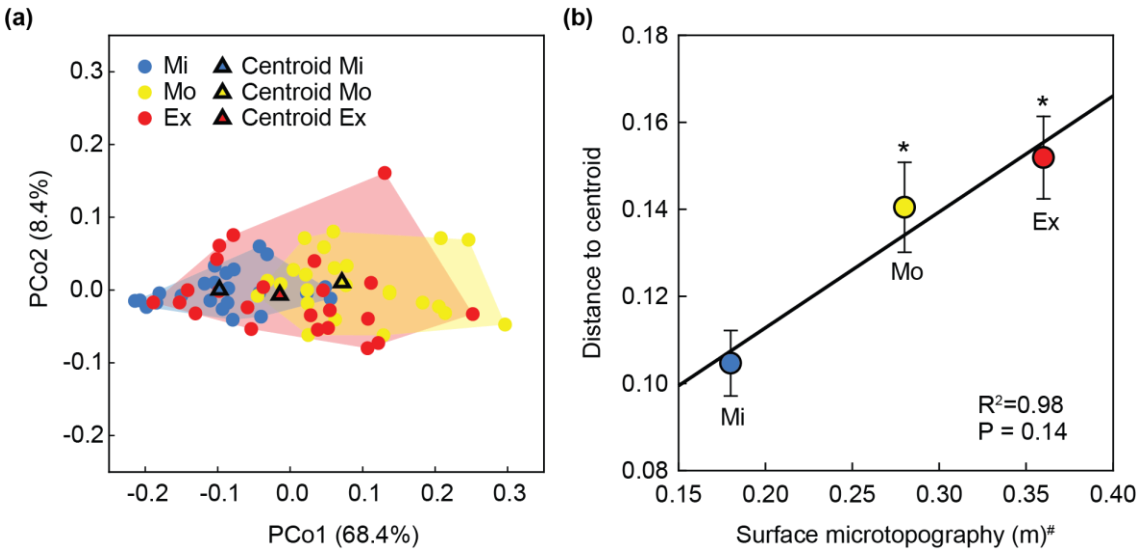

Figure 2.2 (a) The functional gene β-diversity at each site, and (b) its relationship with surface microtopography. (a) Pairwise distances among samples were calculated using Sørensen index, and processed through multivariate homogeneity of group dispersions procedure to compare the β-diversities among sites. The level of dispersion of samples (represented by circular dots) within each site were measured by the distance of each sample to the site centroid (outlined triangles) in the principle coordinates (PCo) plot. Percentiles in parentheses were the portion of community variation explained by each of the two axes. (b) The means and standard errors of the distances to centroid at each site in (a), in correlation with ground surface microtopography. Surface microtopography was a measure of the unevenness of ground surface. Significant ($p<0.05$, asterisks showed) larger distances to centroid were observed for Mo and Ex sites compared with Mi site by Tukey's test. Linear regression line is shown for n=3 sites. #Surface microtopography data are adopted from Schuur 2009.

2.3.2 Effects of permafrost thaw on the abundances of important functional genes

A total of 34,017 functional gene probes were detected, 49.1 % of which showed significantly ($p<0.05$) different abundances among sites (**Table S 3**). These probes belonged to 692 functional genes. Below are the detailed results for selected categories of functional genes that are important in biogeochemical cycles and ecosystem functioning, including those in carbon cycling, nitrogen, phosphorous, sulfur and plant beneficial categories.

<u>C cycling genes</u>

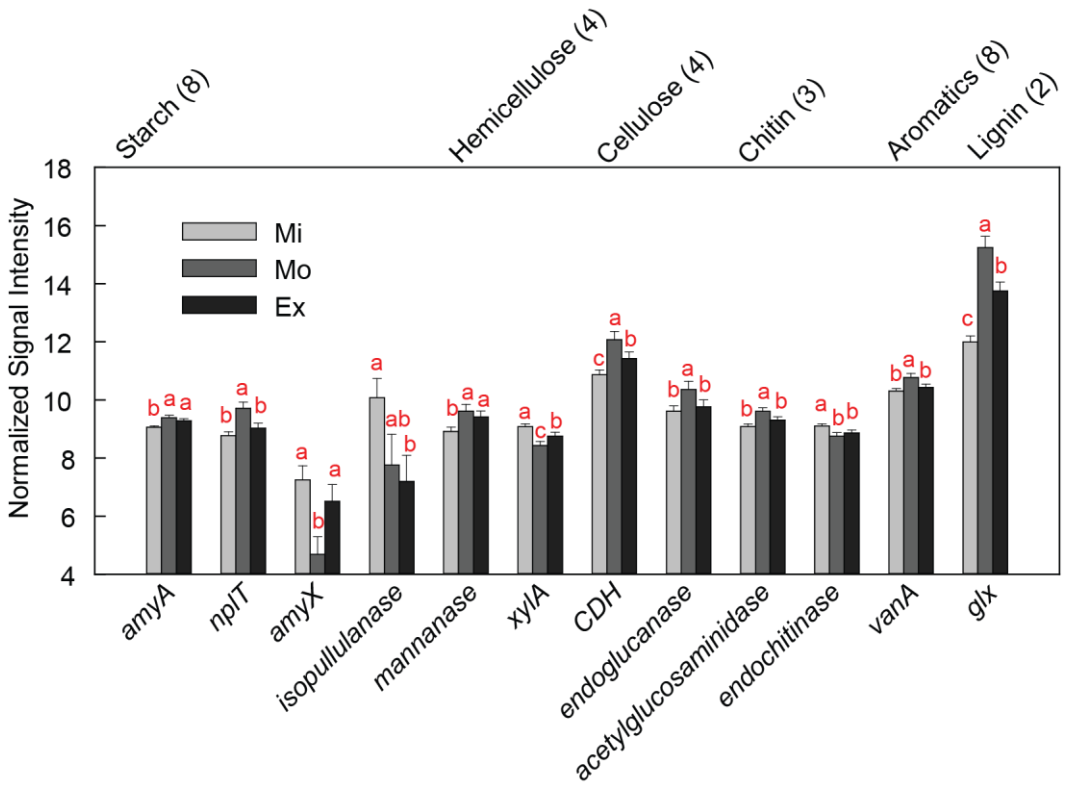

Figure 2.3 Normalized relative abundance of detected carbon degradation genes derived from bacteria and archaea. Only significantly different abundance among sites were illustrated using bars. The order of genes is organized based on the lability of their targeted carbon substrate. The numbers in the parenthesis following the gene subcategory (substrate type) indicates the number of total detected genes in that subcategory. In the subcategory of pectin, only one gene is detected (pectinase) and is not significantly different among sites, so it is not shown in the figure. Significant differences of the means are marked by different letters, based on ANOVA model followed by Fisher's LSD test. Full annotation information of the genes is presented in Table S5.

A total of 3,305 bacterial and archaeal probes, representing 30 genes associated with metabolizing various carbon compounds, were detected. Twelve of these genes were significantly ($p<0.05$) different in abundance between at least two of the three sites (**Figure 2.3**). Eight of these genes (out of 12, 67 %) had the highest abundance at the Mo site. For fungal communities, 2,052 probes belonging to 51 genes were detected, and 28 of these genes differed ($p<0.05$) in abundance at least between two sites (**Figure**

S 3). A majority of these genes (23, 82 %) exhibited the lowest abundance at the Mo site.

Four carbon fixation genes, targeted by 1,019 probes, were detected across all samples (**Figure S 4**). Specifically, *aclB* gene, an indicator for reductive tricarboxylic acid cycle, and the Calvin cycle rubisco gene were at the lowest abundance in the Mo thaw site. The abundance of the *pcc* gene, involved in the 3-hydroxypropionate/4-hydroxybutyrate cycle, was highest in the Mo thaw site.

Three CH_4 cycling genes were detected (**Figure S 4**) with 218, 134 and 196 probes showing positive hybridization signals in the Mi, Mo and Ex sites, respectively. The abundances of all three genes, including the CH_4 oxidation genes *mmoX* and *pmoA,* and methanogenesis gene *mcrA*, had the lowest abundance in Mo site ($p<0.001$). The *mcrA* gene exhibited a lower abundance at the Ex site compared with the Mi site, though the two CH_4 oxidation genes did not.

N cycling genes

Eighteen of the 23 detected nitrogen cycling genes significantly ($p<0.05$) differed in abundances among the three sites (**Figure S 5**). Under Ex thaw conditions, the nitrogen cycling functional potentials were more similar to the Mi site. While the detected ammonification gene *gdh* abundances decreased with thaw progression, the *ureC* gene, responsible for conversion of urea to ammonia, was detected in the highest abundance at the Mo site. Yet, probes targeting *nifH* genes, involved in nitrogen fixation, another ammonium-producing pathway, showed the lowest abundances at the Mo thaw site. The *napA* gene, involved in nitrate reduction to nitrite, was also lowest in abundance at Mo site. For the ammonia oxidizing gene *amoA*, 112 detected probes belonged to archaea,

and 417 belonged to bacteria. There were greater abundances of bacterial and source-organism-unspecified *amoA* genes, but lower abundances of archaeal *amoA* genes in the Mo and the Ex site compared with the Mi site. The abundances of all 8 detected denitrification genes were impacted by thaw. Except for *narG* (involved in the first step of denitrification, the reduction of nitrate to nitrite) and a fungal gene p450nor, encoding a cytochrome p450 nitric oxide reductase, the six other denitrification genes, including *nirK* for both denitrifying and nitrifying pathways, *norB*, *nirS*, *nosZ*, and *nirZ*, all exhibited the lowest abundances at the Mo site. Assimilatory nitrogen reduction genes *nirA*, nitrate reductase and *nir* showed the highest abundance in the Mo site. Overall, microbial functional potentials for organic nitrogen ammonification, ammonia oxidation, and assimilatory processes were higher, while nitrogen fixation, denitrification and nitrogen mineralization potentials were lower at the Mi site.

Other functional categories

GeoChip detected abundance differences of genes among the three sites in many other functional categories, and the numbers and portions of those probes are summarized in **Table S 3**. All of the S assimilation (ATP sulfurylase, PAPS reductase, and sulfate transporter) and sulfite reduction (*dsrA*/*B*) genes showed the lowest abundance in the Mo site (**Figure S 6**). A phosphorus utilization gene, *ppx*, was decreased in both the Mo and Ex thaw sites, compared to the Mi site (**Figure S 6**). For plant beneficial genes, 12 of the 32 (37.5 %) detected had the highest abundances at the Mo site, including genes encoding the enzymes for antibiotic (*pcbC*, *imbA*, *phzF* and *prnB*), antioxidant (*cat*) and hormone (*sped* and *spe*) biosynthesis, pathogen resistance (*sid*), and plant hormone signaling (*acdS*) (**Figure S 7**).

2.3.3 Linkages between microbial functional potentials and soil and plant properties

Table 2.2 Values (mean ± standard error) of soil physical-chemical variables and plant biomass. n = 23, 20, and 16 samples for Mi, Mo and Ex sites for nitrogen and carbon contents, $\delta^{15}N$, $\delta^{13}C$ and bulk density, and n = 17, 23, 22 for Mi, Mo, and Ex sites for soil moisture, respectively. For plant biomass, n=12 observations per location. For soil temperature, n=6 observations for each site. Differences of means among sites were tested using ANOVA followed by LSD test (repeated measures ANOVA was used for daily averaged temperatures data). Different letters denote significant difference of the means. P values <0.05 are in bold.

Variable	Unit	Mi	Mo	Ex	F	p
Gravimetric water content	%	62.1±4.5	66.1±3.5	69.4±3.4	0.91	0.408
‡Growing season temperature	°C	3.1±0.3 ^{b}	3.0±0.1 ^{c}	3.4±0.4 ^{a}	979.00	**<0.001**
‡Winter temperature	°C	-0.1±0.1 ^{b}	-0.1±0.1 ^{c}	0.0±0.1 ^{a}	1148.00	**<0.001**
†N content	%	1.1±0.1	1.3±0.1	1.2±0.1	1.02	0.368
†C content	%	26.7±2.7	30.6±2.7	28.9±2.6	0.58	0.561
†$\delta^{15}N$	‰	0.9±0.1	0.7±0.1	0.9±0.1	1.26	0.292
†$\delta^{13}C$	‰	-26.2±0.2	-26.4±0.2	-26.3±0.1	0.52	0.597
†Bulk Density	g/cm^3	0.4±0.1	0.4±0.1	0.3±0.1	0.26	0.776
*ANPP from vascular plant	g/m^2	187.2±4.1 ^{b}	271.9±9.2 ^{a}	203.6±5.1 ^{ab}	3.96	**0.029**
*Vascular plant biomass	g/m^2	248.9±3.6 ^{b}	370.5±10.9 ^{a}	330.9±5.0 ^{ab}	6.13	**0.005**
*ANPP from non-vascular plant	g/m^2	23.9±1.7 ^{b}	53.2±4.1 ^{ab}	154.9±13.6 ^{a}	5.77	**0.007**
*Non-vascular plant biomass	g/m^2	112.1±4.0 ^{b}	117.3±3.1 ^{ab}	154.8±2.9 ^{a}	3.89	**0.030**

†Reanalyzed from data presented in Hicks Pries 2012.
*Reanalyzed from Schuur 2007.
‡Reanalyzed from Schuur 2009.

A summary of reported plant and soil characteristics are shown in **Table 2.2**. Soil temperatures in different depths are presented in **Figure S 8**. Canonical correspondence analysis (CCA) was performed to establish the linkages of microbial functional gene compositions to plant and soil properties. Variables suggested by forward selection to include in the model consisted of sampling depth, soil moisture, soil carbon and nitrogen content, $\delta^{15}N$, bulk density, vascular plant ANPP and graminoid ANPP. Mo and Ex site communities were separated from those in the Mi site (P = 0.005, **Figure 2.4**a). The Mi site community functional gene potentials exhibited a negative correlation with vascular plant ANPP, the most influential factor in the model, and a

positive correlation with $\delta^{15}N$. The Mo site functional gene composition was related most to high soil bulk density and graminoid ANPP, and that of the Ex site was positively correlated with soil moisture, as well as carbon and nitrogen content. The model explained 30% of the total variation in microbial functional gene composition.

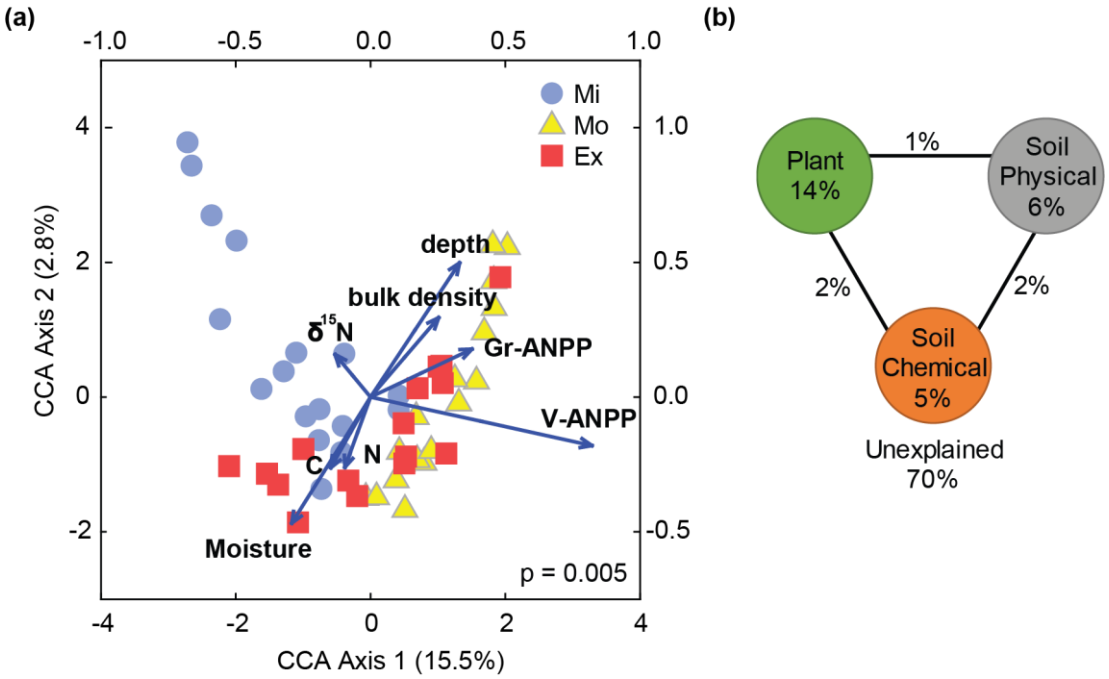

Figure 2.4 (a) Canonical correspondence analysis (CCA) and (b) variation partitioning analysis (VPA) on microbial functional gene profiles and forward selection determined plant and soil variables. 57 sample points (after removing samples having missing soil variable measurements) from the three thawing sites and eight plant and soil geochemical variables were included. Numbers on CCA axis and in VPA diagram show the percentages of explained variations in the microbial functional gene profile. Lower and left axes show scales for microbial functional gene profiles, and the upper and right axes show scales for plant and soil variables. V-ANPP, vascular plant aboveground net primary productivity; Gr-ANPP, graminoid ANPP. In VPA, plant variables include Gr-ANPP and V-ANPP, soil physical properties include moisture, and bulk density, and sampling depth; soil chemical variables include soil nitrogen, carbon, and $\delta^{15}N$ contents.

Variation-partitioning analysis (VPA) was performed to identify individual and interactive contributions of different categories of CCA variables to the variances of microbial community structure (**Figure 2.4**b). The three categories of variables, plant

(vascular plant ANPP and graminoid ANPP), soil physical property (depth, moisture, and bulk density) and soil chemistry (nitrogen and carbon contents, $\delta^{15}N$), explained 14%, 6% and 5% of the total variance, respectively. Interactions between the three groups contributed 5% of the total variance. The majority of the community variations (70 %) could not be explained by the plant and soil variables measured.

Mantel tests were used to examine the relationships between microbial functional gene composition and plant and soil variables (**Table S 4**). Microbial functional gene composition was only significantly ($p<0.05$) correlated with vascular plant and graminoid biomass and ANPP. Non-vascular plant variables and soil geochemical variables were not correlated to microbial functional gene profiles. Controlling for the variations caused by depth did not reveal any significant correlations between soil variables and microbial functional gene composition.

2.4 Discussion

As one of the most vulnerable terrestrial carbon pools, decomposition of organic carbon in thawing permafrost may serve as a positive feedback to global climate change (Schuur and Abbott 2011), but also difficult to predict owing to the complexity of belowground microbial activities. This study observed the tundra microbial functional potentials in sites exposed to varied intensity of permafrost thaw. We found shifts in microbial functional gene profiles from minimally to extensively thawed sites at 15-65 cm, with lower α-diversity and higher β-diversity at the two more severally thawed sites compared with minimal thaw. This is more or less consistent with previous studies at the same site (Deng et al 2015, Penton et al 2016), as well as with other studies which showed thaw related perturbations affected the tundra microbial communities in lab

microcosms (Mackelprang et al 2011, Taş et al 2014), field experiments (Xue et al 2016a), and field observations (Lipson et al 2015). Microbial diversity is expected to increase as permafrost thaws because more substrates become available (Jansson and Taş 2014), yet field evidence is lacking, possibly due to insufficient survey efforts (e.g., sequencing depth) to detect such difference. Conspicuously, difference in microbial functional gene profile was not observed in the surface (0-15 cm) and permafrost (>65 cm) layers. Passive dispersal of microorganism through air or animal carrier (Martiny et al 2006) might easily homogenize the species pool in top soils within the area of our study site. While in continuously frozen permafrost, harsh condition caused limited growth and activity (Rivkina et al 2004) might be the reason of slow microbial succession upon disturbance. The increase of the functional gene β-diversity with thaw is an intriguing finding highlighted by this study. The level of divergence of functional gene potentials from communities within a similar physical distance was strongly correlated with the surface microtopography, a measure of the unevenness of ground surface created by thermokarst depressions (Schuur et al 2009). This indicated that thaw-induced topographical reformation and thus increased versatility of soil environment may be the primary reason for the increase in the heterogeneity in microbial functional gene compositions.

As thaw progressed, a large portion of detected functional genes that are involved in carbon, nitrogen, and other biogeochemical cycling changed in abundances, most of which were not merely increase or decrease from the least to the most thawed sites, but rather showed extreme values at the moderate thaw. On the other hand, vascular plant biomass and ANPP both peaked at moderate thaw, before shrubs took over graminoids

under warmer and extensively thawed conditions (Schuur et al 2007). Tundra soil is carbon rich, but with a large portion being slow carbon (Schuur et al 2008), whose decomposition was primarily stimulated by inputs of fresh and labile carbon, mainly from succeeding plants (Grogan et al 2001). Both the composition and abundance of plant species can affect the belowground microbial assemblages (Bais et al 2006). At moderate thaw, the most abundant carbon degrading genes harbored by bacteria and archaea versus the least abundance of those genes carried by fungi might reflect variations in the amount of litter- and root exudate-derived carbon substrates among sites. Grass-dominance and larger plant biomass at moderate thaw might provide more high-quality litter as well as root exudates for bacteria. In contrast, shrub dominance at the extensively thawed site possibly led to low quality, standing litter (Gavazov 2010, Hobbie 1996), thus supporting a higher fungal abundance, known to be more efficient at attacking recalcitrant substrates than bacteria (Hieber and Gessner 2002, Romaní et al 2006). In fact, the close relation between vascular plant community and the entire detected microbial functional gene profile was reflected in the high percentage variation in microbial community that was explained by plant variables in contract to soil variables. On the contrary, non-vascular plant (e.g., moss and lichen) biomass and productivity were not correlated with microbial functional gene profiles, possibly because their short root systems could not reach deeper soil layers where the microbial samples were collected. These results echoed many studies (De Long et al 2016, DeMarco et al 2014, Jonasson et al 1999, Lipson and Monson 1998, Suding et al 2008) showing that permafrost thaw affects soil microbial communities through above- and belowground biotic interactions.

We observed greater abundances of genes for ammonification and ammonia oxidation in the two sites with greater thaw, especially in the moderately thawed site. As a few studies reported significant correlations between nitrogen cycling process rates and corresponding gene/enzyme abundance (Liu et al 2015, Morales et al 2010, Trivedi et al 2016, Wang et al 2015, Xue et al 2016b), the higher abundances of *ureC* and *amoA* genes might indicate faster nitrogen turnover in thawed soils. This supports the finding that thaw tended to increase plant nitrogen availability, as indicated by higher total canopy nitrogen in the moderate and extensively thawed sites (Schuur et al 2007), which could be associated with faster carbon decomposition and an increased nitrogen limitation after more permafrost is thawed for a longer period of time (Jonasson et al 1999). The relatively low denitrification gene abundance under moderate thaw signaled less mineral nitrogen loss through direct reduction, which was supported by the soil stable isotopic nitrogen content. When there was no difference in $\delta^{15}N$ input to soil from the plant (Schuur et al 2007), the lower $\delta^{15}N$ in the moderately and extensively thawed sites compared with the minimally thawed site potentially indicated lower fractions of ecosystem nitrogen loss through ^{15}N-depleted forms (NO_3^-, N_2O, etc.) (Amundson et al 2003). Considering the high abundance of nitrogen assimilation genes *nirA* and nitrate reductase at the moderate and extensive thaw, the mineralized nitrogen was likely utilized by both plants and microbes. Yet, further studies are needed to directly measure functional processes to confirm these discussions.

We consistently detected the lowest abundances of genes involved in anaerobic processes under moderate thaw, including those involved in methanogenesis (*mcrA*), nitrogen fixation (*nifH*), denitrification (*nirK*, *norB*, *nirS*, and *nosZ*), dissimilatory

nitrogen reduction (*napA*), and sulfite reduction (*dsrA*/*B*). This indicated that functional potentials for anaerobic reactions were more suppressed here, compared with minimally and extensively thawed sites. As contradictory it may seem with reported observations that thaw-induced saturated soil mosaics promote anoxic microbial processes (Coolen and Orsi 2015, Lipson et al 2015, Mackelprang et al 2011, Waldrop et al 2010), the EML study site is located at a well-drained mild slope with short period of visible water bogs only at the Ex sites in early summer. Only when the full soil depth profile is considered, waterlogging impacts deep soils for different lengths of time at the three sites. Thus, such topologic and hydrologic conditions did not result in a detectable increase in soil water content among our sites from our single time-point sampling. Conversely, ground subsidence could facilitate oxygen diffusion into areas below water table and plant roots also transport oxygen to the rhizosphere and the surrounding bulk soil (Husson 2013, Ponnamperuma 1972). At moderate thaw, these processes may have more thoroughly supported aerobic decomposition. Although the extensively thawed site had a greater maximum depression depth and higher plant biomass than the minimal site, soils here may remain saturated for a longer period of time than the other two sites. As thaw continues at EML, we may observe more severe water saturation and, subsequently, decreased oxidative potentials.

Notably, the explained variation in microbial functional potentials by the available plant and soil variables was low, probably because these measured environmental variables represent the conditions at the time of sampling rather than those spanning the sites' histories, which deterministically shape the microbial communities. Low temperatures in permafrost regions tend to preserve a large diversity of historical seed banks (Steven

et al 2006, Willerslev et al 2004) or dormant microbes (Lennon and Jones 2011), that can be captured by DNA-based metagenomic techniques. In addition, stochastic processes (Stegen et al 2012, Zhou et al 2013, Zhou et al 2014) may contribute to the diversity and succession of microbial communities, leading to the existence of rare and opportunistic species, which were captured by the closed-format, highly sensitive microarray (Zhou et al 2015).

In summary, by analyzing the abundances of up to 40,000 functional genes probes in soils collected at EML across a gradient of naturally thawing permafrost, we found substantial differences in the profile of microbial functional potentials at the three stages of thaw. Genes involved in carbon and nitrogen cycling, as well as anaerobic processes, appeared to be most different at the moderately thawed site, potentially resulting from microbial interactions with plant communities, and ground subsidence upon thaw. Although the functional gene abundances were similar at minimally and extensively thawed sites, the later possessed a more divergent functional profile, which was likely related to a more heterogeneous microclimate after thaw intensified. Whether this divergent profile in Ex site will continue, or further developed thaw will serve to converge the communities to a new steady state, remains to be tested. Related studies on multiple functional process rates are still needed to reveal the mechanisms behind the complex responses of the microbial functional genes to long-term permafrost thaw.

Chapter 3: Rapid microbial feedbacks reveal vulnerability of tundra soil carbon to climate warming

3.1 Abstract

Microbial decomposition of soil carbon in high latitude tundra underlain with permafrost is one of the most important, but poorly understood, potential positive feedbacks of greenhouse gas emissions from terrestrial ecosystems into the atmosphere in a warmer world (Graham et al 2012, Schuur et al 2008, Schuur et al 2013, Zhou et al 2012). Using integrated metagenomic technologies, we showed that the microbial functional community structure in the active layer of tundra soil was significantly altered after only 1.5 years of warming, a rapid response demonstrating the high sensitivity of this ecosystem to warming. The abundance of microbial functional genes involved in both aerobic and anaerobic carbon decomposition were also markedly increased by this short-term warming. Consistent with this, ecosystem respiration (R_{eco}) increased up to 38%. In addition, warming enhanced genes involved in nutrient cycling, which likely contributed to an observed increase (30%) in gross primary productivity (GPP). However, the GPP increase did not offset the extra R_{eco}, resulting in significantly more net carbon loss in warmed plots compared to control plots. Altogether, our results demonstrate the vulnerability of active layer soil carbon in this permafrost-based tundra ecosystem to climate warming and the importance of microbial communities in mediating such vulnerability.

3.2 Introduction

Permafrost, defined as "subsurface earth materials remaining below 0 °C for two consecutive years" (Schuur et al 2008), is a unique characteristic of Polar Regions and high mountains. In permafrost underlain high latitude tundra, plant-derived carbon has accumulated over hundreds to thousands of years because low temperatures and saturated soils reduce microbial decomposition of soil organic carbon (Hicks Pries et al 2012, Lee et al 2012). As a result, nearly 50% of the global soil organic carbon is stored in northern hemisphere permafrost and the active layer soils above, although they cover only 16% of the global terrestrial area (Tarnocai et al 2009). High latitude tundra has long been recognized as being highly responsive to climate change (Grosse et al 2011). Recent accelerated warming in the northern high-latitude region (ACIA 2004) has resulted in rapid permafrost degradation, and studies suggest that permafrost could decline by 30-70% by the end of the 21st century (Lawrence et al 2012, Schuur and Abbott 2011). During permafrost degradation, frozen soil becomes biologically active, with microbial decomposition resulting in massive ecosystem carbon loss, which will likely dominate the overall net carbon exchange in permafrost regions (Schuur et al 2008). While plant responses to climate warming in the active layer of the tundra soil have been intensively studied (Natali et al 2012, Walker et al 2006), microbial responses have not been examined until very recently (Coolen and Orsi 2015, Graham et al 2012, Hultman et al 2015, Mackelprang et al 2011, Yergeau et al 2012). Although various observational studies have documented the responses of tundra ecosystems to natural warming (Sturm et al 2001), and some incubation studies revealed microbial community changes upon permafrost thaw in laboratory settings

(Coolen and Orsi 2015, Mackelprang et al 2011), very few studies examined microbial responses to climate warming in tundra ecosystems in the field. Since field experimental warming can directly examine the impacts of temperature increases on the microbial community in situ (Walker et al 2006), an ecosystem warming experiment, Carbon in Permafrost Experimental Heating Research (CiPEHR), was established in September, 2008, in Interior Alaska. The experiment is located in typical moist acidic tussock tundra (Walker et al 2005), a dominant tundra type, on permafrost that is close to the freezing point and thus especially vulnerable to thaw in a warming climate (Schuur et al 2009). In this experiment, snow fences (i.e. increased snow pack for insulation) were used in the soil warming treatment to increase soil temperature, coupled with early spring snow removal to control snow-water equivalents in both warmed and control plots. Soil warming and control treatments were arranged in six replicates, providing sufficient statistical power. This is the first warming experiment to degrade surface permafrost without delaying spring snow melt (Natali et al 2011). To understand how vulnerable the active layer of the tundra soil is to climate warming, a total of 12 subsurface soil samples from a representative depth of 15-25 cm were collected from both warmed and control plots after short-term (1.5 years) warming for geochemical and microbial analyses. These samples represented active layer soil that freezes in winter and thaws in the growing season, and were within the organic horizon along the depth profile. Because soil microbial community structure is tightly linked to changes in the aboveground plant community and soil environmental conditions (Zhao et al 2014), we predicted that short-term warming would result in selective microbial growth, which would be seen as a shift in the active layer microbial community

structure and accompanying gene content, especially in those populations and traits important to both aerobic and anaerobic carbon decomposition and nutrient cycling. Consequently, soil carbon in this tundra ecosystem would be highly vulnerable to climate warming.

3.3 Materials and methods

3.3.1 Site Description and Sampling

The Carbon in Permafrost Experimental Heating Research (CiPEHR) site was established in September 2008 at a moist acidic tundra area of Interior Alaska near the Denali National Park in the Eight Mile Lake region (63º52'59''N, 149º13'32''W). The experimental plots were located in the discontinuous permafrost region where permafrost thaw has been observed in the past several decades. Experimental design and site description were described in detail previously (Natali et al 2011). Briefly, three experimental blocks were located approximately 100 m away from each other. In each block, two snow fences were erected in the winter of each year (October to April) about 5 m apart. The soil warming treatment plots were located 5 m back from the leeward side of the snow fences, while the paired control plots were at the windward side of the snow fences. Soil temperature was increased in the warmed plots due to thicker snow cover on the soil surface and lower wind strength. Snow fences were removed in the spring before snow melt to provide uniform hydraulic conditions in both winter warming and control treatments. From 1976 to 2009, mean monthly temperature in the field ranged from -16 °C in December to 15 °C in July, with an annual mean temperature of -1.0 °C. The average annual precipitation was 378 mm. Only C_3 plant species were observed in this area. Dominant species include *Eriophorum vaginatum*,

Vaccinium uliginosum, some other vascular species, nonvascular feather moss and lichen. In the experimental plots, soil from the ground surface to a depth of 45-65 cm, depending on sampling cores, was rich in organic carbon materials; below that depth was mineral soil with a mixture of glacial till and windblown loess. The active layer depth was about 50 cm.

Twelve soil cores, six from treatment and six from control plots, were taken using electric drills in destructive sampling plots at the six snow fences in the beginning of the 2010 growing season (May), one and one-half years after the initiation of the winter warming treatment. Our analysis provides a snapshot of the soil microbial community response to early stage soil warming. The 15-25 cm depth soil fractions were analyzed in this study.

3.3.2 Environmental and soil chemical measurements

Thaw depth was measured weekly during the growing season (May to September 2010) using a metal depth probe (Natali et al 2011). The thaw depth data presented in this study were the average values for the 2010 growing season.

Constantan-copper thermocouples and CR1000 data loggers (Campbell Scientific) were used to measure and record soil temperature and moisture content at 5, 10, 20 and 40 cm every half hour in flux bases installed in each plot (Natali et al 2011). The soil temperatures in **Figure 3.1** were reanalyzed from previously published data (Natali et al 2012), which represents either growing season or wintertime (December 2009 to March 2010) temperatures averaged over 5-40 cm soil depth. To represent the microclimate of the soil where and when the microbial communities were sampled, the soil temperature data used in canonical correspondence analysis (CCA) (**Figure S 10**) was the average

values at 20 cm depth from December 2009 to May 2010. Volumetric water content from the soil surface to 15 cm depth was measured using site-calibrated Campbell CS616 water content reflectometer probes (Natali et al 2011). Soil moisture data presented in this study were averaged over the 2010 growing season.

To prepare soils for microbial and chemical analyses, visible roots and stones were removed by metal forceps. To measure soil carbon and nitrogen, soil samples (5g) were dried at 70 °C until constant weight, ground to powder, encapsulated in silver foil and fumigated with HCl for 24 hours at room temperature to remove soil inorganic carbon (carbonates). Soil carbon and nitrogen concentrations were analyzed in the Colorado Plateau Stable Isotope Laboratory at the Northern Arizona University on a DELTA V Advantage isotope ratio mass spectrometer (Thermo Fisher Scientific), configured through a Finnigan CONFLO III (Thermo Fisher Scientific) and using a Carlo Erba NC2100 Elemental Analyzer (CE Elantech). The total organic carbon (TOC) and soil nitrogen content of each sample was calculated as the percentage mass of carbon or nitrogen (Avramidis et al 2015).

To measure soil carbon pools, soil samples were processed with a two-step hydrolysis procedure to separate the labile and recalcitrant carbon pools(Rovira and Vallejo 2002). First, 5 N H_2SO_4 was used to hydrolyze dried soil at 105 ºC for 30 min, from which the hydrolysate and wash-offs were collected after centrifugation as labile pool 1, containing mainly polysaccharides. Second, the residue was then shaken continuously overnight at room temperature with 26 N H_2SO_4, followed by hydrolysis at 105 ºC for 3 hours with acid diluted to 2 N. The hydrolysate and wash-offs were recovered as labile pool 2, containing mostly cellulose. The recalcitrant carbon pool consisted of the

remaining organic C. The organic carbon in Labile pools 1 and 2 was analyzed using a Shimadzu TOC-V CPH PC-Controlled TOC Analyzer (Shimadzu Corporation) and the organic carbon in the recalcitrant carbon pool was analyzed using a PerkinElmer Optima 2000DV ICP-OES spectroscopy (PerkinElmer) in the Environmental and Agricultural Testing Service laboratory at North Carolina State University.

3.3.3 Aboveground plant communities

Aboveground plant community investigations were conducted as described previously (Natali et al 2011, Natali et al 2012). In brief, above ground biomass and net primary productivity (ANPP) were determined by a nondestructive point-frame method using a 60×60 cm point frame with a grid size of 8×8 cm (Walker 1996). At each of the 49 intersecting grid points, a metal rod (1 mm diameter) was placed vertically through the plant canopy. Species identity and tissue type (leaf, stem or fruit) were recorded for every "hit" with the rod. Above-ground live biomass for each vascular plant species, moss and lichen was estimated by applying allometric equations developed for this site to the average number of pointframe "hits" per plot (Schuur et al 2007). Vascular plant ANPP was estimated as the sum of the current year's apical growth (leaves, stems, flowers and fruits) and secondary growth. The ratio of biomass between each tissue type and total plant was determined from destructive harvesting of a site adjacent to CiPEHR (Shaver et al 2001). Secondary growth was evaluated using growth rates determined from tussock tundra at Toolik Lake, Alaska (Shaver et al 2001). Moss NPP was measured by the cranked wire method, which measures vertical growth of moss using a stainless-steel reference wire inserted at the moss surface (Clymo 1970, Schuur et al 2007). Three to five cranked wires were placed in four moss types in each treatment at

all fences to measure the growth from mid-May to mid-September. Feather moss NPP was estimated as the product of linear growth per stem, stem density, biomass per unit stem growth and percent cover. Allometric equations developed for EML watershed (Schuur et al 2007) as well as percent cover was used to convert the vertical growth of other types of moss into biomass. Moss NPP was the sum of all types of moss NPP. Current year's fully formed green leaves from six vascular plants found across plots were collected at peak biomass (mid-July) for measuring foliar nitrogen and at the end of the growing season (late September) for senescent nitrogen (Natali et al 2011). At least three leaves from two to three individuals in each plot were collected each time. Leaves were dried at 60 °C, finely ground, and analyzed on a continuous flow isotope ratio mass spectrometer (Thermo Fisher Scientific) coupled with a Costech elemental analyzer (Valencia, CA, USA).

3.3.4 Decomposition

Weighed cellulose filter paper (Fisher brand P8 09-802-1B) were placed into fiberglass mesh bags and placed vertically at 0-10 cm in the field soils in September 2009 and collected in September 2010. The bags were rinsed and dried at 60 °C for weighing. The percent mass loss was calculated to represent decomposition rate.

3.3.5 Ecosystem carbon flow

Ecosystem carbon flux measurements were described previously (Natali et al 2011, Natali et al 2014). Growing season net ecosystem exchange (NEE) and ecosystem respiration (R_{eco}) were measured from May to September 2010 using an automated CO_2 flux system coupled to the flux chambers (Natali et al 2011). R_{eco} was determined with night measurements. Gross primary productivity (GPP) was estimated as the difference

between NEE and R_{eco} (values are positive for carbon flowing from atmosphere to terrain and vice versa). Winter respiration was estimated based on a parameterized winter respiration model, adjusted using in-plot winter respiration measurements in March and April 2009 using an infrared gas analyzer in a portable CO_2 flux system. In winter, there was no photosynthetic activity and R_{eco} represents mainly microbial respiration. The carbon flux data used for analysis in this study were reanalyzed from previous published datasets (Natali et al 2014).

3.3.6 Soil DNA extraction

Soil DNA was extracted using a PowerMax Soil DNA Isolation Kit (MO BIO), and the quality was assessed based on spectrometry absorbance at wavelengths of 230 nm, 260 nm and 280 nm (ratios of absorbance at 260/280 nm around 1.8, and 260/230 nm > 1.7) detected by a NanoDrop ND-1000 Spectrophotometer (NanoDrop Technologies). Then it was quantified with Pico Green using a FLUOstar OPTIMA fluorescence plate reader (BMG LabTec) before used for gene array labeling and sequencing library preparation.

3.3.7 GeoChip analysis

GeoChip 4.2 is a comprehensive gene array containing 107,950 probes designed for covering 792 functional gene families from 11 major functional categories including carbon, nitrogen, phosphorus and sulfur cycling (He et al 2007, Tu et al 2014). 1µg DNA from each sample was mixed with random primers and denatured before dNTP, fluorescent dye Cy-3 dUTP and DNA polymerase were added for labeling at 37°C for 6 hours, followed by heating at 95°C for 3 min. Labeled DNA was purified and dried up. For hybridization, DNA was resuspended in hybridization solution containing sample tracking control, formamide, SSC, SDS, Cy3-labeled alignment oligo, Cy5-labeled

alignment oligo and Cy5-labeled common oligonucleotide reference standard target. After denaturing, the mixtures were deposited onto the glass microarray and hybridized at 42 °C for 16 hours. Then the arrays were washed and dried, and scanned by a MS 200 Microarray Scanner (NimbleGen) at 532 nm and 635 nm. NimbleScan software version 2.5 (NimbleGen) was used to grid and process the images to transform them into signal intensity. The raw signals from NimbleScan were submitted to the Microarray Data Manager on our website (http://ieg.ou.edu/microarray/), cleaned, normalized and analyzed using the data analysis pipeline. Briefly, spot signal to noise ratio (SNR) and minimum intensity cutoff was used as standard to remove unreliable spots. Both the universal standard and functional gene spot intensities are used to normalize the signals among arrays. Data were log transformed after cleaning and normalization. A total of 48,188 functional gene probes were detected across all samples in this study.

3.3.8 Illumina MiSeq sequencing of 16S rRNA gene amplicons

DNAs were amplified for the V4 region of 16S rRNA genes using primer set 515F and 806R, and sequenced in one run on a MiSeq using 2 x 150 pair end format (Wu et al 2015). Raw sequences were assembled using RDP's paired-end reads Assembler. Any assembled sequences with any ambiguous bases ("N") were discarded. 5.28% of the remaining reads were identified as chimeras using Uchime (Edgar et al 2011) and removed. The remaining sequences were clustered into OTUs using Uclust (Edgar 2010) at 97% identity, and randomly resampled to the depth of 42,684 reads per sample. Representative sequences chosen by Uclust from each OTU were annotated taxonomically using the RDP Classifier (Wang et al 2007) with the confidence cutoff 0.5. Finally, 512,208 sequences in 23,677 OTUs were obtained.

3.3.9 454 pyrosequencing of nifH gene amplicons

nifH genes from the DNA samples were amplified using the primer pair *nifH* Poly F (5'- TGCGAYCCSAARGCBGACTC -3') and Poly R (5' - ATSGCCATCATYTCRCCGGA -3') and sequenced on the 454 GSFLX Titanium platform at Macrogen, Inc. (Seoul, Korea) (Huse et al 2007, Meyer et al 2008, Ronaghi et al 1998). After trimming primers, the sequences were cleaned using LUCY (Chou and Holmes 2001). Sequences with "N", those containing frameshift(s) detected by FrameBot (Wang et al 2013), and those indendified as chimera by Uchime (Edgar et al 2011) based on the Zehr *nifH* Database (Zehr et al 2003) were all removed from downstream analyses. The remaining 162,523 sequences were clustered into 2,643 non-singleton OTUs using CD-HIT (Li and Godzik 2006) at 0.95 identity, which was an arbitrary but strict enough cut-off to identify different species based on previous studies on *nifH* and other nitrogen cycling related genes (Mao et al 2011, Palmer et al 2009, Pereira e Silva et al 2013). Finally, 2,643 non-singleton OTUs were normalized to relative abundance (scale all the sample sequence numbers to the largest one) for statistical analyses. The representative sequence for each OTU was assigned taxonomic information based on the FrameBot (Wang et al 2013) nearest neighbor match with an identity cut-off of 0.5.

3.3.10 Shotgun metagenome sequencing analysis

Each soil metagenome was prepared using the TruSeq Kit and sequenced at the Los Alamos National Laboratory Genome Facility using the Illumina HiSeq 2000 in one flow cell lane with a 2 × 150 bp paired-end kit (Wu et al 2015). A total of 3.24 billion reads were generated from the 12 samples, with both phylogenetic and functional

information extracted. After data processing, it was found that one of the samples from the control (C1) did not produce enough useful sequence during shotgun sequencing and thus this sample was removed from all subsequent analyses. For phylogenetic analysis, the metagenome reads were trimmed (Luo et al 2011) and searched against representative OTU sequences from GreenGenes (DeSantis et al 2006) using BLAT (Kent 2002). Paired reads that both matched GreenGenes reference sequences were identified as 16S reads and were extracted for further analyses. These 16S reads were subsequently searched against the 99%-clustered GreenGenes OTU sequences. The reads were assigned to the taxon that was the lowest common ancestor of the two reads in a pair. 797,898 reads were assigned to 23,167 OTUs in total. For functional subsystem analysis, 25 million reads were randomly resampled from each sample. Open reading frames (ORFs) were predicted on non-16S encoding reads using FragGeneScan (Rho et al 2010). The translated amino acid sequences were then searched against the M5NR database (Wilke et al 2012) using BLAT. Reads matching genes incorporated in the SEED database (Overbeek et al 2005) were assigned to the corresponding best-matched subsystem(s). The numbers of assigned reads were taken as a proxy of abundance of the SEED subsystem(s). An approach combining re-sampling techniques, the DESeq package (Anders and Huber 2010), and binomial testing with adjusted *p*-values (Benjamini and Hochberg 1995) was then applied to identify significantly differentially abundant subsystems (pathways) under warming vs. control plots, as described previously (Luo et al 2013a).

3.3.11 Annotating shotgun sequences based on GeoChip genes

An ecological functional gene-oriented metagenomic analysis pipeline (EcoFun-MAP), has been developed to fish out sequence reads of important environmental functional genes from shotgun metagenome sequence data. EcoFun-MAP is a method designed for annotating metagenomic sequences by comparing them with functional genes used to fabricate GeoChip. In the preparation of the reference databases, keyword queries were submitted to the NCBI (Geer et al 2010) online GenBank for 308 functional genes to retrieve candidate reference sequences, from which 5 to 200 distinct representative sequences from each gene were manually selected functional gene seed sequences (FGSS's). The selected FGSS's were aligned using both global and local algorithms in ClustalW (Larkin et al 2007), and the resulting alignments were used as input for another program HMMBUILD (Eddy 1998) to build both global and local HMMER[64] models (FGSS-HMM). Next, the candidate reference sequences for each gene were searched back against corresponding FGSS-HMM using HMMSEARCH (Eddy 1998). The output sequences, termed "functional gene reference sequences" (FGRS's), were clustered into OTUs for each gene using CD-HIT at the similarity threshold of 95%. In addition, BLAST databases were constructed on the FGRS's with MAKEBLASTDB (Camacho et al 2009). To this end, two reference databases involved in the method were established: FGSS-HMM and FGRS-BLAST. For annotation, sequences from HighSeq were resampled to the minimal number of reads in a sample, and were quality trimmed by Btrim (Kong 2011). All trimmed nucleotide sequences were translated into protein sequences using FragGeneScan (Rho et al 2010). HMMSEARCH was used for annotating the predicted protein sequences with the FGSS-HMM database, and both

global and local model hits were counted as valid results. Also, all FGSS-HMM confirmed sequences were compared together against the FGRS-BLAST database with BLASTN (Camacho et al 2009). Only best hits (Rank No. 1 in BLAST results) between probes and sequences were kept as final processing results.

3.3.12 Statistical analysis

Statistical analyses were carried out using R software version 2.15.1 using the package vegan (v.2.0-6) (Oksanen et al 2013) when not specified. Detrended correspondence analysis (Oksanen et al 2013) was performed to visualize the overall microbial community composition among samples. Three complementary non-parametric multivariate analyses, non-parametric multivariate analysis of variance (Adonis) (Zapala and Schork 2006), analysis of similarity (ANOSIM) (Clarke 1993), and multi-response permutation procedure (MRPP) (Van Sickle 1997), were used to test the differences in soil microbial communities between warming and control treatments. CCA (Hotelling 1992) was performed to determine the linkage between environmental variables and microbial community composition. For selecting environmental variables, those containing redundant information were reduced to minimum number, keeping only the variables distinct the most among samples. Also, the final sets of variables should have the variance inflation factors (VIF) all < 20. Finally, soil temperature, soil moisture and GPP remained in the CCA model (**Figure S 10**a) based on GeoChip data. Labile carbon pool 1 and 2 (%), and soil nitrogen content (%) were selected for 16S rRNA gene-based analysis (**Figure S 10**b). The significance of the CCA model was tested by analysis of variance (ANOVA). Based on CCA results, variation partitioning analysis (VPA) was performed to determine the contribution of each individual variable

or groups of variables to total variations in soil microbial community compositions. CCA was also used to determine correlations between abundance of subcategories of functional genes and the individual environmental variables (**Table S 9**). Two-tailed t-tests were performed to examine whether the differences between warming and control treatments were significant based on various variables (i.e., soil carbon contents, aboveground biomass, and total bacteria, archaea and fungi abundance) using Microsoft Excel 2010. ANOVA (Chambers et al 1992) was performed to test the treatment effect on the abundance of each functional gene involved in carbon and nitrogen cycling for GeoChip or relative abundances of OTUs of certain genus or phylum groups. In addition to the warming treatment effect, the probe or OTU also factored into the model for partitioning the variance of probes within each functional gene. Response ratio (RR) was used to compute the effects of warming on functional genes relevant to GeoChip probes from shotgun sequences using formula described by Luo et al (2006). Raw shotgun metagenome, 16S rRNA and nifH amplicon gene sequences are available in the European Nucleotide Archive (http://www.ebi.ac.uk/ena) under study no. PRJEB10725. GeoChip raw and normalized signal intensities can be accessed through the Gene Expression Omnibus (GEO) database under Series GSE77866.

3.4 Results and Discussion

3.4.1 Warming influence on plant and soil, and ecosystem carbon fluxes

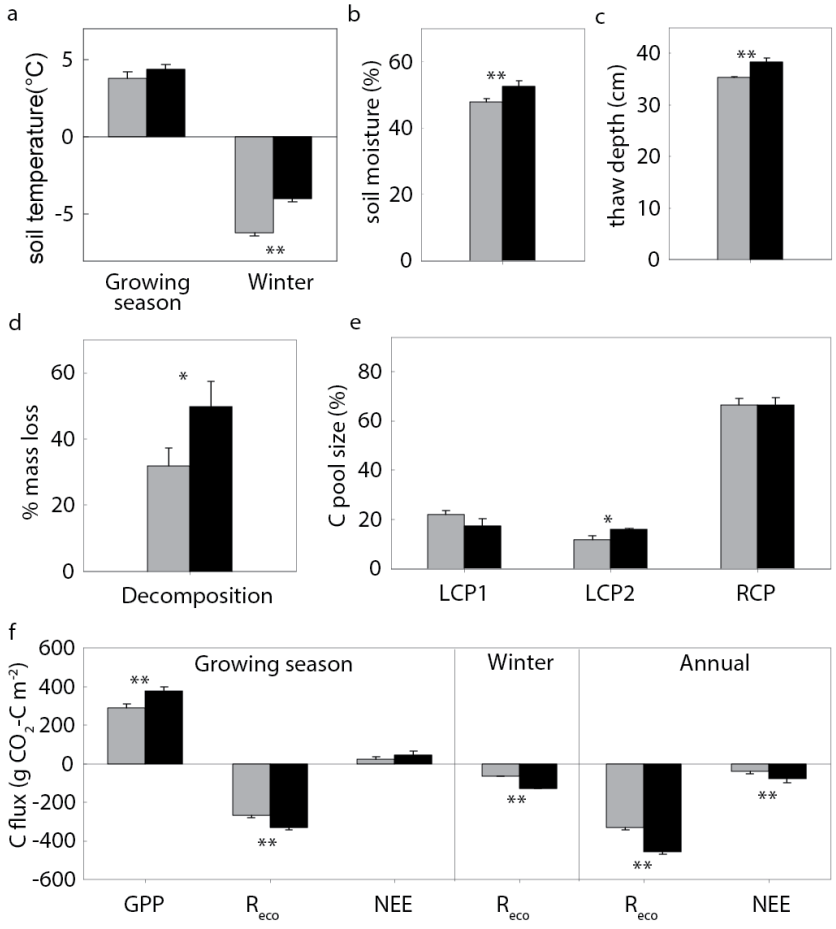

Figure 3.1 Warming effects on soil variables and ecosystem carbon fluxes. Gray bars represent control plots and black bars represent warmed treatment plots. (a) Soil temperature in both growing season (May to September 2010) and wintertime (December 2009 to March 2010) averaged across 5, 10, 20 and 40 cm; (b) soil moisture; (c) Maximum thaw depth; (d) Standard cellulose filter paper decomposition rate (mass loss) in the field; (e) Proportion of soil carbon pools in total organic carbon, including labile carbon pool 1 (LCP1, mainly polysaccharides) and 2 (LCP2, mostly cellulose), and recalcitrant carbon pool (RCP); (f) Growing season (May to September 2010), wintertime (October 2009 to April 2010) and annual ecosystem carbon fluxes. Positive values indicate carbon sink, and negative values represent carbon source. Error bars represent standard error of the mean. The differences between warmed and control plots were tested using two-tailed t tests, indicated by ** when $p<0.05$, or * when $p<0.10$. Panels a, b, c, d, and f were reanalyzed from previously published data (Hicks Pries et al 2013b, Natali et al 2012, Natali et al 2014).

Short-term soil warming altered several environmental attributes (e.g., plant, soil microclimate and soil properties) of the tundra (Natali et al 2011, Natali et al 2012, Natali et al 2014). First, soil temperature (5-40 cm) increased by 2.3 °C (from -6.2 °C to -4.0 °C) in response to warming in wintertime and by 0.6 °C (from 3.8 °C to 4.4 °C) during the growing season in 2010 (**Figure 3.1**a), which led to a substantial surface permafrost thaw as indicated by an increased thaw depth (8.8%, $p<0.001$; **Figure 3.1**c). Similarly, soil moisture increased in response to warming (over 10%, $p=0.03$; **Figure 3.1**b). Second, GPP increased (30.3%, $p=0.02$; **Figure 3.1**f), mainly due to enhanced growth of graminoids (57.5% increase in biomass, $p=0.05$). Warming also extended the growing season length through earlier bud break and delayed senescence (Natali et al 2012). In addition, the percentage of mostly-cellulose fraction of the labile carbon pool (Rovira and Vallejo 2002) in total soil organic carbon was higher (36.1%, $p=0.06$) in warmed than control soils (**Figure 3.1**e). The carbon amount of this pool under warming tended to increase as well, but not statistically significant (**Figure S 13**). Together, these results indicated that environmental attributes of the tundra soil were altered rapidly by short-term warming.

3.4.2 Warming influence on microbial communities and functional genes

The observed alterations in the soil microclimate (temperature, moisture, thawing depth), soil carbon, and GPP in response to warming would be expected to cause significant changes in the microbial communities in the active layer of tundra soil. Consistent with this expectation, the microbial community functional gene structure was markedly different between warmed and control plots as revealed by the detrended correspondence analysis (DCA) of the GeoChip data (**Figure S 9**a), indicating increases

in certain genes and possibly the organisms that host these. Three different non-parametric multivariate statistical tests (ANOSIM, Adonis, and MRPP) showed that the functional community structure differed substantially between warmed and control plots (**Table 3.1**).

Table 3.1 Significance tests on the effects of warming on the microbial community functional structure detected by GeoChip hybridization. Three different permutation tests were performed, including multiple response permutation procedure (MRPP), analysis of similarity (ANOSIM) and permutational multivariate analysis of variance (Adonis), based on Euclidean, Horn or Bray distance. Bold values indicate $p<0.05$.

	MRPP		**ANOSIM**		**Adonis**	
	δ	p	R	p	F	p
Euclidean	69.02	**0.04**	0.38	**0.02**	1.69	**0.04**
Horn	0.06	**0.04**	0.36	**0.02**	1.20	0.23
Bray	0.09	**0.03**	0.30	**0.02**	1.28	0.21

However, significant differences in the overall community structure were not detected with 16S rRNA gene-based amplicon and shotgun metagenomic sequencing approaches (**Figure S 9**b and c). This is most likely due to the high heterogeneity of soil environments, low taxonomic resolution of the experimental approaches, and/or high noise associated with random sampling (Zhou et al 2015). Canonical correspondence analysis (CCA) revealed that soil temperature, moisture and plant GPP were the main significant variables related to the microbial community functional structure ($F=1.68$, $p=0.005$; **Figure S 10**a). This is also consistent with our central hypothesis that warming-induced changes in plant productivity and soil microclimate significantly alter the soil microbial community structure. In addition, soil community DNAs were shotgun sequenced and a total of 3.24 billion raw sequences were obtained for these samples (**Table S 6**). Although the overall metagenome structures were not separable into warmed vs control groups (**Figure S 9**c, **Figure S 11** and **Table S 5**), a small

portion (7.4%) of total subsystems, genes associated with microbial physiological attributes and ecosystem processes, were significantly different between warmed and control plots ($p<0.05$; **Figure 3.2**d). In particular, warmed plots were enriched in genes associated with pathways related to labile carbon utilization (**Table S 7**). Our above results indicated that the microbial communities in the active layer of tundra soil were responsive to warming.

Soil warming also significantly impacted a number of microbial functional and phylogenetic groups important for carbon decomposition. First, more than half (54.5%) of the detected carbon decomposition genes were increased by warming based on GeoChip signal intensities ($p<0.05$; **Figure 3.2**a), including those involved in degrading starch (e.g. *amyA* encoding α-amylase), hemicellulose (e.g. *ara* encoding arabinofuranosidase), cellulose (e.g. cellobiase), chitin (e.g. endochitinase), aromatics (e.g. *vdh* encoding vanillin dehydrogenase) and lignin (e.g. glyoxal oxidase, phenol oxidase). Also, the total fungal functional gene intensity detected by GeoChip was more abundant in warmed plots than control plots (4.7%, $p<0.001$; **Figure S 12**a). Increases of the genes involved in recalcitrant carbon decomposition (**Figure 3.2**a) suggest the possible degradation of old recalcitrant carbon and thus a potential positive feedback to climate warming. In addition, shotgun metagenome sequence data revealed that a substantial portion (19.5%, 8 of 41) of carbon degradation pathways was increased by warming ($p<0.05$; **Figure 3.2**d, **Table S 7**), including those for cellulose, mannose metabolism, carbohydrate hydrolases, fructooligosaccharides and raffinose utilization, lactose and galactose uptake and utilization, L-fructose utilization, xylose utilization, chitin utilization, and N-acetylglucosamine utilization. More specifically, many

individual genes involved in labile carbon degradation (e.g. starch, hemicellulose and cellulose), which were identified from metagenome sequences using GeoChip genes as queries, were increased (95% confidence interval; **Figure 3.2**e). Overall, since these functional genes directly participate in aerobic carbon degradation, their higher abundance could enhance carbon decomposition and hence contribute to positive climate feedback.

The potential for accelerated carbon decomposition was supported by several independent pieces of evidence. First, the cellulose decomposition rate measured by adding external cellulose substrate was higher under warming (**Figure 3.1**d). Also, both winter R_{eco}, derived almost exclusively from heterotrophic soil respiration, and growing season R_{eco}, including both autotrophic (from plants) and heterotrophic soil respiration, increased with warming (100% and 24%, $p<0.05$; **Figure 3.1**f) (Natali et al 2014) . In addition, strong correlations were observed between both growing season and wintertime R_{eco} and the functional gene groups involved in degrading almost all carbon compounds targeted by GeoChip, including starch, hemicellulose, cellulose, chitin, aromatics and lignin (**Table S 9**), suggesting that changes in abundance of these genes could be important in mediating R_{eco} (Lau et al 2015).

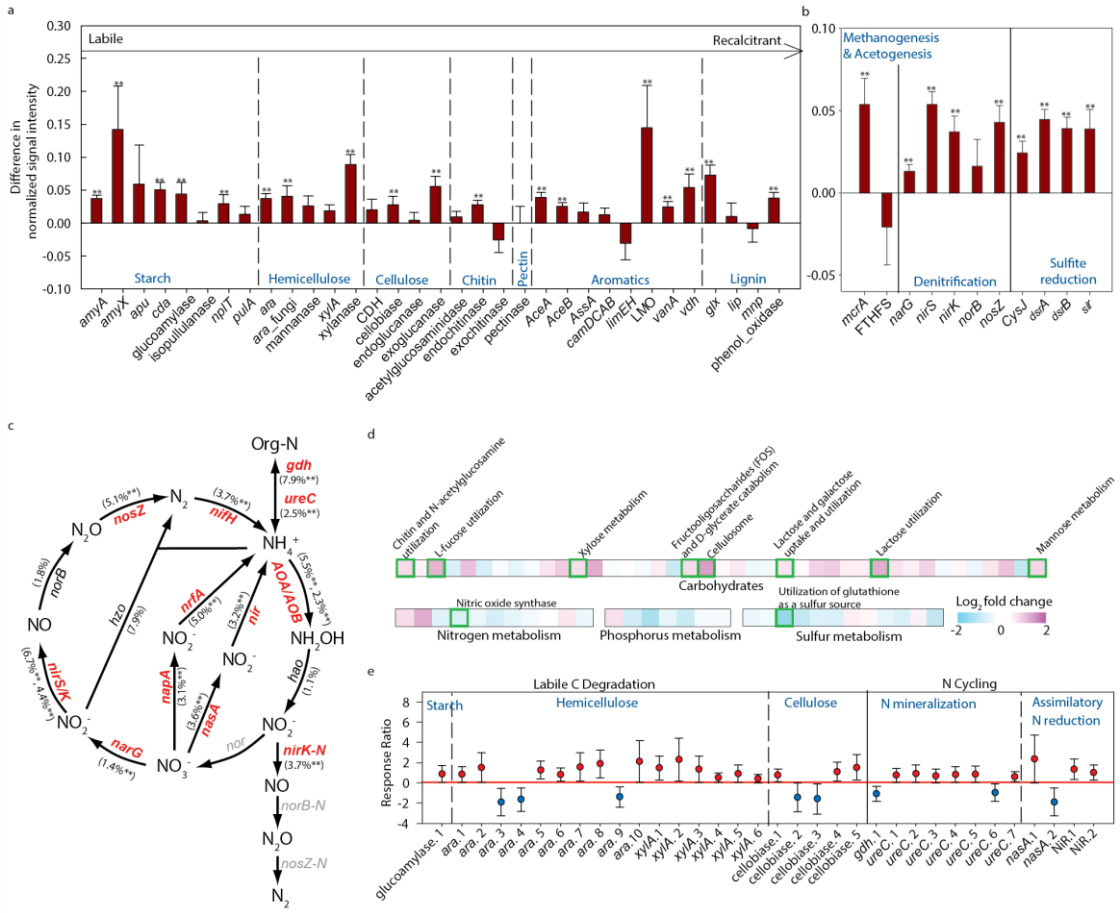

Figure 3.2 Warming effects on functional genes involved in biogeochemical cycling processes. (a) Carbon degradation based on GeoChip data. The targeted substrates were arranged in order from labile to recalcitrant C. GeoChip data is presented as the signal difference between warmed and control plots (Warmed-Control). Error bars represent standard error. Significance is indicated by ** when $p<0.05$. (b) Anaerobic processes from GeoChip data; (c) Nitrogen processes based on GeoChip hybridization. The percent change in nitrogen gene abundance in response to warming is indicated in parenthesis. Genes where change in abundance was significant ($p<0.05$) are labeled in red. Gray-colored genes were not targeted by the version of GeoChip used here, not detected or not applicable. (d) Abundance of subsystems involved in carbon, nitrogen, phosphorus and sulfur cycling from metagenomic shotgun sequence data. Changes in subsystems are indicated as fold change ($\log_2$ (warmed/control)) in abundance. Significant differences between warmed and control plots are highlighted with green boxes. (e) Response ratios showing significant changes in abundance of gene clusters involved in carbon and nitrogen cycling in the metagenomic shotgun sequence data. These gene clusters were identified by searching the shotgun sequence datasets using GeoChip genes as queries. Each cluster on the x-axis represents a group of sequences among which the similarities are ≤ 95%. Error bars indicate 95% confidence intervals of abundance differences between warmed and control groups. The full names of the genes in this figure are listed in **Table S 11**.

Permafrost thawing induced by warming often increases soil water content and creates a mosaic of flooded areas interspersed within dry areas, which may potentially enhance anaerobic carbon decomposition (Coolen and Orsi 2015, Schuur et al 2008). Since water is heterogeneously distributed spatially and temporally, oxygen would also be expected to be unevenly distributed in the soil (Natali et al 2011). GeoChip hybridization-based analysis revealed that genes involved in several important anaerobic respiration processes, such as denitrification, methanogenesis and sulfate reduction, were increased by warming ($p<0.05$; **Figure 3.2**b). Shotgun metagenome sequence analysis also revealed that the pathway for denitrification (marginally) increased in response to warming ($p=0.08$; **Table S 10**). These results were consistent with laboratory incubation studies, where methanogenic pathways were increased within several days after permafrost thaw (Coolen and Orsi 2015, Mackelprang et al 2011). Although some upland permafrost areas were observed to be CH_4 sinks (Lau et al 2015), for our studied site, significantly increased CH_4 emission rates after several years of warming have been reported (Natali et al 2015). Since CH_4 and N_2O have 25 and 298 times the warming potential of CO_2 per mole (IPCC 2007), respectively, anaerobic microbial responses are most likely of considerable importance.

Estimates show that CH_4 emission in northern wetlands, including tundra, accounts for 25% of the global CH_4 release from natural sources (Liebner and Wagner 2007). GeoChip analysis revealed that warming increased the gene encoding methyl coenzyme M reductase A (*mcrA*), a key enzyme in methanogenesis ($p<0.01$; **Figure S 12**b). While 16S rRNA sequence analysis detected two methanogens (*Methanobacteria* and *Methanomicrobia*; **Figure S 12**d), the relative abundance between warmed and control

plots was not significantly different for either methanogen. Warming, however, resulted in a greater abundance of *pmoA*, a gene encoding particulate CH_4 monooxygenase subunit A ($p=0.01$; **Figure S 12**b), suggesting that more of the CH_4 produced could be oxidized in the aerobic upper soil horizon at the warmed plots. Similar findings were reported in recent studies on both incubated permafrost soils (Mackelprang et al 2011) and active layer samples in situ (Hultman et al 2015, Lau et al 2015).

Warming also increased genes involved in nitrogen cycling (**Figure 3.2**c and e), microbial phosphorus utilization and sulfur metabolism (**Figure S 12**c). Most (82.4%) of the GeoChip-detected functional genes involved in nitrogen cycling were increased in response to warming ($p<0.05$; **Figure 3.2**c), consistent with the previous finding that warming enhances nutrient cycling (Zhou et al 2012). For example, the abundance of N_2-fixing bacteria was higher in response to warming ($p<0.05$; **Figure 3.2**c), and two bacterial Classes (Opitutae and Deltaproteobacteria) detected by PCR amplification of the *nifH* gene had higher abundance in warmed samples ($p<0.05$; **Figure S 12**e). Also, the abundance of key genes (e.g. *gdh* and *ureC*) in nitrogen mineralization was higher in warmed than control soil ($p<0.05$ or 95% confidence interval; **Figure 3.2**c and e). In addition, warming appeared to increase nitrification and denitrification processes as indicated by increased *nirK* and *amoA* genes based on GeoChip data (**Figure 3.2**c). The increase in *amoA* could potentially lead to higher nitrate concentrations, which is also supported by the greater abundance of genes for various reductive processes that use nitrate as an electron acceptor, such as *narG*, *nirS/nirK* and *nosZ* for denitrification, *napA* and *nrfA* for dissimilatory nitrate reduction to ammonium, and *nasA*, *nirA* and *nirB* for assimilatory nitrate reduction (**Figure 3.2**c and e). Microbial phosphorus

utilization genes (phytase and *ppx*) and eight of the 11 detected sulfur metabolic genes had higher abundance in warmed than in control plots (**Figure S 12**c). Although the significant increase in abundance of the genes involved in nutrient cycling processes observed in warmed plots may potentially enhance the rates of nutrient cycling, more in-depth studies are necessary to determine the rates and extent of stimulation of different nutrient-cycling processes.

The increased abundance of nitrogen cycling genes (particularly those involved in nitrogen mineralization, nitrogen fixation and nitrification) and other nutrient cycling genes could increase nutrient (especially nitrogen) availability in soil, which is important for ecosystem carbon dynamics because nitrogen is a limiting factor for plant growth in most tundra ecosystems[12]. That warming enhanced plant nitrogen uptake is supported by the observation that from 2009 to 2010 plant foliar nitrogen mass increased in warmed plots (35%, $p<0.01$), while remaining unchanged in control plots (Natali et al 2012). The enhanced plant nitrogen uptake could in turn affect GPP, which increased in response to warming ($p<0.05$; **Figure 3.1**f). Moreover, almost all genes involved in nitrogen cycling (18 of 19) and most carbon degradation genes (22 of 33) showed significant correlations with GPP ($p<0.05$; **Table S 9**). Increased N_2-fixation, mineralization and nitrification could counteract the potential higher nitrogen loss from soil due to increased plant nitrogen uptake, denitrification and nitrate leaching. As a net result, the soil nitrogen availability appeared not to be affected by warming (Natali et al 2011).

3.4.3 Summary, importance and implication

In summary, our results highlight the importance of microbial community mediated feedbacks of the active layer to warming, as illustrated in a conceptual model (**Figure 3.3**). In response to warming, deeper thaw depth increased the amount of carbon accessible for decomposition. Within the active layer, soil carbon is also more vulnerable to degradation through the following mechanisms: First, short-term soil warming altered the active layer microbial community structure, demonstrating rapid responses by these communities; annual R_{eco} released 127 g more carbon m^{-2} from warmed plots compared with controls, resulting in 38.6% more carbon loss from soil. Also, warming increased the abundance of functional genes involved in anaerobic processes, which could lead to a greater positive feedback by releasing more CO_2, CH_4 and N_2O (**Figure 3.3**). In contrast, the potentially higher nutrient availability resulting from the increased abundance of nutrient cycling genes would also stimulate plant growth (**Figure 3.3**). In this study, increased GPP did not completely offset the carbon loss from the warming-induced R_{eco} increase. The net carbon loss from warmed plots doubled in 2010 (**Figure 3.1**f), and was estimated to increase more in actual climate warming scenario (Natali et al 2014). However, it should be noted that the experimental results reported in this study were derived from the active layer of the Alaskan tundra soil. To generalize whether the results observed are applicable to permafrost requires further analyses with actual permafrost.

Overall, whether the tundra soil acts as a carbon source or sink depends on plant and microbial responses to climate warming. Our results indicate that the soil carbon is highly vulnerable to climate warming and this vulnerability is determined by a set of

complex microbial feedbacks to the temperature increase. Improved predictions by ecosystem models to climate warming (Friedlingstein et al 2006) may be possible through better assessment of microbial functional capacities and their responses.

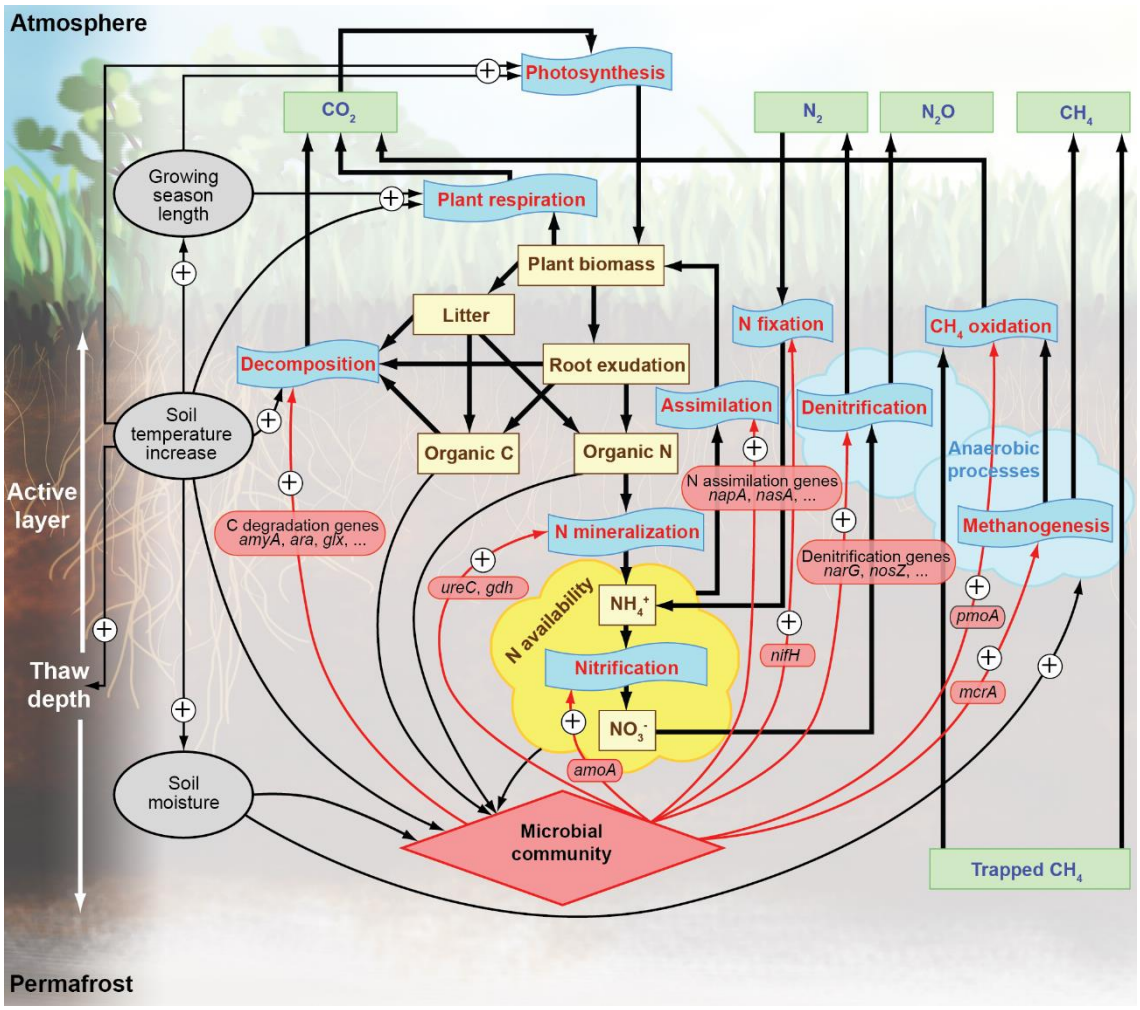

Figure 3.3 A conceptual model of the impact of warming on the active layer of tundra ecosystem processes. Greenhouse gas pools are represented by green square frames, material pools by yellow square frames, and biological processes by frames in a shape of blue punched tape. Material flows are indicated by thicker black arrows. Impacts of environmental attributes (e.g. soil temperature) and microbial community are marked by narrow arrows in black and red, respectively, and labeled with a "+" if increases in gene abundance were observed in this study.

Chapter 4: Differential microbial sensitivity to experimental warming: a comparative metagenomic analysis of soils from two ecosystems

4.1 Abstract:

Climate warming has been differentially increasing the global surface temperature, with the greatest temperature elevation observed in the northern high-latitude regions. Although tundra and underlain permafrost in those areas were predicted vulnerable to climate warming, few quantitative comparisons were reported between tundra and other grassland ecosystems, especially of the composition and structure of soil microbial communities and their functional diversity. Here, we compared the early responses of soil microbial composition and functional gene abundance to experimental warming between a tundra site and a temperate tall grass prairie using several metagenomic technologies, including functional gene microarray, amplicon sequencing, and metagenomic shotgun sequencing. Despite distinct species and functional gene pools in soils from the two ecosystems, genes involved in carbon and nitrogen cycling showed positive responses to warming at both sites, but with 36% more significantly responding genes and a greater magnitude of response for 10 genes at the tundra site. The functional gene compositions were correlated with temperature, moisture, ecosystem respiration and gross primary production at the tundra sites, but mostly with substrate related variables, plant biomass and nitrate concentration, at the prairie, implying different limiting factors in microbial growth and functions. Our results revealed the higher sensitivity of tundra soil microbial communities to warming, compared with those from temperature prairie, and provided field evidence in supporting that northern high-latitude regions might be more vulnerable to climate warming.

4.2 Introduction

Climate warming has increased global surface temperature 0.15 to 0.2 °C per decade on average during the past four decades, but unevenly heated different regions of earth's surface (Hansen et al 2010). The greatest temperature changes were observed in the northern high-latitude regions of the northern hemisphere (Hansen et al 2006), where the temperature has increased at rates twice the global average (Comiso et al 2008, Kortsch et al 2012). Climate warming could trigger abrupt changes in ecosystems in those regions (Kortsch et al 2012), accelerated by their positive feedbacks to the warming effect (Dufresne et al 2002, Friedlingstein et al 2001, Scheffer et al 2006, Walter et al 2006). Therefore, many ecosystems in the Arctic and subarctic, including sea ice, boreal forest, permafrost and tundra, are predicted as tipping elements, or potential tipping elements in the Earth's climate system (Duarte et al 2012, Lenton et al 2008). Current trend of climate change, if not reversed or slow down, is evaluated to have immense potential to push these tippling elements of the Earth system to pass their tipping points, the critical thresholds at which small perturbations can qualitatively shift the state of the system to one with distinctive characteristics, within the next century (Lenton et al 2008, Lenton 2011, Lenton 2012). On the other hand, many other ecosystems, such as temperate grassland and forest, has not been considered as tipping elements so far based on current thoughts (Lenton et al 2008). For example, compared with greatly changed landscapes (Serreze et al 2000) caused by shrinking permafrost and tundra loss in the northern high-latitude regions, including ground subsidence (Nelson et al 2001), thermokarst formation (Jones et al 2011), and expansion of the shrubland (Sturm et al 2001), the natural grassland ecosystems in temperate regions

worldwide were much less reported under significant succession during the past century with recorded global temperature and CO_2 level increases. The difference of ecosystem sensitivity to climate warming could be due to both the difference in the observed temperature increase regime, and varied level of sensitivity and resilience of the ecosystem per se.

The influence of warming were contrasted across different ecosystems in some reports for soil physical-chemical properties, soil and ecosystem functional process rates (i.e., respiration, primary production, nitrogen mineralization, CH_4 uptake, and nitrous oxide emission), distribution of nutrients in plants and microbes, and aboveground plant growth (Beier et al 2008, Lu et al 2013, Luo et al 2013b, Peñuelas et al 2004, Rustad et al 2001, Schmidt et al 2002), but rarely, especially quantitatively, for the composition and structure of soil microbial communities. Soil microbial communities play fundamental roles in the functions of terrestrial ecosystems, and are critical drivers of the carbon cycle between land and the atmosphere. Intensive literatures reported the responses of soil microbial community to climate warming through physiological adaptation, community compositional changes, biomass increase or decrease, with evidences derived from both observations on functions, such as reparation rate, temperature sensitivity and enzyme activity, and molecular techniques like genomics and transcriptomics profiling (Bradford 2013, Deng et al 2015, Hartley et al 2007, Jassey et al 2013, Nie et al 2013, Pailler et al 2014, Peltoniemi et al 2015, Rousk et al 2013, Semenova et al 2015, Streit et al 2014, Tucker et al 2013, Wang et al 2014, Yoshitake et al 2015, Zhang et al 2013, Zhang et al 2005, Ziegler et al 2013). Yet, how

the influence of warming on the microbial community differs across terrestrial ecosystems, and what causes such difference, are less tested and summarized.

In this study, we quantitatively compared the soil microbial communities in two contrast ecosystems, a high latitude tundra and a temperate tall grass prairie, of their early responses to experimental warming. According to predictions of the Earth's tipping element, the subarctic tundra will be more vulnerable in response to temperature changes than the temperate grassland. We hereby hypothesize that the microbial community in tundra soils is also more sensitive to warming, and imposes greater responses than the prairie communities. A previous publication (Xue et al 2016a) has metagenomically characterized the rapid responses of the microbial functional genes, along with greatly altered soil physical-chemical properties and ecosystem carbon flux, in the tundra soils after only two winters of warming treatment. Here we presented results from similar microbial analyses of soils collected also after one and half years of warming, with a similar level of temperature increase, from an Oklahoma tall grass prairie. We applied several metagenomic techniques, including functional gene array hybridization, amplicon sequencing of 16S, 28S and *nifH* genes, and metagenomic shotgun sequencing, and quantified the magnitude of difference in the responses of the microbial functional genes to warming at sites representing the two ecosystems. Our results indicated that although the background community composition differed in the two sites, warming increased the abundance of functional genes involved in carbon and nitrogen in both sites, but with a greater magnitude and more influenced genes in the tundra site. Functional gene composition in the two sites might be driven by varied environmental factors, which lead to their differed responses to warming. Our study

provided field evidence in supporting that the tundra ecosystem in northern high-latitude region harbors more responsive soil microbial communities than temperate prairie does to climate warming.

4.3 Material and methods

4.3.1 Sites Description and Sampling

This study analyzed soil microbial communities from two field warming experiments, one in the Carbon in Permafrost Experimental Heating Research site (CiPEHR, 63º52’59’’N, 149º13’32’’W) in Healy, Alaska (AK site), and the other in the Kessler Atmospheric and Ecological Field Station (KAEFS, 34°58'54"N, 97°31'14"W) in central Oklahoma (OK site). The AK site (Natali et al 2011, Xue et al 2016a) represented a cool moist acidic tundra ecosystem underlain with discontinuous permafrost at the depth of >1 m, with an annual mean temperature of –1.0 °C (monthly averages ranged from –16 °C in December to 15 °C in July) and average annual precipitation of 378 mm. This area was covered only by C_3 plant species, dominated by *Eriophorum vaginatum, Vaccinium uliginosum*, moss and lichen. The top 0.45-0.65 m soil was carbon-rich, below which was mineral soil with a mixture of glacial till and windblown loess. The OK site (Li et al 2013, Xu et al 2013, Xu et al 2016) was located on an herbivore grazing-excluded temperate tall grass prairie, with the mean annual temperature of 16.3ºC (monthly averages ranged from 3.3ºC in January to 28.1ºC in July), and average annual precipitation of 967mm. The plots were dominated by C_3 forbs and grasses in spring, and by C_4 grasses in Fall. The soil was sandy loam texture with a water holding capacity of 37%.

The experimental setting of AK CiPEHR experiment was detailed in previous publications (Natali et al 2011, Xue et al 2016a). Briefly, there were six field-replicated sets of control and warmed plots. The winter warming treatment was achieved by setting up snow fences in between each control and warmed plot pair, and let more snow accumulate on the warmed plot to insulate heat transfer from ground to the atmosphere. Before the snow started to melt in spring, excessive snow was removed from above the warmed plots to ambient cover depth, to prevent a difference in hydrological conditions between treatment and control. The snow fences were placed every winter starting from late 2008. Twelve soil cores, one from each plot, were sampled in May 2010, the beginning of growing season, after two winters (1.5 years) of warming treatment. Soils from 15-25cm were analyzed in this study. At OK site, there were four pairs of field replicated control and warmed plots. The warming treatment was achieved by infrared radiators hung at 1.5m above the plot. The radiators were powered and working non-stop since spring 2009. In control plots, wood "dummy" heaters were used to simulate shading effect in warmed plots. Eight surface (0-15cm) soils cores, one from each plot, were sampled in Oct 2010, after about 1.5 years of warming treatment. Samples from both sites were transported to the laboratory and stored at -80 °C immediately until analyses. Any observable plant root materials were picked out before the soil was processed.

The AK and OK sites represented very different grassland ecosystems in terms of ambient temperature, soil physical-chemical properties, and vegetation type. They made a valid comparison with regard to answering our question on how different ecosystems respond initially to climate warming because of three reasons. First, both sites were

located in areas that no human activities other than site maintenance occurred, allowing the study of natural responses of ecosystems under climate change. Second, although warmed through different approaches, the temperatures in warmed plots were increased by similar levels at the two sites. Third, both sites were operated for a similar length of time at sampling. Although AK plots were not artificially warmed in the growing season, the winter warming effect was observed to linger during the summer (Natali et al 2011). We used surface/subsurface soils for analysis because these layers contain more organic carbon, and are the depths in which microbes interact intensively with plants in mediating carbon cycling. At AK, top 0-5 cm layers of soils were mostly under decomposed plant debris, thus subsurface fractions were used in the analysis.

4.3.2 Field observations

The field measurements at AK site were described in detail in Xue et al (2016a). Here we summarize the environmental observations in OK site.

Temperature and moisture. Soil temperature was continuously monitored by thermocouples installed at the depth of 7.5cm in the center of each plot. The hourly average data was stored in an SM19 Storage Module (Campbell Scientific). Soil volumetric water content was measured once or twice every month between 10 am and 3 pm using a manual time domain reflectometry (Soil Moisture Equipment Corp., Santa Barbara, CA, USA) at 10 cm depth. The soil temperature and moisture data at the OK site presented in this study were the annual average for 2010.

Plant biomass. The peak aboveground plant biomass was estimated by a simplified pin-contact method (Frank and McNaughton 1990, Sherry et al 2008) at the peak biomass season in fall (Luo et al 2009). A 0.5m x 1m frame, containing 5x10 10cm by 10cm

cells, was held at 0.7m (this height covered all the plants) above the ground surface. A pin was held perpendicular to the ground at the corner of each cell to record green (live plant) and brown (standing litter) hits with the pins. This process was also done in biomass harvested plots (samples not included in this study) before the plants were clipped at 10 cm above the soil surface. The clipped plants were separated into C_3 and C_4 plants and oven-dried at 65 °C for 48 h for biomass. With the regression relationship between pin-hits and the directly weighed biomass in clipped plots, we estimated the biomass in the unclipped (warmed and control) plots.

Ecosystem carbon fluxes. Ecosystem gas exchange was measured with a transparent cubic chamber (0.5 m in length) attached to an infrared gas analyzer (IRGA; LI-6400, Li-Corp.) once or twice a month on clear, sunny days between 10 am and 3 pm (Niu et al 2008). Two small fans ran continuously to mix the air inside the sealed chamber during the 90-s measurement periods. Nine consecutive recordings of CO_2 concentration were taken at 10-s intervals. CO_2 and H_2O flux rates were determined from the time-courses of the concentrations to calculate the NEE (Steduto et al 2002). Following the measurements of NEE, the chamber was vented and sealed again, and covered with an opaque cloth to avoid light and thus photosynthesis. After the CO_2 concentration in the chamber began to steadily increase (usually 0.5 min after the chamber was covered), the CO_2 exchange measurements were repeated to estimate ecosystem respiration (R_{eco}). Gross primary productivity (GPP) was estimated as the difference between NEE and R_{eco}. The NEE, R_{eco} and GPP data at the OK site presented in this study were the annual average in 2010.

Soil respirations. Soil respiration (R_s) and heterotrophic respiration (R_h) were measured using an LI-8100 portable soil CO_2 fluxes system attached to a 10-cm survey chamber once or twice a month, avoiding days immediately after rainfall events. R_h was estimated by setting the chamber on top of a shallow PVC collar (10 cm in diameter and 5 cm in height) installed at 2-3 cm deep in the soil (Zhou et al 2007) and measure the CO_2 concentration inside. Small living plants inside the PVC collars were clipped at the soil surface to eliminate leaf respiration. R_h measurements took place on a deep collar (70 cm in height) that were inserted at 70 cm below the soil surface to prevent new roots from going in. After old root inside of the collar died and being decomposed, CO_2 efflux from the deep collars represented R_h (Zhou et al 2007). Autotrophic respiration (R_a) is calculated as the difference between R_s and R_h.

4.3.3 Soil geochemical and microbial analysis

After sampling, soils from both AK and OK sites were processed together using the same methods for soil geochemical and microbial analyses. Soil geochemical analyses included soil carbon, nitrogen, $\delta^{13}C$ and $\delta^{15}N$ stable isotope analysis and soil labile and recalcitrant carbon pool fractionation. Microbial analyses included DNA extraction, functional gene array (GeoChip 4.2) hybridization, amplicon sequencing of 16S rRNA genes, and nifH genes, and metagenomic shotgun sequencing. Methods used in those analyses, downstream data processing procedures, and data processing results for AK site were described in detail in Xue et al (2016a). Here we summarized the results for OK communities. After data cleaning and processing, a total of 44,736 functional gene probes were detected by GeoChip hybridization, 198,520 sequences in 12,516 OTUs were recovered from 16S rRNA gene sequences, and 250,844 sequences in 5,185 OTUs

were retrieved from nifH sequences. Statistics for metagenomic shotgun sequences were summarized in **Table S 5**.

In addition to the above analysis, we also performed 454 pyrosequencing of 28S rRNA gene amplicons to investigate the fungal communities in the two sites. Primer pair LR0R (5'- ACCCGCTGAACTTAAGC -3') and LR3 (5'- CCGTGTTTCAAGACGGG -3') (the 28S rRNA gene position in Saccharomyces Cerevisiae)(Vilgalys and Hester 1990), combined with sample-identifying 8-mer tag sequences by the 2 bp spacer sequences, was used to amplify the 28S rRNA genes of the community DNA samples. The primers were synthesized by Eurofins. The PCR system, containing 50 mM KCl, 10 mM Tris-HCl at pH 8.3, 0.1% Triton X-100, 2.5 mM $MgCl_2$, 200 µM dNTPs (Invitrogen), 5 units of Taq polymerase, 0.1µg BSA (New England Biolabs Inc., Ipswich, MA, USA), 0.4 µM each primer and 12.5 ng DNA template in a volume of 100 µL, was kept under the following thermocycling conditions: 3 min at 94°C for initialization; then 35 cycles of 1 min at 94°C for denaturation, 45 s at 53°C for annealing, and 1 min at 72°C for extension; and 15 min at 72°C for final elongation. Five to ten 100 µL PCR reactions were performed for each sample, and the products were pooled together, purified by agarose gel electrophoresis, recovered using QIAquick Gel Extraction Kit (Qiagen), and quantified with PicoGreen using an FLUOstar Optima (BMG Labtech, Jena, Germany). Equimolar uniquely-tagged amplicons from each sample were then combined into one library for 454 pyrosequencing at Macrogen, Inc. (Seoul, Korea) using 454 GSFLX Titanium platform. Raw sequences were split by tags and trimmed to remove primers. The sequences were then cleaned using LUCY (Chou and Holmes 2001) by setting the following

parameters: the maximum average error at 0.01, the maximum error at the ends at 0.01, the minimum score at 21, window size at 50, minimum length at 200 and allowed N number at 10. Sequences containing unidentified base N and detected by UCHIME to possibly generate chimeras were removed (Edgar et al 2011). A total of 326,245 qualified sequences for AK samples and 255,760 qualified sequences for OK samples were obtained and clustered to OTUs at a similarity of 0.97 using CD-HIT (Li and Godzik 2006). The OTU singletons were removed. The representative sequence of each OTU was identified phylogenetically in RDP Classifier (Wang et al 2007) with the confidence cutoff 0.5. Finally, 325,636 sequences in 1,172 non-singleton OTUs for AK samples and 250,844 sequences in 5,185 non-singleton OTUs for OK samples were normalized to relative abundance and included in statistical analyses.

Notably, for 16S rRNA genes sequencing and metagenomic shotgun results, sequences from AK and OK were processed as one sequence pool and annotated to species (OTUs or functional guilds) together, thus in downstream analysis, we were able to line up same species in the two sites by their OTU or functional guild IDs. The 28S and *nifH* sequences were annotated separately for AK and OK, thus we only compared the community response to warming within each site, but did not compare sequences between sites.

4.3.4 Statistical analysis

We performed the following statistical analysis to test the warming effect on microbial communities and environmental variables. (i) Multi-response permutation procedure (MRPP) (Van Sickle 1997), a non-parametric analysis for multivariate data, was used to test the differences of soil microbial communities between warming and control

treatments, and between AK and OK sites with the distance matrix constructed using Bray-Curtis distance (Bray and Curtis 1957). (ii) Two-tailed t tests were performed to test the significance of differences between warming and control treatments for the environmental variables (i.e., soil geochemistry, plant biomass, and ecosystem carbon fluxes). For environmental variables measured at multiple time points (temperature, moisture, GPP, R_{eco}, and NEE), repeated measure ANOVA was performed. (iii) Analysis of variance (ANOVA) (Chambers et al 1992) was performed to test the treatment effect on abundances of each function gene involved in carbon and nitrogen cycling for GeoChip or relative abundances of OTUs of certain genus or phylum groups. Other than warming treatment effect, the probe or OTU was also considered a factor in the employed model for partitioning the variance from various probes within each gene catalog. (iv) Canonical correspondence analysis (CCA) (Hotelling 1992) was performed to determine the linkage between each environmental variable and the microbial community composition in various functional categories. (v) Response ratio (Hedges et al 1999) was used to determine the magnitude and direction of warming induced change for each microbial species (OTU for sequencing data, probe for GeoChip data, functional clusters for EcoFun-MAP processed shotgun sequencing data, and subsystems) that were present in both warming and control samples. (vi) To quantitatively compare the magnitude of functional gene abundance changes between AK and OK sites, we introduced the ratio of response ratios as follows, based on the calculation of response ratio.

The response ratio of a functional gene abundance to treatment, as introduced by (Hedges et al 1999), was calculated as

$$L = \ln(\bar{X}_W) - \ln(\bar{X}_C)$$

where $\bar{X}_W$ and $\bar{X}_C$ are the sample mean of probe signal intensities in warmed and control groups, respectively. Variance of L is calculated as

$$v = \frac{(s_W)^2}{n_W \bar{X}_W^2} + \frac{(s_C)^2}{n_C \bar{X}_C^2}$$

where n_W and s_W denotes the samples size (the product of probe number in each gene and the number of biological replicates) and the standard deviation of probe signal intensities in warming group. n_C and s_C denote sample size and intensity standard deviation of the control group. So, the standard error of each response ratio L is

$$SE_L = \sqrt{v} \quad (1)$$

And the 95% confident interval λ satisfies

$$L - z_{0.025}\sqrt{v} \leq \lambda \leq L + z_{0.025}\sqrt{v} \quad (2)$$

where $z_{0.025} = 1.96$ is the point lower than which 97.5% of the total area was included in standard normal distribution.

To compare the magnitude of warming effect in AK with that in OK site, we calculated the ratio of response ratios as

$$R = \ln\left(\frac{\frac{\bar{X}_{W_{AK}}}{\bar{X}_{C_{AK}}}}{\frac{\bar{X}_{W_{OK}}}{\bar{X}_{C_{OK}}}}\right) = \ln\left(\frac{\bar{X}_{W_{AK}}}{\bar{X}_{C_{AK}}}\right) - \ln\left(\frac{\bar{X}_{W_{OK}}}{\bar{X}_{C_{OK}}}\right) = L_{AK} - L_{OK}$$

Standard errors of L_{AK} and L_{OK} are calculated using equation (1). The standard deviation is calculated as

$$SD_L = SE_L\sqrt{n}$$

where n is the sample size of each gene for each site. The pooled variance of R is

$$s_p^2 = \frac{(n_{AK} - 1){s_{LAK}}^2 + (n_{OK} - 1){s_{LOK}}^2}{n_{AK} + n_{OK} - 2}$$

The standard error for R is estimated as

$$SE_p = s_p \sqrt{\frac{1}{n_{AK}} + \frac{1}{n_{OK}}}$$

Then the 95% confidence interval is calculated with equation (2).

4.4 Results

4.4.1 Soil property, plant and ecosystem responses to by warming

Table 4.1 Summary of soil and plant attributes at the OK site (mean ± standard error). Significance was tested by two-tailed t test to compare control and warming samples or repeated measure ANOVA for soil microclimate and ecosystem carbon exchange variables. The significance was tested by two tailed t test, labeled with * when $p<0.05$.

	Soil and ecosystem attribute	Control	Warming	p
Soil Microclimate	Soil Temperature (°C)	16.17±0.12	18.51±0.18	**
	Soil Moisture (%)	10.59±0.56	9.17±0.55	**
Soil C and N	Labile C pool 1 (%)	35.25±5.27	25.97±1.36	
	Labile C pool 2 (%)	21.74±1.08	30.21±2.26	**
	Recalcitrant C pool (%)	43.02±4.62	43.82±1.77	
	TOC (mg C g^{-1} dry soil)	9.09±1.71	12.85±1.68	
	$\delta^{13}C$ (‰)	-22.28±0.79	-22.38±0.63	
	Total N (%)	0.07±0.01	0.08±0.01	
	NH_4^+ (mg N g^{-1} dry soil)	38.35±5.15	52.20±4.86	
	NO_3^- (mg N g^{-1} dry soil)	8.69±2.98	6.26±0.36	
	$\delta^{15}N$ (‰)	5.14±0.34	4.38±0.35	
Plant biomass (g m^{-2})	C_3	451.1±57.4	395.3±39.2	
	C_4	110.8±26.0	91.0±16.6	
	Total	561.90±39.66	486.26±48.68	
Ecosystem C exchange (g-C m^{-2} $month^{-1}$)	Net ecosystem exchange	20.10±5.66	55.58±7.39	**
	Ecosystem respiration	-135.77±4.47	-117.15±10.82	
	Gross primary productivity	155.87±7.44	172.73±13.16	

The AK soil and ecosystem properties were presented in (Xue et al 2016a). Here we presented data in OK and compare the changes in the two sites (**Table 4.1**). Observed soil temperature during the one and half years of warming increased similar degrees

(2.3 °C, -6.2 °C to -4.0 °C, in winter at AK, and 2.3 °C, 16.2 to 18.5 °C, averaged across the entire year at OK, $p<0.01$). Moisture was increased at AK for 10% (47.8 to 52.7%, $p<0.01$) but decreased at OK for 13% (10.59 to 9.17%, $p<0.01$). Both sites had increased portion of the labile carbon pool that consisted mainly of cellulose in the total soil organic carbon (36.1% in AK, 39% in OK). AK warming resulted in the significantly altered pattern of ecosystem carbon flow, including increased plant productivity and ecosystem respiration. While no significant changes in these parameters were observed in OK, although slightly increased GPP and decreased R_{eco} resulted in a larger amount of carbon being sequestrated, as indicated by increased NEE under warming (176.5%, $p=0.01$). While the two ecosystems were subjected to a similar level of artificial warming for a comparable length of time, soil and plant properties were differentially affected.

4.4.2 Microbial community responses to warming

Table 4.2 Summary of permutation tests to investigate warming effects on soil microbial community composition based on GeoChip hybridization, OTUs for 16S rRNA, 28S rRNA and *nifH* genes detected by amplicon sequencing, and genes or subsystems detected by metagenomic shotgun sequencing. Bray-Curtis distance was used in the multiple response permutation procedure (MRPP). *nifH* and 28S sequences were separately processed for AK and OK, thus no comparison was performed between sites.

Detection approaches	**Targeted genes/groups**	**Warming vs. Control in AK ***		**Warming vs. Control in OK**		**AK vs. OK**	
		δ	P	δ	P	δ	P
Microarray	GeoChip probes	0.09	**0.03**	0.04	0.52	0.07	**0.001**
Amplicon sequencing	16S sequences	0.63	0.26	0.53	**0.08**	0.60	**0.001**
	nifH sequences	0.40	0.70	0.66	0.59	-	-
	28S sequences	0.76	0.73	0.66	**0.04**	-	-
Metagenomic shotgun sequencing	EcoFun-MAP	0.34	0.55	0.30	0.77	0.32	**0.001**
	Subsystems from shotgun sequences	0.05	0.77	0.02	0.41	0.03	**0.001**

* Data published in Xue et al (2016a).

Overall, all four techniques revealed fundamentally different microbial community taxonomic and functional composition in AK and OK sites (**Table 4.2**), with higher diversity in OK samples than in AK (**Table S 13**, **Figure 4.1**b, d, e, and f). Warming altered the microarray detected functional gene composition in AK (Xue, M. Yuan et al. 2016), while changed the fungal community composition, and marginally affected bacterial and archaeal taxonomy in OK (**Table 4.2**).

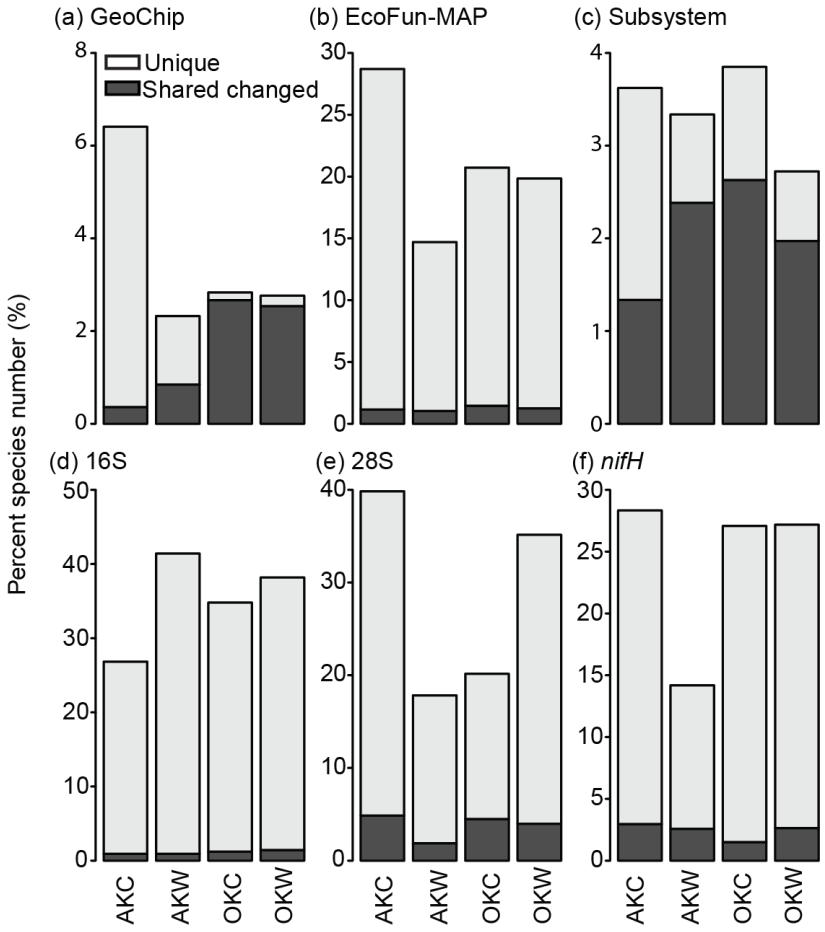

Figure 4.1 Percentage of species that were uniquely present in control or warmed samples, and those shared but with response ratios significantly differed from zero. The dark grey bars in AKC and OKC groups represent species with negative response ratios, or decreased in abundance in response to warming. The dark grey bars in AKW and OKW denote the species with increased abundance under warming.

In the open-format detections (i.e., 16S, 28S and nifH sequencing), species that were uniquely present in either control or warmed samples consisted of a significant portion

all the detected species (**Figure 4.1**d, e, and f). This is also true for the EcoFun-MAP processed shotgun sequences (**Figure 4.1**b). Notably, using the same technique, the GeoChip functional gene array, AK samples had much larger portions of unique probes than OK samples (**Figure 4.1**a). In five of the six data sets for AK, control samples had more unique probes than warming (**Figure 4.1**a, b, c, e, and f). For OK, unique OTUs were much less in control samples compared with warming only in 28S community (**Figure 4.1**e), while in other data sets, similar portions of unique OTUs were detected for control and warming.

Detailed changes of species detected by different techniques in response to warming were presented in **Figure 4.2Figure 4.2**. In all the datasets, species responded both positively and negatively to warming treatment, and the responding species distributed across the entire detected functional or taxonomic spectrums. In 16S data, differential responses of certain groups were observed (**Figure 4.2**d). For example, subgroups from Acidobacteria and Proteobacteria tended to only increase when warmed. **Figure 4.2**g and **Figure 4.3** summarized the values of response ratios that were confidently different from zero. For all the three function-related datasets and 16S community, AK species had a larger positive response than OK (**Figure 4.3**a, b, c, and d). Negative responses of species were also larger in EcoFun-Map and 16S data (**Figure 4.3**b, d). NifH OTUs, in the opposite, tend to have larger response ratios at OK compared with AK (**Figure 4.3**f).

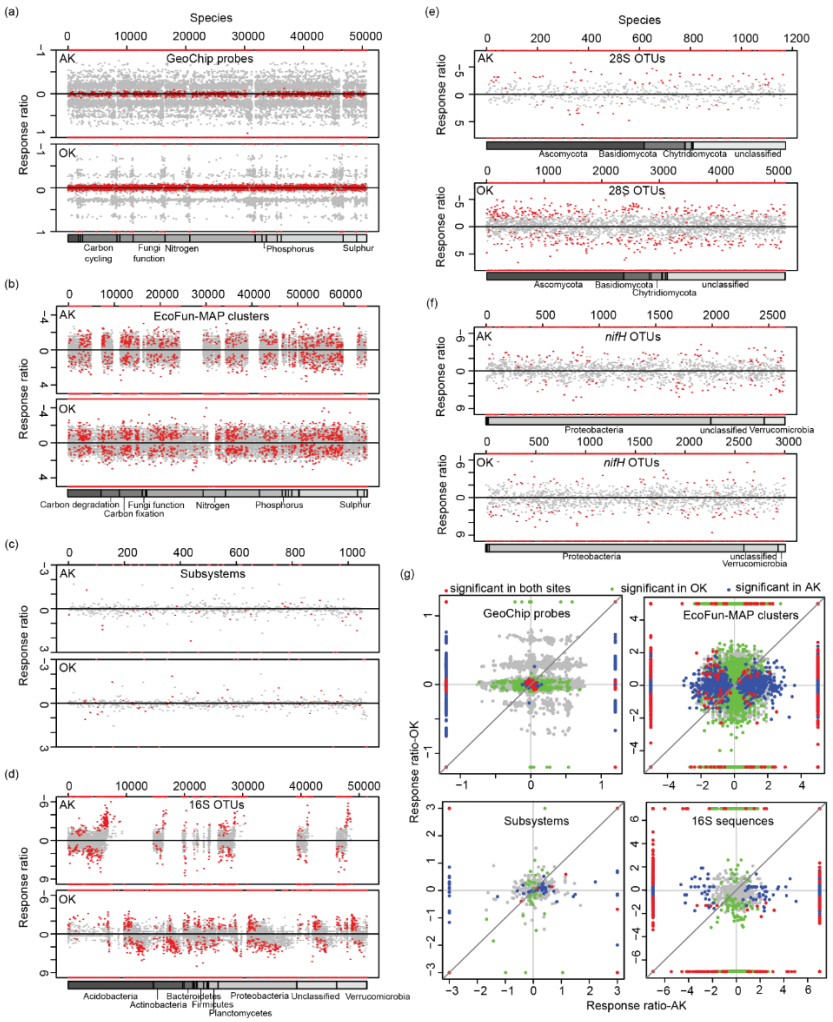

Figure 4.2 Response ratios of all the species to warming in the two sites detected by six different metagenomic techniques. Panels (a)-(f) present response ratios of GeoChip functional gene probes, EcoFun-MAP fished out functional gene clusters from shotgun sequences, shotgun sequences annotated subsystems against the GreenGene database, 16S amplicon sequences, 28S amplicon sequences, and *nifH* amplicon sequences, respectively. In each plot, negative response ratios mean decreased abundance by warming, and vice versa. If the 95% confidence interval of a response ratio does not overlap with zero, the value is marked with a red dot. Grey dots therefore mean that the response ratios are not confidently differed from zero. Red dots sitting on the upper and lower frame of the plots denote the species uniquely present in control and warmed plots, respectively. For (a) through (d), identical species are at the same location on x-axes for AK and OK. (a), (b), and (d) have the annotation of major functions and taxonomic groups underneath the plots. In (c), around 1500 subsystems of functions were not categorized into a higher level. In (e) and (f), species were separately plotted for AK and OK, with their own annotations. (g) summarized the response ratios of common species in AK and OK, with the 1:1 line plotted in order to compare the response ratios of species in the two sites. Those at the edge of plots were species uniquely present in control or warmed group.

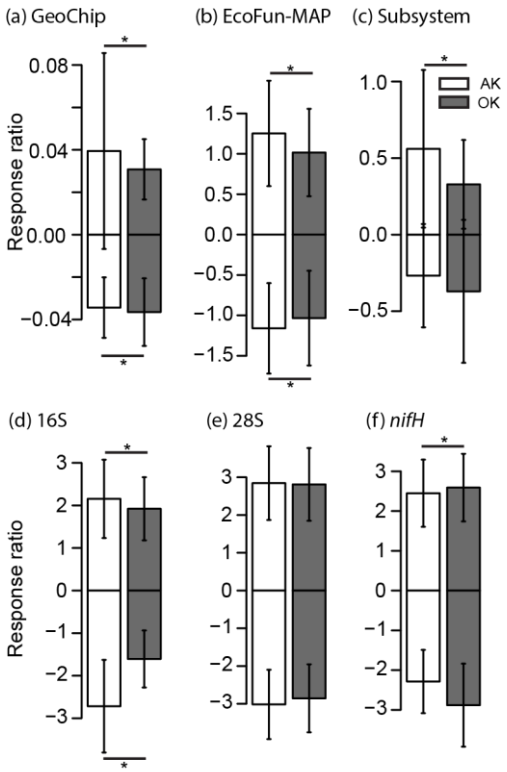

Figure 4.3 Means and standard deviations of the response ratios significantly differed from zero. Positive and negative response ratios were separately calculated. Asteroids mark significant ($p<0.05$) difference of the means in AK compared with in OK by student T-test.

4.4.3 Responses of functional genes related to carbon decomposition, anaerobic respiration, and nitrogen cycling

Warming tended to increase the abundance of carbon degradation related genes in both sites ((Xue et al 2016a), **Figure S 14**). While more than half of the detected carbon degradation genes were increased in abundance after only one and half years of warming in AK, Only 18.2% (6 of 33) of detected carbon decomposition genes based GeoChip data were increased by warming ($p<0.05$, **Figure S 14**a), including *amyA* gene encoding α-amylase for starch degradation, *ara* gene encoding arabinofuranosidase and the gene encoding mannanase for hemicellulose degradation, the gene encoding endochitinase for chitin degradation, *vanA* gene encoding vanillate O-demethylase

oxygenase for aromatics degradation and the gene encoding phenol oxidase for lignin degradation. Moreover, the magnitudes of changes between warming and controls were much greater at AK than OK, demonstrated by the ratio of response ratios analysis (**Figure 4.4**a).

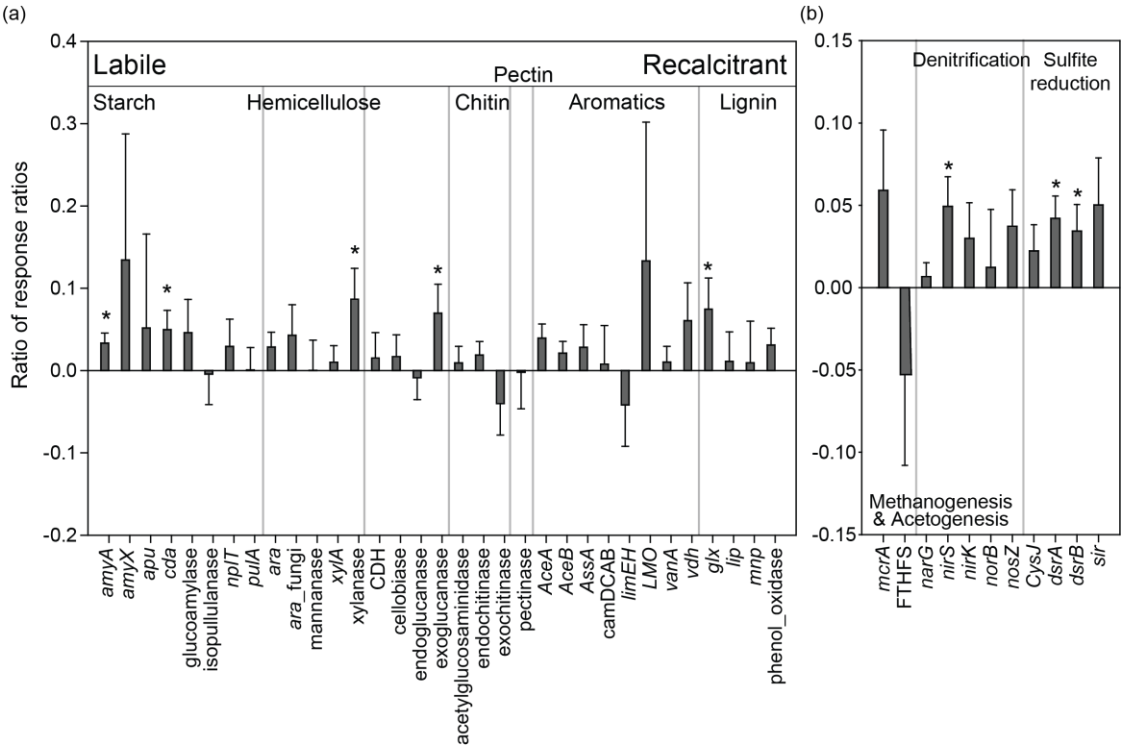

Figure 4.4 The ratio of response ratios between AK and OK sites for (a) carbon degradation genes and (b) anaerobic respiration genes. Asteroids indicate significant different of the ratio of response ratios as the 95% confident interval had no overlap with zero. In (a), the functional genes were arranged so that the targeted substrates are from labile to recalcitrant for decomposition.

Regarding genes involved in anaerobic processes, no more than half of the detected genes (45.5%, 5 of 11) were significantly stimulated by warming at the OK site ($p<0.05$; **Figure S 14**b), including *narG*, *nirS* and *nosZ* genes for denitrification, *dsrA* and *dsrB* genes for sulfite reduction, and 9 of those genes significantly increased in abundance at AK site (Xue 2016). Moreover, the magnitudes of changes between

warming and controls for *nirS, dsrA* and *dsrB* were significantly greater at AK than OK site (**Figure 4.4**b).

Warming also increased gene involved in nitrogen cycling at both sites. In nitrogen cycling, nearly half of genes (47.1%, 8 of 17) were increased in abundance by warming at the OK site ($p<0.05$; **Figure S 15**), including *ureC* gene for ammonification, *amoA* gene from bacteria for nitrification, *napA* and *nrfA* gene for dissimilatory nitrogen reduction, *narG*, *nirS* and *nosZ* genes for denitrification, and *nifH* gene for nitrogen fixation. Compared with AK site, genes for the assimilatory nitrogen reduction pathway (*nasA* and *nir*) did not change in abundance at OK site. The magnitudes of warming-augmented nitrogen gene abundance changes for *nirS* and *nifH* were significantly greater at the AK than OK (**Figure S 15**).

4.4.4 Microbial functional guilds in correlation with environmental conditions

Many of the AK microbial functional attributes related to carbon degradation, nitrogen, phosphorus and sulfur cycling were correlated with soil temperature and moisture (Xue et al 2016a). While for the OK functional gene composition of the 19 functional subcategories, none was correlated with soil temperature, despite detected functional gene abundance changes under warming (**Figure S 14** and **Figure S 15**). Only the functional gene composition for anammox pathway was correlated to soil moisture (**Table 4.3**). Instead, the functional structure of a majority of these functional subcategories were significantly or marginally significantly correlated with soil substrate related variables: 18 with the C_4 plant biomass, 15 with the C_3 and C_4 biomass ratio, and 16 with nitrate concentration (**Table 4.3**). The mass correlations of microbial functional structures with soil and ecosystem respirations at AK site were not observed

at OK (**Table 4.3**). This indicated that different environmental factors cast major impacts on the microbial functional community at the two sites.

Table 4.3 CCA between the structure of each functional gene group involved in C/N/P/S cycling and each environmental attribute for the OK site. The functional community structure was determined by GeoChip hybridization. The significance is represented by ** when $p<0.05$ and * when $p<0.10$. Environmental attributes without significant correlation to any of the functional gene groups are not listed. A similar table for AK site was presented in Xue et al (2016a).

Category	Subcategory	[a]Environmental atributes									
		Moist.	NEE	R_a	C_4	C_3:C_4	LP1%	LP2%	LP3%	NO_3^-	NH_4^+
C degradation	Starch				**	**				**	
	Hemicellulose				**	**				*	
	Cellulose				**	*				*	
	Chitin				**	**				*	*
	pectinase									**	
	Others				**	*				*	
	Lignin				**	**				**	
N	Ammonification				**					*	
	Anammox	*	*		**		**	*			**
	Assimilatory N reduction				**	**				*	
	Denitrification				**	**				**	
	Dissimilatory N reduction				**	**				*	
	Nitrification				**	**				*	
	nifH				**	**				**	
P	Phosphorus utilization				**	**				*	
S	Adenylylsulfate reductase			*	**	**				*	
	Sulfide oxidation				*				*		
	Sulfite reductase				**	**				*	
	Sulfur oxidation				**	**				*	

[a]Environmental attributes include soil moisture (Moist.), net ecosystem exchange (NEE), autotrophic (root) respiration (R_a), peak biomass of C_4 species (C_4), ratio between C_3 and C_4-biomass (C_3:C_4), soil labile carbon pool 1 (LP1%), soil labile carbon pool 2 (LP2%), soil labile carbon pool 3 (LP3%), soil nitrate (NO_3^-) and ammonia (NH_4^+) contents.

4.5 Discussion

Findings from several metagenomic techniques were synthesized in this study to investigate the soil microbial community's early responses to climate warming in two contrast ecosystems, a sub-arctic moist acidic tundra and a temperate tall grass prairie.

Although soils in the two ecosystems bore pronouncedly distinct species pools and functional potentials, functional genes involved in carbon degradation, anaerobic respiration and nitrogen cycling were detected with increased abundance at both sites. However, more functional genes were significantly increased, with a larger magnitude of response, were observed at the tundra site compared with the prairie, under a similar level of temperature elevation after the same length of time of warming treatment. Soil temperature and moisture were strongly correlated with functional gene compositions in the tundra site, while substrate-related variables were major covariates with the community structure at the prairie. Our results indicated that soil microbial communities were differentially affected by temperature increase in distinct ecosystems, and that contrasting plant or edaphic factors might play a role in influencing the sensitivity of the microbial functional genes in response to warming.

The ratio of response ratios revealed larger magnitudes of functional gene changes in the tundra compared with the prairie by direct quantification of the responses between the two sites. Northern permafrost region received extensive attention in climate change research due to its enormous size of carbon storage, and the vulnerability of this carbon to decomposition upon warming (Schuur et al 2008). The tundra and permafrost loss were evaluated as potential "tipping elements" of the earth's climate system (Lenton et al 2008). Many studies have documented altered tundra and permafrost microbial community composition, functional potential, and biochemical pathway under conditions of climate change related thaw (Coolen and Orsi 2015, Mackelprang et al 2011), hydrological reformation (Lipson et al 2015), temperature increase (Mikan, Schimel et al. 2002, Schimel, Bilbrough et al. 2004, Allison and Treseder 2008), plant

community succession (Sturm, Racine et al. 2001, Schuur, Crummer et al. 2007, Lantz, Kokelj et al. 2009), and fire (Taş, Prestat et al. 2014). While warming effect on temperate grassland microbial communities were also investigated in many field experiments (Zogg, Zak et al. 1997, Zhang, Parker et al. 2005, Briones, Ostle et al. 2009, Castro, Classen et al. 2010, Ma, Lü et al. 2011, Hayden, Mele et al. 2012, Nie, Pendall et al. 2013, Luo, Rodriguez-R et al. 2014), direct and quantitative contrast of the tundra to other ecosystems in terms of soil microbial responses to climate change factors is limited. Here, we provided field evidence in supporting that at the early phase of warming, microbial community in tundra soils was more sensitive, and imposed larger scales of changes in the abundances of responding species as well as functional genes in comparison with those from the temperate prairie. (Rustad, Campbell et al. 2001) et al reported in a meta-analysis that plant productivity had a larger positive response to warming in cooler ecosystems, but soil respiration and net nitrogen mineralization in tundra and grasslands showed no significant difference in the magnitude of response to warming. Yet (Beier, Emmett et al. 2008) concluded that in short term, the aboveground processes were more sensitive to warming than belowground processes by observing European shrublands with a temperature gradient. Our study observed larger positive responses of both plant productivity and soil microbial functional genes. We could capture the rapid response of belowground community composition to warming potentially because the high sensitivity of microarray to targeted sequences (Zhou, He et al. 2015), as by amplicon or shotgun sequencing, warming influence was not reflected on the entire detected community. This consequently implies that northern permafrost region might be more vulnerable

and contributable to future climate conditions over some other ecosystems. Furthermore, since observations here were based on temperature manipulations of a similar level at the two sites, the warming influence on tundra ecosystem might be even larger compared with the prairie in real climate scenarios, for the predicted global temperature increase will be larger at northern latitudes (Hansen, Ruedy et al. 2010). Multiple mechanisms may explain the differences in the sensitivity and the magnitudes of microbial responses to warming in the two ecosystems. Different limiting environmental factors might exist for microbial growth and function at the two locations. The tundra site was featured with an annual average temperature below freezing point, even much lower than the optimal growth temperature for most psychrophiles (D'Amico, Collins et al. 2006), but with abundant soil organic materials and high nitrogen availability. Upon warming treatment, communities in the tundra likely directly responded to raised temperature, and covaried with other variables that closely related to temperature, such as moisture. Strong correlations between the community structure with soil and ecosystem respirations could resulted from either covariation of temperature with respiration rate, or direct increase in microbial biomass. In tundra soil, substantial portions of organic carbon and nitrogen pools remain inaccessible to microbial consumption (Schuur, Bockheim et al. 2008), thus no correlations were observed between them and the community structure. Oklahoma prairie, on the other hand, had comfortable temperatures for most microorganisms, temporally highly variable amount of moisture, but limited soil substrate, especially soil nitrogen, similar as reported for many grassland ecosystems (Vitousek and Howarth 1991, LeBauer and Treseder 2008). As major microbial substrates came from plant-

derived organic materials, the community structure varied with plant biomass, but not soil temperature, the increase of which did not significantly alter the plant biomass. During the first 1.5 years of operation, increased carbon sequestration (indicated by NEE) at the prairie site was consistent with the increase in cellulose fraction of the carbon pool. Whether the increase in soil substrate and available nutrient in response to warming will continue, and whether soil microbial communities will indirectly respond to the substrate change, are to be answered with future observations.

In summary, by the quantitative comparison of the magnitude of warming influence on soil microbial community composition and functional gene abundances in two different ecosystems, we reported more sensitive and stronger responses of the tundra communities at the early phase of the warming experiment. The difference in the limiting environmental factors at the tundra and prairie sites, and whether warming treatment altered these limitations for the microbial community, might be important mechanisms driving the observed difference in community succession in both ecosystems. Admittedly, whether the significant community shifts after only one and half years of warming at the tundra site would continue or acclimate in the long term remains elusive. However, given the rapid initial response and high sensitivity of the tundra soil communities to warming, and the huge amount of carbon storage suspected to be accessible to these microbes, the tundra ecosystem might be more contributable than other ecosystems to future climate condition and carbon cycle, such as the temperate prairie.

Chapter 5: Warming facilitates the interconnection of grassland soil microbial communities

5.1 Abstract

Soil microbial community is a critical component of terrestrial ecosystems, whose response to climate change could potentially alter the global carbon balance. Although intensive reports have shown that warming can influence the soil microbial community composition and structure, little is clear about how the microbial interactions among themselves would be influenced. Here, soil microbial co-occurrence networks were constructed using 16S rRNA gene amplicon sequences extracted from monthly samples collected in a long-term field warming experiment on a Central Oklahoma grassland. We observed substantially larger and more connected networks for warmed communities compared with control, despite huge variation in network structures along season. The increase in network complexity under warming was concurrent to decreased phylogenetic diversity, reflecting environmental filtering and increased functional association in altered soil and vegetation conditions. A portion of identified keystone taxa, which play important roles in network topology, reoccur in different networks, representing a preserved prominent group in grassland soils across the season and under warming. The structure of microbial networks introduced a dimension beyond species abundance, which revealed more complicated responses of microbial communities to climate warming.

5.2 Introduction

The global temperature increases and warming related climate changes have become not only a scientific, but also political and economic concern globally (Pachauri et al 2014). A huge amount of carbon, an order of magnitude larger than released by human society, is cycled among the land, ocean, and atmosphere, where the even larger amount of carbon is stored (Stocker 2014). The disturbance from the changing climate could lead to changes in carbon cycles, either releasing more carbon into the atmosphere and create a positive feedback, or sequestrate more carbon into land and ocean to mitigate greenhouse effect (Hansen et al 2013, Kirschbaum 2000, Luo 2007, Soden and Held 2006). The scenarios of carbon sequestration depend on the responses and interactions of ecosystem components to climate change. Soil microbial communities were found to be critical mediators in terrestrial carbon cycles in different terrestrial ecosystems (Bardgett et al 2008, Davidson and Janssens 2006). On the one hand, soil microbes perform major activities of organic matter decomposition; on the other hand, they also transform organic materials into soil nutrients need by the plant to fix carbon, and involve in carbon mineralization processes. Understanding how soil microbial communities perform under diverse types of disturbance related to climate change is a critical component of climate change biology.

Rich literatures have reported and discussed the compositional, structural and functional change of soil microbial communities in response to warming (Bradford 2013, Deng et al 2015, Hartley et al 2007, Jassey et al 2013, Nie et al 2013, Pailler et al 2014, Peltoniemi et al 2015, Rousk et al 2013, Semenova et al 2015, Streit et al 2014, Tucker et al 2013, Wang et al 2014, Yoshitake et al 2015, Zhang et al 2013, Zhang et al 2005,

Ziegler et al 2013). The responses depend on ecosystem and climate regime under study, and the interaction of warming with a wide range of other factors (Castro et al 2010, Cavaleri et al 2015, Docherty et al 2012, Walter et al 2013), such as precipitation (Liu et al 2016, Zhang et al 2013), moisture (A'Bear et al 2014, Rousk et al 2013), nutrition level (Hines et al 2014, Melle et al 2015), and the intensity of disturbances like clipping or grazing (Crowther et al 2015, Steven et al 2015, Walter et al 2013, Zhang et al 2005). Furthermore, seasonality is one of the most common characteristics of terrestrial ecosystems, and is often related to dramatic variations in the soil environment, including temperature, moisture, and the life cycles of vegetation. Studies found that warming could influence plant and animal phenology, such as flowering time, migration, etc., by altering the patterns of seasonal environmental changes (Hughes 2000, Körner and Basler 2010, Sherry et al 2007). Microbial communities were also found subject to great seasonal variation (Contosta et al 2015, Dumbrell et al 2011, Edwards and Jefferies 2013, Gilbert et al 2012, Giovannoni and Vergin 2012, Gou et al 2015, Kuffner et al 2012, Lara et al 2011, Mironova et al 2012, Schadt et al 2003, Slaughter et al 2015, Takahashi and Hada 2012, Yu et al 2016), and likely influenced by warming through altered seasonality of the environmental factors (Baer et al 2014, Baldrian et al 2013, Jassey et al 2011, Lv et al 2014, Puissant et al 2015). These studies provided valuable information on how warming may influence soil microbial community's diversity, composition, and dynamics by altering the seasonality of terrestrial ecosystems. However, little is known about how the interactions among different microbial species and populations change in response to warming and across seasons.

In the environment, microorganisms exist in constant interactions with each other, only through which they can survive and perform ecosystem functions critical to the entire biosphere (Bassler and Losick 2006, Fuhrman 2009, Hallam and McCutcheon 2015, Keller and Surette 2006, Konopka 2009). In recent years, the analysis of complex microbial communities realized by high-throughput meta omics technologies has gone beyond the richness, abundance, and composition of the community assemblage. Network analysis has become a computational tool to infer the massive potential interactions among microbial species from abundance observations, skipping the seemingly impossible task to directly search for interacting microbial species from a vast pool of possibilities. Studies of microbial networks from human microbiome (Duran-Pinedo et al 2011, Faust et al 2012), soil (Barberan et al 2012, Lupatini et al 2014, Zhou et al 2010, Zhou et al 2011), rhizobiome (Shi et al 2016), groundwater (Deng et al 2016) and ocean (Gilbert et al 2012, Lima-Mendez et al 2015, Steele et al 2011) revealed that the microbial communities are highly organized and interactive in responding to environmental perturbation and performing ecological functions. The depiction of their interactions or niche sharing patterns greatly promoted our understanding of microbial community assemblage.

To characterize the soil microbial interactome in different seasons, and reveal how warming could influence these interactions, we built microbial co-occurrence networks based on 16S rRNA genes amplicon sequences from soil samples collected monthly in a long-term grassland warming experiment. Networks were constructed using a random matrix theory (RMT)-based network inference approach (Deng et al 2012) for different seasons under both control and warming. These networks were then analyzed and

compared to address the following questions: (1) Are soil microbial networks differ along the season alternation? (2) Does warming have an impact on the network structure? (3) Are there potential keystone taxa that are particularly important in network topology? If yes, do they change along the season or by warming? (4) How do the environmental conditions relate to the network structure? Our results captured the change of microbial network complexity along the season, and discovered that warming facilitate the interconnection of microbial communities in grassland soils.

5.3 Materials and Methods

5.3.1 Study site and experimental design

As described previously (Li et al 2013, Xu et al 2013, Xu et al 2016), the field experiment (ca. 34º59'N, 97º31'W) is part of the Kessler Atmospheric and Ecological Field Station (KAEFS), located in central Oklahoma on a tall grass prairie with grazing excluded for decades. Local mean annual temperature from 1948 to 2012 was 16.3 ºC, with monthly means ranging from 3.5 ºC in January to 28.1 ºC in July. Annual precipitation was 895 mm, with monthly totals 33 mm in January to 126 mm in May (Oklahoma Climatological Survey). The soil is 51% sand, 35% silt, and 13% clay with a water holding capacity of 37%. The site has two peaks of plant biomass, usually in late April/early May and late August/early September. Spring dominant species are C_3 grass *Bromus arvensis*, and C_3 forbs *Solanum dimidiatum*, *Croton glandulosus*, and *Vicia sativa*. Summer dominant species are and C_4 grasses *Tridens flavus* and *Sorghum halepense*. From July 2009, the temperature of experimental plots was manipulated to simulate climate warming. Each of the four biological replicate blocks contained a pair of 2.5 × 1.75 m plots, one for experimental warming and the other was complementary

control. Two infrared heaters (165 × 9 × 15 cm; Kalglo Electronics, Bethlehem, PA, USA) were installed at about 1.5 m above the warmed plots to achieve whole ecosystem warming, each working for an area of 2.5 m × 1.75 m. In control plots, two wood bars of the same dimensions were installed as "dummy" heaters to mimic the shading effect.

5.3.2 Field measurements, soil sampling and physical-chemical analysis

Soil Temperatures at 7.5cm were recorded every 15 min by thermocouples (T-type; Campbell Science Inst., Logan, UT, USA) installed at the center of each plot. Soil volumetric water contents (VWC) for 0-15 cm were measured every 30 min by TDR meters (ESI Environmental Sensors Inc., Sidney, BC, Canada) installed in each plot. All data were stored and transferred using the CR10X data loggers (Campbell Scientific). In correspondence to the monthly soil sampling, both monthly averages of temperatures and the three-day averaged temperatures before sampling time were calculated. Soil respiration and heterotrophic respiration were measured monthly between 10:00 and 15:00 local time using a LI-8100 Portable Soil CO_2 Fluxes System (LI-COR. Inc., Lincoln, NE, USA) attached to either a shallow (5 cm) or a deep (70 cm) PVC collar (80 cm^2 in area) chamber installed in each plot (Li et al 2013). The CO_2 flux from the shallow collar represents soil respiration from both plant root and soil microorganism, and that from the deep collar only consists of heterotrophic respiration due to root exclusion. Ecosystem carbon exchange (Xu et al 2013) was measured monthly between 10:00 and 15:00 local time on sunny days using an LI-6400 (LI-COR) Portable Photosynthesis System attached to a transparent chamber (0.5 m × 0.5 m × 0.7 m, with fans circulating the air inside). The chamber was placed and sealed on a metal frame in the plot, and covered all the vegetation inside the frame. Carbon flux measured with the

chamber exposed to sunlight was used to calculate NEE and that when the chamber was completely covered with a light-prove cover was estimated as ecosystem respiration (R_{eco}). The difference between NEE and R_{eco} was considered instantaneous gross primary productivity (GPP) of the covered vegetation. Peak aboveground plant biomass was estimated based on a point-frame method coupled with direct biomass collection in clipped plots (Luo et al 2009). The point-frame method was used to survey each plant species and litter coverage at both clipped and unclipped plots. Afterward, the aboveground biomass in clipped plots was collected, completely dried at 65 ºC and weighed. The regression relationship developed between point-frame hits and weighed biomass in clipped plots was then applied to unclipped plots for biomass estimation. Every month in 2012, one surface (0-15cm) soil sample core (2.5 cm diameter) was taken from each of the eight warmed and control plots for soil physical-chemical and microbial analysis. Samples were put on ice and transferred to -80 ºC freezers within 3 hours until process. Visible roots were picked out from soil samples before processing. Soil gravimetric water content (GWC) was estimated by drying about 10 g of soil at 65 ºC until constant weight, and calculate the percentage of water weight in wet soil weight. Soil pH was estimated by measuring the pH of a 1:5 soil-to-water mass ratio (dried soil equivalent weight) mixture using an Accumet Excel XL15 pH Meter (Fisher Scientific) with a combined calibrated electrode. The oven-dried soil was ground and analyzed for soil total carbon, total nitrogen, ammonia NH_4^+ and nitrate NO_3^- concentration in the Soil, Water and Forage Analytical Laboratory at Oklahoma State University. For determining soil total carbon and nitrogen, samples were treated with 1 N HCl for 24 hours to remove soil inorganic carbon (carbonates), and applied to a dry

combustion carbon and nitrogen analyzer (LECO, St. Joesph, MI, USA). For soil NH_4^+ and NO_3^-, samples were kept shaking with 1 M KCl for 30 min, filtered through a Fisher P4 qualitative filter (Fisher Scientific) and applied on a Lachat 8000 flow-injection analyzer (Lachat, Milwaukee, WI, USA).

5.3.3 Microbial community analysis

Soil total DNA was obtained using a freeze-grinding method followed by the SDS-based lysis and phenol-chloroform extraction (Zhou et al 1996), and purified through the columns provided in the MoBio PowerSoil DNA isolation kit (MoBio Laboratories, Carlsbad, CA, USA). The quality and purity of DNA were controlled by measuring the spectrometry absorbance at wavelengths of 230 nm, 260 nm and 280 nm using a NanoDrop ND-1000 Spectrophotometer (NanoDrop Technologies Inc., now NanoDrop Products by Thermo Fisher Scientific), and ensuring that A260/280 ≈1.8, and A260/230 ≥ 1.7. The quantity of DNA was analyzed with the PicoGreen using an FLUOstar OPTIMA fluorescence plate reader (BMG LabTech, Jena, Germany).

To determine the microbial taxonomic composition, 16S rRNA gene amplicon library was prepared and sequenced on an Illumina MiSeq platform in 2 × 250 bp pair-end format (Wu et al 2015). DNAs were PCR amplified for the V4 region of 16S rRNA genes using the Illumina adapted primer set 515F and 806R according to a previous protocol (Caporaso et al 2011). One hundred ng of amplicons from each sample were combined, run on 1 % agarose gel at 100V for 45 min, collected and purified through the QIAquick Gel Extraction Kit (Qiagen) column. The purified amplicons were further quantified with triplicates through PicoGreen and diluted to 2 nM, and used to prepare

the sequencing library following the protocol provided by Illumina. The library was then sequenced on an Illumina MiSeq.

An in-house data processing pipeline on the Galaxy platform was used to pre-treat the 16S rRNA sequences. More than 8 million raw sequences were retrieved by matching the sample barcode with zero error base. After using Btrim (Kong 2011) to remove low quality and short sequences, more than 6 million sequences were combined from forward and reverse reads through FLASH (Magoč and Salzberg 2011). Then, all combined sequences containing ambiguous base N, or were out of the length range of 247 to 258 bases were removed. Uchime (Edgar et al 2011) was used to detect and remove chimera. Then, Uclast (Edgar 2010) was used to generate the OTU (operational taxonomic unit) table by tagging the sequences with a similarity of >97% to the same OTU. The OTU with only one sequence in all the samples (singletons) were removed from the downstream analysis. Finally, the OTU table was randomly subsampled so that the total sequence number in every sample was 17,297. 70,022 OTUs were left after subsampling. The representative sequence for each OTU was searched against the RDP classifier (Wang et al 2007) to give each OTU a taxonomic information. The cutoff of the phylogenetic assignment confidence level was set to 0.5. A phylogenetic tree was constructed to calculate the phylogenetic diversity of the community. All the 70,022 representative sequences, one for each detected OTU in the whole data set, were applied to PyNAST (Caporaso et al 2010) for alignment with reference to the GreenGene 16S database (DeSantis et al 2006). The 68,846 successfully aligned sequences were then used to build a phylogenetic tree using FastTree (Price et al 2010).

5.3.4 Molecular Ecological Network (MEN) analysis

Molecular ecological networks were constructed using the 16S rRNA sequences from the above samples using the methods and MENA pipeline described in (Deng et al 2012). First, two all-timepoint (AT) networks, one for control and one for warming treatment, were constructed, each using 48 samples from all replicates and time points. Only OTUs that were present in 29 or more (>60%) samples were included in each network construction to obtain robust data association estimations. Then, to study the dynamics of microbial interactions along time, eight separate-season (SS) networks were constructed, each containing 12 samples from 4 field replicates and 3 time points of each season. The 3 time points were combined to acquire enough sample for reliable data association calculations. Samples from different months were grouped as follows. Spring, summer, and fall referred to February to April, May to July, and August to October, respectively. Winter is represented by sampling time points of January, November, and December in the same calendar year (2012). For the SS networks, OTUs with >75% (9 samples) occurrence were used for construction.

Before network construction, the data association matrices were calculated based on Spearman's rank. An improved Random Matrix Theory (RMT)-based approach (Deng et al 2012) were applied to detect a range of acceptable data association strength cutoffs (similarity thresholds, S_t) for each network. S_t defines the minimum data association strength between two nodes in a network. For the ten data sets, different ranges of acceptable S_t's were detected. However, for network comparison purpose, the same cutoff was adopted for AT or SS networks. The cutoff value was determined as the midpoint value of the overlapped S_t ranges (**Table S 14**).

The network topological properties, module separation, key-stone taxa identification, and eigengene analysis were all performed according to Deng et al (2012) using the MENA (http://ieg2.ou.edu/MENA/) pipeline. Networks were visualized using Gephi 0.9.1 and Cytoscape 3.5.0. The nodes in each network were separated into modules using the Greedy modularity optimization algorithm (Newman 2006b). Modularity measures how connected the nodes are within a network. For each node, its within-module connectivity (Z_i) and among module connectivity (P_i) were calculated (Guimera and Nunes Amaral 2005), and based on which its topological role in the network was interpreted based on classification introduced in pollination networks (Olesen et al 2006). Nodes with P_i>0.62 and Z_i>2.5, highly connected to the entire network, were identified as network hubs; those with Pi>0.62 were connectors; those with Z_i>2.5, highly connected within modules, were assigned module hubs. Nodes with P_i<0.62 and Z_i<2.5 were peripherals that had moderate connectivity both within and among modules. Network hubs, module hubs, and connectors were identified as keystone species that played important roles in the network topological structure, and potentially also in the biological interactome.

For each of the modules containing ≥8 nodes, an eigengene was calculated based on methods introduced in Deng et al (2012) to summarize the species abundance information from this module as a centroid. Eigengenes from the same network were then clustered based on their distance matrix to reveal the organization or relationship of different modules. Furthermore, the correlation of each eigengene-environmental variable pair was calculated as Pearson's product-moment to reveal the potential links between the environment and each module.

5.3.5 Statistical analysis

To reveal the differences of environmental conditions, microbial communities and their network properties between treatments and among seasons, as well as to discover the links amongst the three aspects, the following analyses were performed. 1) Analysis of variance (ANOVA) was performed to test the difference of means between treatment, among months, and among the two combined for the following dependent variables: soil, plant, and ecosystem fluxes variables, microbial taxonomic and phylogenetic hill numbers, the distances of microbial communities to their centroids in the PCoA space, and the abundances of different microbial taxa. For temperature data, repeated measures ANOVA was used to control the variation caused by different observation time points. 2) A multivariate permutational procedure, the permutational multivariate analysis of variance (Adonis) (Anderson 2001) was used to test how different the entire microbial communities' composition was under different treatment and sampling time. Bray-Curtis distance (Bray and Curtis 1957) was used to calculate the distance matrix in this test. 3) Paired student t-tests were applied to test whether the network properties, as well as soil, plant, and ecosystem fluxes variables were significantly different in warmed and control conditions. 4) The test of multivariate homogeneity of groups variances (Anderson et al 2006) was used to calculate the distances of microbial samples to their group centroids based on treatment, sampling month, as well as sampling season. The difference of the average distances to group centroids indicates varied beta-diversity, or heterogeneity, of samples among groups. 5) Microbial community's taxonomic diversity was estimated as the hill number (Hill 1973), or the effective number of species, for q=1, based on species composition and abundance. This estimation was a

near approach to Shannon entropy. 6) Microbial community's phylogenetic diversity was also estimated as the hill number for q=1, but based on the phylogenetic tree constructed using the OTUs' representative sequences. 7) Hierarchical clustering was used to calculate the distances between any pairs of module eigengenes within a network. 8) Pearson correlation was used to compute the strengths and significance of links between module eigengenes and climate, soil, plant, and ecosystem fluxes variables. All the statistical analyses were performed using R version 3.4.0 (Team 2014) with packages vegan version 2.4-3 (Oksanen et al 2013), agricolae version 1.2-4 (De Mendiburu 2014), and ieggr version 2.2.

5.4 Results

5.4.1 The seasonality of and warming effect on ecosystem and soil microbial communities

The environmental conditions showed strong seasonal fluctuations and influences by warming treatment (**Figure 5.1**). Except for soil total nitrogen content, all other variables, including soil temperature, moisture, total carbon content, nitrate and ammonia nitrogen contents, pH, respiration fractions, and ecosystem carbon exchange fractions, all significantly differ ($p<0.05$) by sampling month. Warming increased soil temperature at 7.5cm constantly during the entire year by an average of 4.3 °C ($t_{11,\ paired}$ =19.03, $p<0.001$), and decreased soil moisture by 0.02 (20.7%, $t_{11,\ paired}$ =3.01, p=0.001) on average, though more obviously in winter and early spring, when there was little vegetation or litter cover. Warmed soils had greater nitrate on average (4.5 mg-N kg-soil^{-1}, 71.2%, $t_{11,\ paired}$ =2.82, p=0.017) than control, mostly contributed by their higher nitrate concentrations in the second half of year. Soil respiration peaked in spring and

was similar from warmed and control soils, resulted from the counteraction of increased heterotrophic respiration (0.43 μmol-C m^{-2} s^{-1}, 54.4%, $t_{11, paired}$ =3.19, p=0.009) and decreased autotrophic/root respiration (0.74 μmol-C m^{-2} s^{-1}, 33.4%, $t_{11, paired}$ =4.34, p=0.001) by warming. Although not significantly different throughout the entire year, ecosystem respiration and gross primary productivity were lower in warmed than control plots in March and September, the two months in which plant biomass peaked, due to the negative impact of warming on plant biomass (**Figure S 16**).

The soil prokaryotic community composition echoed the seasonal fluctuation of and warming effect on the environment, and was significantly different both between warming and control, and among sampling months (**Table 5.1**). Month as a main effect explained a substantial portion (16%) of community variance. The β-diversity, or heterogeneity within treatment, was higher for warmed communities (**Figure S 17**a, b). As for the relative abundance of microbial taxa, warming tends to increase Actinobacteria in April, Gemmatimonadetes in May, Euryarchaeota in Jun, and BCR1 in October. Warming decreased the relative abundance of a few taxa in February through April and September through December. More taxa (7 known taxa and unclassified bacteria in warming, 3 taxa in control) had significant ($p<0.05$) different relative abundance across time in warmed than control soils (**Figure S 18**). Warming and season had differential effects on the microbial taxonomic and phylogenetic diversities, indicated by the Hill numbers (**Figure 5.3** and **Table 5.2**). Taxonomically, the microbial communities were most diverse in fall, and least diverse in winter, but not significantly different between warming and control. On the contrary, the microbial

phylogenetic diversity only differed between treatments but not among seasons, with a lower diversity in warmed plots.

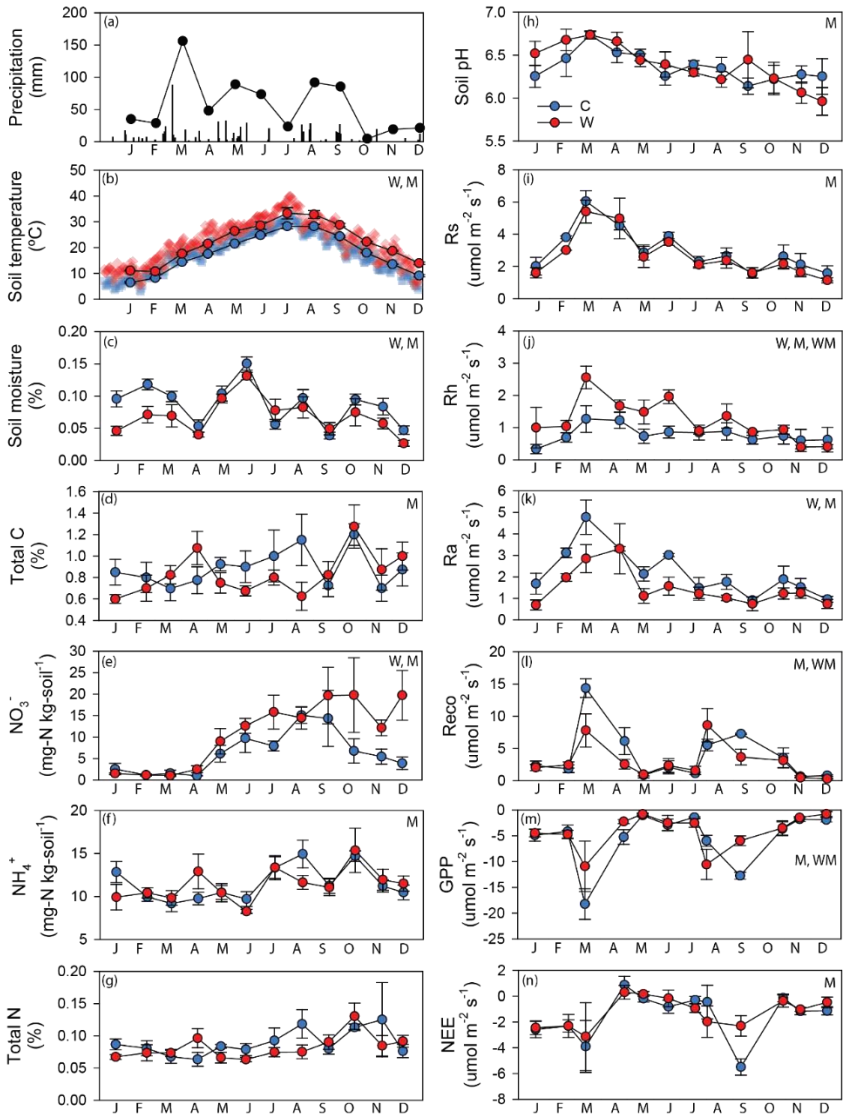

Figure 5.1 Environmental variables, soil physical-chemical properties, and ecosystem carbon fluxes. Dots represent accumulative precipitation in each calendar month in the year of soil sampling in (a), monthly averaged temperature in replicated plots in (b), and averaged values for measurements in replicated plots (n=4) in (c) through (n). Blue and red colors denote control and warming, respectively. In (b), daily average temperatures are marked with blue squares for control plots, and red diamonds for warmed plots. Error bars are standard errors. At the upper right corner for (b) through (n), W, M, or WM indicate that observations are significantly different by warming treatment, sampling month, or their interaction, respectively, tested using ANOVA. Total carbon, NO_3^-, NH_4^+, and total nitrogen refer to corresponding substrate concentrations measured from soil samples. R_s, R_h, and R_a denote soil total respiration, heterotrophic soil respiration majorly from microbes, and autotrophic soil respiration derived from plant roots. R_{eco}, ecosystem respiration that included both aboveground and belowground, plant and soil microbial respirations. GPP, gross primary productivity. NEE, net ecosystem exchange, the difference between GPP and R_{eco}. For GPP and NEE, negative values meant carbon gain for soil, and vice versa.

Table 5.1 Dissimilarities of microbial community compositions by warming treatment, sampling months, and their interaction, tested using Permutational Multivariate Analysis of Variance (Adonis) with Bray-Curtis distance.

	F	R^2	Pr(>F)
Warming	2.81	0.03	**0.001**
Month	1.54	0.16	**0.001**
Warming × Month	0.98	0.10	0.628

Table 5.2 ANOVA and LSD test results on community diversities based on the model: Hill number (taxonomic or phylogenetic) ~ Season*Treatment. Means and standard errors are shown. Significant differences between groups are indicated by different letters following the standard errors. The interaction of season and warming has no considerable influence on both taxonomic and phylogenetic hill numbers (p>0.05).

By season (n=24)						
	Spring	Summer	Fall	Winter	$F_{3,88}$	p
Tax.	2211±116 ^{ab}	2481±132 ^{ab}	2587±122 ^{a}	2124±95 ^{b}	3.486	**0.019**
Phyl.	10.59±0.19	10.73±0.22	11.04±0.19	10.44±0.24	1.583	0.199
By treatment (n=48)						
	Control		Warming		$F_{1,88}$	p
Tax.	2437±90		2265±81		2.138	0.147
Phyl.	10.98±0.14 ^{a}		10.43±0.15 ^{b}		7.276	**0.008**

5.4.2 Characteristics of networks

Eight separate season (SS), and two all-time point (AT) networks were constructed to explore the co-occurrence features of microbial members under warmed condition, and along seasonal environmental changes (**Figure 5.2**). The SS networks were constructed with S_t=0.8925. Network sizes (n) ranged from 392 to 575 in node numbers, and link numbers ranged from 288 to 1067. The AT networks for control and warmed communities were built with S_t=0.6305, with 661 and 903 nodes, and 1717 and 4104 links, respectively. All networks were scale-free, as indicated by the good fit of the node degree distributions to power-law functions (R^2 from 0.880 to 0.968). They were also modular, as indicated by high modularity (M). By retaining the numbers of nodes

and links in each network, the randomly rewired networks are significantly different from the corresponding empirical ones, indicating that the empirical networks are unlikely formed as such by chance. The empirical networks had much higher average clustering coefficients (*avgCC*), meaning they are highly clustered. The average path lengths (*GD*) and harmonic geodesic distances (*HD*) of empirical networks tended to be lower in control group, and higher in the warmed group, than random networks in SS networks. Modularity showed the opposite trend. In AT networks, all these four network properties were higher in empirical than random networks.

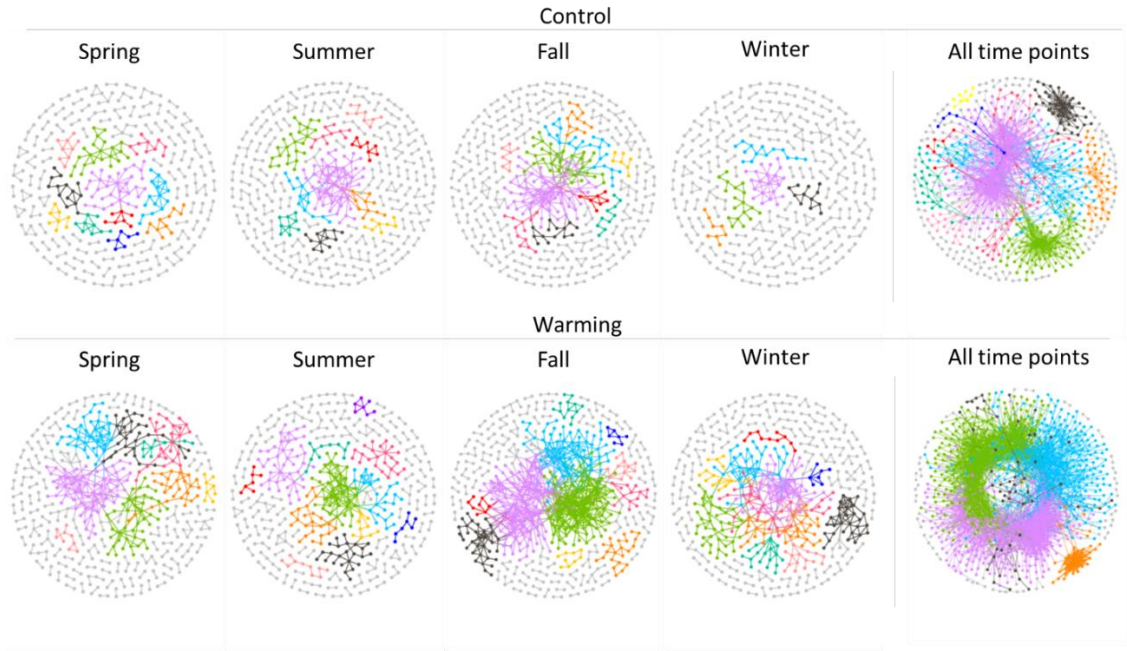

Figure 5.2 Co-occurrence networks for microbes in warmed and control soils from separate seasons and all-time points. Modules separated using Greedy algorithm are uniquely colored in each network for modules with >6 nodes, and in gray for modules with ≤6 nodes. Topological properties of each network are presented in **Table 5.3**.

Table 5.3 Topological properties of all the empirical networks, and the means and standard deviations of 100 random networks generated for each empirical network by keeping the number of nodes and links the same but rewiring the links. The majority rules of selecting OTUs for network construction are to include OTUs present in >75% (9) samples for separate seasons data sets, and those present in >60% (29) samples for combined-timepoints data sets. For separate seasons networks, their topological properties were compared between warming and control treatments. ↑ and ↓ following the network property names indicate the direction of value change under warming compared with control for separate season networks, and * and ** mark p values <0.1 and <0.05, respectively, by one-tailed paired T-tests. ↑ and ↓ after the numbers of properties for each network mean that those numbers are above or below the mean±standard deviation ranges, respectively, of corresponding random network properties.

Network Index	Separate season networks								All timepoints networks	
	Sp-C	Sm-C	Fl-C	Wt-C	Sp-W	Sm-W	Fl-W	Wt-W	C	W
No. of OTUs for construction	1501	1542	1680	1572	1463	1507	1339	1427	2070	1888
Similarity threshold (S_t)	0.8925	0.8925	0.8925	0.8925	0.8925	0.8925	0.8925	0.8925	0.6305	0.6305
Empirical Networks										
Network size (n) ↑**	392	458	479	396	497	473	575	501	661	903
No. of links ↑**	336	416	477	288	570	494	1067	600	1717	4104
No. of positive links/portion	310/92%	396/95%	414/87%	268/93%	519/91%	450/91%	945/89%	545/91%	1553/90%	3665/89%
No. of negative links/portion	26/8%	20/5%	63/13%	20/7%	51/9%	44/9%	122/11%	55/9%	164/10%	439/11%
R^2 of power-law	0.958	0.958	0.918	0.959	0.933	0.968	0.880	0.947	0.912	0.890
Average degree (*avgK*) ↑**	1.714	1.817	1.992	1.455	2.294	2.089	3.711	2.395	5.195	9.090
Average clustering coefficient (*avgCC*) ↑*	0.144 ↑	0.094 ↑	0.092 ↑	0.085 ↑	0.132 ↑	0.117 ↑	0.185 ↑	0.135 ↑	0.252 ↑	0.335 ↑
Average path (*GD*) ↑*	3.777 ↓	3.884 ↓	5.630	2.457 ↓	7.917 ↑	5.642	5.015 ↑	6.154 ↑	5.027 ↑	4.114 ↑
Harmonic distance (*HD*) ↑*	2.450 ↓	2.810 ↓	4.200 ↓	1.720 ↓	5.712 ↑	3.903 ↓	4.040 ↑	4.779	4.219 ↑	3.640 ↑
Modularity (*M*)/Modules ↓**	0.949/115 ↑	0.895/138 ↑	0.810/133 ↑	0.969/138 ↑	0.845/113 ↓	0.875/112 ↑	0.709/100 ↓	0.843/105 ↓	0.630/60 ↑	0.563/37 ↑
Random Networks										
Average clustering coefficient (*avgCC*)	0.003±0.002	0.003±0.002	0.004±0.002	0.002±0.002	0.005±0.003	0.005±0.003	0.017±0.003	0.005±0.003	0.039±0.004	0.052±0.003
Average path (*GD*)	8.268±0.767	6.178±0.280	5.676±0.204	5.784±1.124	5.686±0.115	5.753±0.161	4.145±0.044	5.452±0.114	3.649±0.033	3.254±0.016
Harmonic distance (*HD*)	6.263±0.476	5.162±0.186	4.879±0.139	3.780±0.674	4.993±0.084	4.971±0.108	3.770±0.033	4.809±0.077	3.351±0.023	3.011±0.011
Modularity (*M*)	0.895±0.008	0.855±0.007	0.809±0.008	0.951±0.007	0.748±0.007	0.794±0.007	0.523±0.005	0.728±0.006	0.403±0.004	0.272±0.003

5.4.3 Warming and season affected network topology

Despite the lower numbers of OTUs (9% for both SS and AT) selected for network construction, networks for warmed samples were always larger (*n* 19% more for SS, and 37% more for AT) compared with corresponding control. This indicated that the abundances of more species covaried in the warmed communities compared with control. In addition, compared with control, warming networks had 0.88 (50%) more links on average in SS networks, and 3.9 (75%) more links in AT networks. The higher average degree (*avgK*) in warming networks showed that the microbial communities there had a more complex structure of interconnections. Warming also led to networks with larger average clustering coefficient (37% for SS, 33% for AT), fewer modules (18% for SS, 38% for AT) and lower modularity (10% for both SS and AT), which together meant that species in warmed communities were more likely to form a few highly interconnected groups. For SS networks, the average path distance and harmonic geodesic distance were 57% and 65% higher under warming, but in all-timepoint networks, those values were 18% and 14% lower under warming, as the warming network formed much fewer but larger modules than control (**Figure 5.2** and **Figure 5.4**).

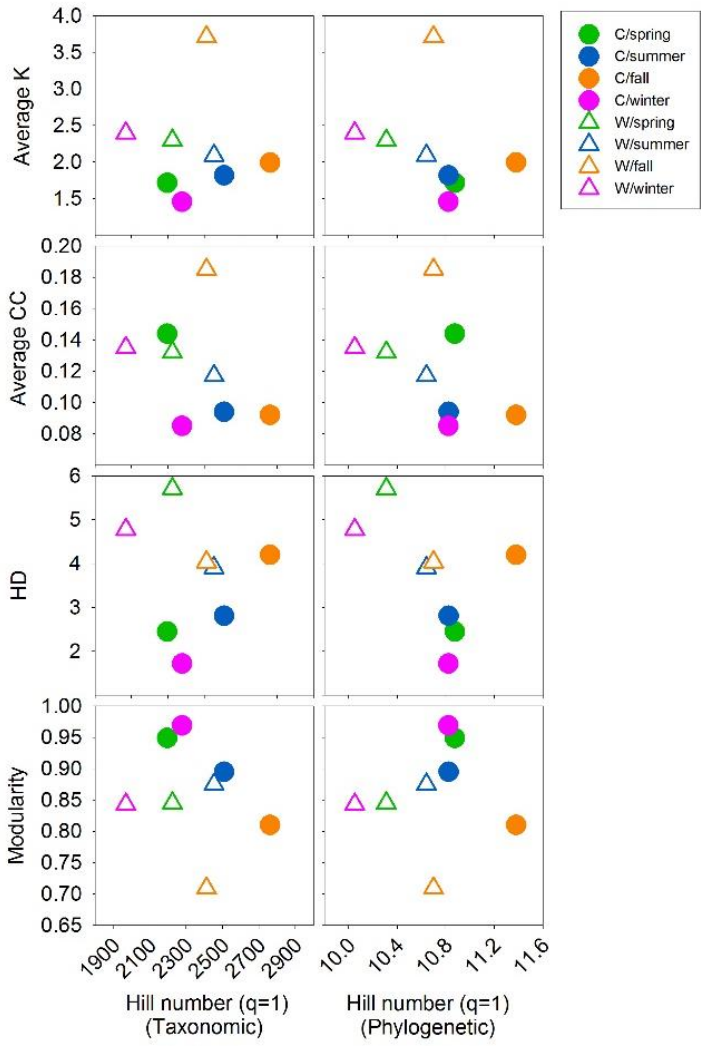

Figure 5.3 The properties of separate seasons networks plotted against the taxonomic or phylogenetic diversity, indicated by hill number of q=1. Average K, average node degree; Average CC, average clustering coefficient; HD, harmonic geodesic distance. Filled circles represent control, and open triangles denote warmed communities or networks. The differences of diversities among groups were tested by ANOVA as shown in Table 5.2. T-tests were performed to test the difference of means for network properties in

Season also affected both the size and complexity of the SS networks. Smaller and simpler networks were obtained from spring and winter communities, while the largest and most complex networks were for fall in both warmed and control plots. Notably, under warming, spring and winter networks reached comparable sizes and complexity with the fall network under control.

Warmed and control networks had distinguished relationships with the diversity of the microbial communities that they represented, as the two group clearly separated when their network properties were plotted against the community Hill numbers (**Figure 5.3**). Compared with control, warmed networks had a higher average degree, average clustering coefficient, harmonic geodesic distance, lower modularity, while the communities had lower taxonomic and phylogenetic diversities. The community diversity and network properties defined samples by treatments better than along the seasons.

5.4.4 Network modularity in microbial communities

To further identify the groups of species within which intensive interactions or strong covariations occurred, each network described above was separated into modules. The larger modules with more than 7 nodes were illustrated in **Figure 5.4**. Generally, species tended to co-occur rather than co-exclude, as positive links accounted for 87-92% of all links in these networks (**Figure 5.4**). Similar to the overall network structure (**Figure 5.2**), warming networks had larger modules, and formed more links both inside and among modules. Fall networks module structures were also more complicated than other seasons.

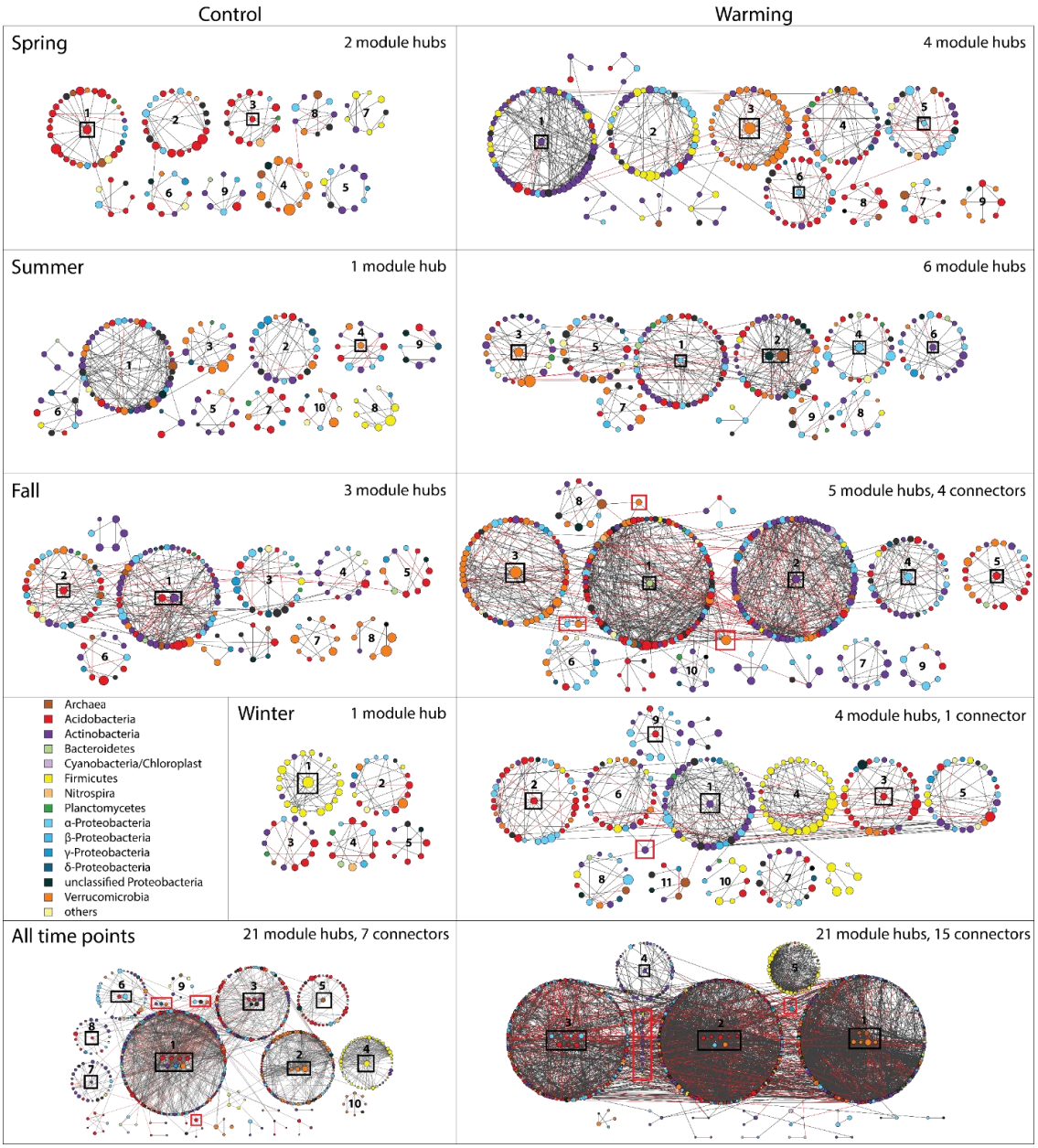

Figure 5.4 Network modules separated using Greedy algorithm. In each network, modules with ≥8 nodes are represented by circularly arranged nodes. Small modules with <8 nodes are only shown if they are linked to larger modules. Nodes within a module are highly connected, and those between modules are less linked. Nodes are colored based on their taxa, and their sizes are proportional to log-transformed abundance (scales different for separate-season and all-timepoint networks). Module hubs are moved to the center of modules and in black lined boxes. Module connectors are boxed in red. Positive links are in black and negative links are in red. The IDs of modules in each network are assigned based on module sizes.

The membership of modules had an obvious phylogenetic signature, as seen in the dominance of taxa in many major modules (**Figure 5.4**). The taxonomy of members in major modules changed over time, and differed between treatment. For example, in spring, Acidobacteria dominated the largest three modules (modules 1, 2, and 3) in control network, but Actinobacteria, and Verrucomicrobia dominated the largest and third largest modules (modules 1 and 3) in the warming network, while Acidobacteria only occurred more in smaller modules (modules 6 and 8). In summer, there was less dominance of any taxa. Interestingly, Firmicutes tended to occur and form large modules only in winter. They occurred or form small modules in spring control (module 7), spring warming (module 1 and 2), and summer control (module 8) networks, and nearly disappeared in summer warming and fall networks. The AT networks preserved such phenomenon and both consisted of one Firmicutes-dominant module (module 4 and 5 in control and warming networks, respectively). Generally, Actinobacteria, Acidobacteria and Verrucomicrobia tended to dominate large modules, while Proteobacteria only sparsely occurred in different modules, although they were the most abundant phylum in every month (**Figure S 18**).

5.4.5 Module hubs and connectors as keystone taxa

Based on the criteria described before, all the nodes were categorized based on the within module connectivity (Z_i) and among module connectivity (P_i) into one of the four network topological roles: peripheral, module hub, connector, and network hub (**Figure 5.4**, **Figure S 19** and **Table S 15**). No network hubs were present in any of our networks. The connectors were only present in relatively complex fall-warming, winter-warming and AT networks, and there are more connectors in fall (4 connectors) than in

winter (1 connector), and in AT-warming (5 connectors) than in AT-control (7 connectors) networks. SS warming networks always have more module hubs than control. Along season, fall networks had the most module hubs and connectors (**Figure 5.4**). The number of connectors and module hubs was consistent with the complexity of networks.

In most cases but not always, the module hubs are from the relatively abundant phylum/phyla in the modules (**Figure 5.4** and **Table S 15**). For example, module 3 and 5 in spring-warming had Verrucomicrobia and Proteobacteria as their hubs, respectively. However, some modules hubs were low-abundance or non-dominant species, such as the Bacteroidetes hub in module 1 of the fall-warming network, and the archaea hub in module 2 of the summer-warming network. In the AT warming network, the largest module 1 had mixed member phylogenetic profiles, but all its six modules were from Verrucomicrobia or Archaea. As for connectors, Verrucomicrobia and Actinobacteria were the most important for fall-warming and AT warming networks, respectively (**Figure 5.4**). The relative abundance of module hubs ranged from 0.028-2.534%, spreading from low to high abundance in the community. Connector OTUs were with lower abundance, ranging from 0.011-0.686% (**Figure S 20**). Abundant taxa in the community (**Figure S 19**) also were more abundant in the taxonomic profile of the keystone taxa (**Figure S 18**). Notably, some OTUs occurred as keystone taxa in more than one networks (**Table S 15**). OTU_70085, belonging to the Spartobacteria class in the Verrucomicrobia phylum, were present in four networks, spring-warming, fall-warming, AT-control and AT-warming, as module hubs. OTU_90925, a GP1 species belonging to the phylum of Acidobacteria, and OTU_132165, from

Spartobacteria class of Verrucomicrobia phylum, were both module hubs in three networks. Additional 14 OTUs, 3 Acidobacteria, 3 Actinobacteria, 3 Proteobacteria, 3 Verrucomicrobia, 1 Firmicutes, and 1 Crenarchaeota, served as module hubs or connectors in two networks.

5.4.6 Links between module eigengenes and environmental conditions

To reveal the higher order organization of networks, each module was decomposed into a single representative abundance profile, the module eigengene, to compare with other modules in the network. The module eigengenes explained 61-82% variations in SS networks, and 25-62% variations in AT networks, of the module members abundance profiles (**Table S 16**). The hierarchical clustering of the eigengenes was used to represent the dissimilarities among modules in terms of their module members abundance profiles (**Figure 5.5** and **Figure S 21**). The ten modules sizing larger than 8 nodes in the AT-control network was clustered into two major groups. The AT-warming network had five distinct modules, with the Firmicute-dominant module (module 5) being the most different one (**Figure 5.5**). Most of the modules in SS network formed clusters (**Figure S 21**).

The eigengene abundance profiles were correlated to the environmental profile to reveal the relationship of the modules and the environmental variables (**Figure 5.5** and **Figure S 21**). Generally, modules in fall networks had more significant correlations with the soil, plant and ecosystem carbon flux variables, while winter and spring networks had less. The microbial substrate-related variables (nitrate, ammonia, total nitrogen and total carbon contents) were significantly correlated to at least one module in all the networks, and to several modules in more complex networks, e.g., fall-control, fall-warming, and

AT networks. In fall-control and fall-warming networks, different module clusters correlated to these substrate-related variables in different directions (positive for one cluster and negative for the other). In AT-warming network, correlations with these variables were all negative. For the AT networks, networks in control and warming had different correlation profiles. Control network modules correlated to GPP and NEE, but warming network modules correlated to soil temperature, heterotrophic respiration, and rainfall. However, they both had modules correlate to plant biomass and richness, and one module that was negatively correlated to the soil moisture. In SS networks, soil moisture was significantly correlated to one or more modules in all networks except for winter. Rainfall only correlated to fall network modules.

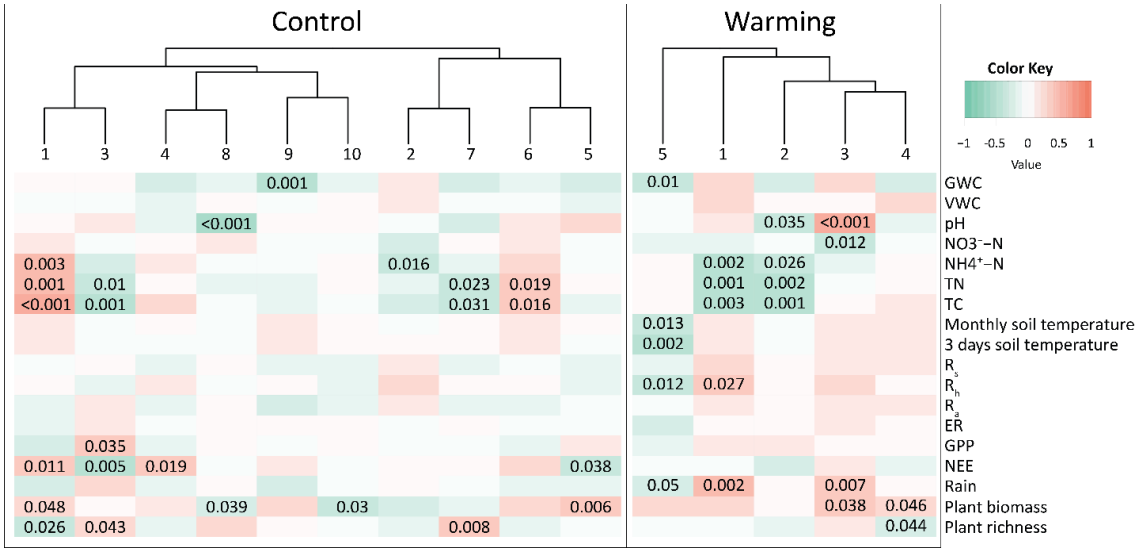

Figure 5.5 Module eigengenes' correlations with environmental variables for the control and warming networks containing all time points. An eigengene was calculated for each module to represent all nodes within each module. Clusters show the hierarchical clustering of eigengenes for modules numbered as in **Figure 5.3**. The Pearson correlation coefficient of each eigengene-environmental variable pair is indicated by the color key. Numbers on top of the heatmap listed p values of all significant ($p<0.05$) correlations. Variables were defined as in the legend of **Figure 5.1**.

5.5 Discussion

Interactions of microbial taxa in an ecosystem embody a dimension beyond species diversity and composition in our understanding of microbial community assemblage (Fuhrman 2009, Hallam and McCutcheon 2015). These interactions result in consequent covariation, co-existence or co-exclusion, of species abundances (Faust et al 2012). In this study, we revealed that networks representing such abundance covariations were much more complex when the soil system was exposed to long-term elevated temperature. In addition, although network structures succeeded along season, reaching the most complex state in fall and returning to the simplest in winter, warming facilitated the interconnection of microbial species in every season. We distinguished network modules that possibly formed through species interactions or similar responses to the fluctuation of environmental conditions, and identified potential keystone species that played important roles in network topological structures. These observed patterns gained us novel insights into the dynamics of soil microbial interactome along season alternation, and how climate warming may influence it.

Network size and complexity are meaningful topological properties in reflecting the interactome of microbial communities (Faust et al 2012, Proulx et al 2005). The larger and more complex networks under warming than in control could be due to the increase of both direct and indirect covariations. Covaried abundances of two species may be resulted directly from interaction, or indirectly through responses of both to a third factor, such as the environmental condition (Berry and Widder 2014, Faust et al 2012, Lima-Mendez et al 2015). Studies reported that changes in environmental parameters, such as pH (Barberan et al 2012) and factors influencing the substrate or food

availability (Foster et al 2012, Zhou et al 2011), can alter community assemblage and network structures. In our study, warming treatment not only increased soil temperature, but also caused a series of ecosystem level adjustments, such as decreased moisture, increased soil nitrate availability, decreased plant biomass and altered plant species composition. These warming related changes acted as an environmental filter, causing decreased alpha diversity of the soil microbial community, as also observed in other field warming experiments (Sheik et al 2011, Wang et al 2017). The selectively preferred species under warmed condition were either more adaptable to the altered physical-chemical environment, such as heat or drought, or were more efficient in performing functions related to warming-preferred ecosystem processes, such as the decomposition of C-rich substrates carbon substrates (Nie et al 2013, Xue et al 2016b). Accordingly, warming may promote both the functional associations, and the covariation of microbes to the soil environment. Whether such tightened interconnections would continue with time, and what influence would this changed network of the microbial community cast on the ecosystem functions remain yet to be answered.

The succession of network structure over time was more likely due to different mechanisms. This was reflected by that along season, higher microbial diversity generated larger and more complex networks. As from winter to fall, the environmental conditions became supportive to more species that were involved in versatile activities. In addition, because most plant species grow and senescent annually in our field site, the structure of networks observed in this study could be tangled with both rhizosphere's environmental filtering and niche sharing (Shi et al 2016), and plant litter

provided substrate amendment (Deng et al 2016, Zhou et al 2011). Notably, Deng et al (2016) described that after substrate enrichment in groundwater, the competition among microbes significantly increased the number of negative links in the network. We also observed the highest portion of negative links in fall networks, when the substrate was the most abundant. In control plots, where plant biomass was higher than warmed plots, the portion of negative links in the fall network was also higher. Therefore, the network structure change along season was more likely resulted from differed microbial activity, especially substrate availability associated with the aboveground vegetation.

In ecological networks, organisms form modules when there are intensive interactions among them but limited interactions to outsiders (Newman 2006a, Ravasz et al 2002). A module could be formed by members that are habiting similar niche, functionally associated, physically contacting, or phylogenetically close (Olesen et al 2007). Many modules in this study had a clear phylogenetic signature, reflecting common life history strategy, as also observed in a study on soil microbial communities in various ecosystems (Barberan et al 2012). This might either be due to their functional association, or the common physiological traits of the taxa. For example, Actinobacteria, a phylum containing known carbon degraders (Das et al 2007), dominated larger modules under warming than control, where the warmer temperature was more favorable to carbon decomposition activity as observed in a nearby field study (Nie et al 2013, Zhou et al 2012). In particular, it dominated large modules in fall, winter and spring under warming, while occurred only separated in modules in summer, coinciding the amount of litter or left-over litter amount in the field. Firmicutes, the well-known spore-former that stands harsh conditions (Filippidou et al 2016), nearly

disappeared in summer and fall, when conditions were favorable for most other taxa. It became abundant and form large modules in winter to occupy niches vacated by those who could not survive cold and drought. On the contrary, Proteobacteria, a phylum with versatile physiology and functions, although abundant in almost all networks, never dominated modules. Although the modules' phylogenetic profiles change over time and differ between treatments in this study, these profiles were more distinguishable from those reported in other biological systems, like microcosm rhizosphere (Shi et al 2016), groundwater (Deng et al 2016), and ocean (Lima-Mendez et al 2015), rendering unique types of microbe-microbe interactions in grassland soils.

Compared with control, the variation in module membership profiles was larger under warming. In other words, warming networks contained less comparable modules over time. For example, under control, spring, summer and winter all had Firmicutes-dominated modules, but under warming, this only occurred in winter, with one module partly dominated by Firmicutes in spring. Also, under warming, the phenomenon of one phylum dominating a module was more common than in control. This is consistent with the observation that warming increased the temporal beta-diversity of community assemblage, and might reflect previous reports (Hagerty et al 2014) that increased species turnover rate in response to warming. Whether the more complex network structures upon warming are related to this finding will need further hypothesis-driven examination.

Microbial species that are important in network topological structures are proposed also critical in community assemblage and ecosystem functioning (Berry and Widder 2014, Paine 1995). This study identified keystone species based on a node's connectivities

within or between modules, as introduced in pollination network models (Olesen et al 2006). Using the same identification criteria, one of the module hubs in rhizosphere microbial networks (Shi et al 2016) were found to be highly possible to have quorum sensing ability, which potentially drove the distribution of other microbes in that module. A nitrogen fixation gene, nifH, was assigned module hub, likely due to the importance of nitrogen fixation process in grassland soils under elevated CO_2 treatment (Zhou et al 2011). A sulfur reducing bacteria had the highest connectivity in the network representing Uranium-polluted groundwater microbial community assemblage immediately after substrate amendment, and with time, its role as a module hub diminished, reflecting the anaerobic oxidation activities (Deng et al 2016). In our observation, there were two types of module hubs. First, most of the module hubs were from the dominant, or relatively abundant phyla in all the module members. This could represent the tight relationship, similar responses to environmental changes, and/or the major functions that species of close phylogeny perform. Second, a few modules were highly connected by taxa rare to the module, such as the Bacteroidetes hub in the fall-warming network, and the archaea hubs in the summer-warming and AT-warming networks. Links from these module hubs to other nodes might reflect functional association and signaling. The Bacteroidetes node was a species from the class Sphingobacteria, which were known to produce sphingolipids, compounds important in signal transmission and cell recognition in plants, animals and fungi (Heung et al 2006). Species in the family Chitinophagaceae was also described to hydrolyze cellulose and degrade chitin (Rosenberg 2014), which might be an important process in the litter-rich fall season. Crenarchaeota consisted only small portion of sequences of the detected

16S genes, yet three OTUs belonging to this phylum were detected as four module hubs, three of which are in warming networks. The only Crenarchaeota module hub in SS networks was for summer-warming. Notably, all these Crenarchaeota OTUs belonged to the class Thermoprotei, known for resisting high temperature and also found in hot springs, thermo-vent, etc (Brochier-Armanet and Forterre 2006). These module hubs might be putative keystone taxa that influence the community structure and functions, from which further hypothesis could be developed about the type of interactions between them and other module members. While module hubs had relative abundances ranging from relatively low to high, connectors had lower abundances, and only occurred in the most complex networks in this study. In the fall-warming network, three of the four connectors were Verrucomicrobia, potentially indicated important roles and wide spread of this phylum in grassland soils (Fierer et al 2013). For AT-networks, connectors in control network had diverse classifications, while Actinobacteria accounted for most of the connectors in warming network. Since Actinobacteria also had higher relative abundance in warmed plots, this might imply selective growth of this group under warmed condition, or the higher potential for carbon degradation under warming. Unlike rhizosphere networks (Shi et al 2016), which had differed species but preserved taxa detected as module hubs or connectors, we observed many OTUs that occurred in more than one, and up to four networks as keystone species. Such consistency, in contrast with the variation in keystone taxa's identities in different networks, highlighted the preserved prominent members and their potential functionalities in grassland soil along season and upon warming.

In summary, this study revealed the co-occurrence patterns of grassland soil microbial communities along season alternation and the influence of experimental warming on the microbe-microbe interaction networks. The networks were most complex in fall, and least complex in winter. Warming facilitated the interconnection of microbial species, and generated larger and more connected networks. While the seasonal succession of network structure may result from substrate driven changes in community compositions, the increased network complexity while decreased phylogenetic diversity in response to warming reflected environmental filtering, and functional associations among selectively favored species under altered ecosystem and soil conditions. Keystone species identified as module hubs or connectors were either representative of module phylogenetic compositions, or potentially important in ecosystem functioning, and were more preserved compared to previous reports. This work provided an important contrast to the rich literature on the global change biology of soil microbial composition and structure, and demonstrated that the quantity, density, and potential type of microbial interactions could also be greatly altered by warming.

Chapter 6: Summary and output

This dissertation presented several lines of field evidence in supporting that the soil microbial community could be influenced by climate warming with changes in community composition and structure, functional potential, and the structures of the interactions among themselves. The responses of microbial communities to warming and permafrost thaw were closely related to soil environment and plant communities, and were often related to changes in the abundance of genes related to carbon and nutrient cycling. Different ecosystems exhibit distinct patterns of response, and soils in northern high-latitude tundra were more sensitive and vulnerable when the temperature was higher. Findings from this work could be valuable implements for earth system models in predicting the future climate condition and carbon cycling, and sources of formulating hypothesis towards the fundamental and mechanistic understanding of soil microbial community's ecosystem functions.

We first presented observations of microbial functional diversity across a natural gradient of degrading permafrost that was induced by regional climate warming. we found changed abundances of microbial functional genes related to carbon and nitrogen cycling, and increased community heterogeneity in tundra soils undergoing permafrost degradation in Alaska. These changes were likely related to both thaw-caused ground subsidence and plant community successions. This study provided critical information on the functional diversity of microbial communities in tundra soils in response to long-term permafrost thaw, illustrated the importance of plants in shaping soil microbial communities during the succession of tundra above thawing permafrost, and

demonstrated how thaw-induced tundra topological reform affects microbial functional potential and diversity.

Then, by comprehensive ecosystem and microbial analyses, findings from the CiPEHR experiment revealed rapid responses of the tundra soil microbial community to climate warming. This study also discovered several mechanisms by which the microbial community could feedback to warming: 1) warming stimulated not only aerobic respiration but also anaerobic decomposition; 2) nitrous oxide and CH_4 emissions from anaerobic processes are likely to further amplify positive carbon feedbacks to warming; and 3) warming greatly enhanced nutrient cycling processes such as nitrogen mineralization, nitrogen fixation and phosphorus utilization, which promotes observed increases in plant growth and potentially dampen the positive feedbacks. These results demonstrated the vulnerability of the northern permafrost ecosystem to climate warming and the importance of microbial feedbacks in mediating such vulnerability.

Third, we focused on the questioned of whether different ecosystems had similar or contrast responses to climate warming. By quantitatively comparing the magnitude of warming influence on soil microbial functional gene abundances in tundra and temperate prairie soils, we found stronger responses of the tundra communities with a larger magnitude of gene abundance change, and higher portions of disappeared or appeared species, compared with the temperate prairie at the early phase of the warming experiment. The difference in the limiting environmental factors for microbial growth and functions might be important mechanisms driving the observed difference in community succession in the two ecosystems. Activities of the microorganisms in the high-latitude tundra soils were limited by the cold temperature but not the substrate,

while the prairie soils were substrate limited. Warming of soil instantly alleviated the cold stress in the tundra, but did not affect substrate input the short-term. Analyses in Chapter 4 provided further evidence on the vulnerability and sensitivity of northern high-latitude tundra to climate warming, and implied that the tundra ecosystem might be more contributable than some other ecosystems, such as temperate prairie, to future climate condition and the carbon cycle.

Fourth, we explored warming effect on the microbial interaction network using time series samples from an Oklahoma prairie. By constructing microbial co-occurrence networks for different seasons under both warming and control, we discovered larger and more complex networks for warmed samples compared with control in every season. This result implied that warming facilitated microbial interactions. We also found phylogenetic signatures in module formation, and identified potential keystone species in microbial functions through network topological features. Although rich literature reported the warming effect on microbial diversity, composition, community structure, and functions, the increased interconnections of microorganisms by warming were first captured by the study conducted in Chapter 5, which revealed a previously undescribed dimension of microbial community assemblage under warming effect. How such change in the interaction of microbial species would affect the overall function of soil microbial community will need further research.

Although our understanding of the earth's climate, its future, its influence on and its interaction with life on earth is still vague and uncertain, the human being will never stop the journey of exploration. Being a small part of the huge effort of this exploration,

this dissertation offered unique and novel insights into our knowledge of how the tiny life in the soil can make big impacts in a warmer world.

Listed below are the individual manuscripts, published or in preparation, in relation to this dissertation. Chapter 2 and Chapter 3 in this dissertation presented contents in the published journal articles 1 and 2 below. The Publishers of the journals granted the author to re-use these published materials in this dissertation by copyright policies.

Peer reviewed journal papers published:

1. **Yuan, M.**, Zhang, J., Xue, K., Deng, J., Deng, Y., Wu, L., He, Z., Van Nostrand, D. J., Schuur, E., Luo, C., Konstantinidis, K., Cole, J., Tiedje, J., Luo, Y., and Zhou, J. Microbial functional diversity covaries with permafrost thaw-induced environmental heterogeneity in tundra soil. ***Global Change Biology***. In press
2. Xue, K.*, **Yuan, M.***, Shi, Z., Qin, Y., Deng, Y., Cheng, L., Wu, L., He, Z., Van Nostrand, J., Bracho, R., Natali, S., Schuur, E., Luo, C., Konstantinidis, K., Wang, Q., Cole, J., Tiedje, J., Luo, Y., and Zhou, J. (2016) Tundra soil carbon is vulnerable to rapid microbial decomposition under climate warming. ***Nature Climate Change***, 6: 595-600.
3. Xue, K.*, **Yuan, M.***, Xie, J., Li, D., Qin, Y., Hale, L., Wu, L., Deng, Y., He, Z., Van Nostrand, J., Luo, Y., Tiedje, J., and Zhou, J. (2016) Annual removal of aboveground plant biomass alters soil microbial responses to warming. ***mBio***, 00976-16

4. Cheng, L., Zhang, N., **Yuan, M.**, Xiao, J., Qin, Y., Deng, Y., Tu, Q., Xue, K., Van Nostrand, J., Wu, L., He, Z., Zhou, X., Leigh, M., Konstantinidis, K., Schuur, E., Luo, Y., Tiedje, J., and Zhou, J. Warming enhances old organic carbon decomposition through altering functional microbial communities. ***ISME Journal***. In press
5. Feng, W., Liang, J., Jung, C., Chen, J., Zhou, J., Hale, L., **Yuan, M.**, Wu, L., Bracho, R., Schuur, E., Luo, Y. Long-term warming intensifies stable soil carbon decomposition by enhancing potential microbial catabolic abilities in grassland. ***Global Change Biology***. In press
6. Johnston, E., Rodríguez-R, L., Luo, C., **Yuan, M.**, Wu, L., He, Z., Schuur, E., Luo, Y., Tiedje, J., Zhou, J., and Konstantinidis, K. (2016) Metagenomics reveals pervasive bacterial populations and reduced community diversity across the Alaska tundra ecosystem. ***Frontiers in Microbiology***, 183801.
7. Tu, Q., **Yuan, M.**, He, Z., Deng, Y., Xue, K., Wu, L., Hobbie, S., Reich, P., and Zhou, J. (2015) Fungal communities respond to long-term elevated CO2 by community reassembly. ***Applied Environmental Microbiology***, 81(7): 2445-2454.
8. Deng, J., Gu, Y., Zhang, J., Xue, K., Qin, Y., **Yuan, M.**, Yin, H., He, Z., Wu, L., Schuur, E., Tiedje, J., and Zhou, J. (2015) Shifts of tundra bacterial and archaeal communities along a permafrost thaw gradient in Alaska. ***Molecular Ecology***, 24: 222-234.
9. Wu, L., Wen, C., Qin, Y., Yin, H., Tu, Q., Van Nostrand, J., Yuan, T., **Yuan, M.**, Deng, Y., and Zhou. J. (2015) Phasing amplicon sequencing on Illumina Miseq for robust environmental microbial community analysis. ***BMC Microbiology***, 15: 125.

10. Luo, C., Rodriguez-R, L., Johnston, E., Wu, L., Cheng, L., Xue, K., Tu, Q., Deng, Y., He, Z., Shi, J., **Yuan, M.**, Sherry, R., Li, D., Luo, Y., Schuur, E., Chain, P., Tiedje, J., Zhou, J. and Konstantinidis, K. (2014), Soil microbial community responses to a decade of warming as revealed by comparative metagenomics. ***Applied Environmental Microbiology***, 80(5): 1777-1786.
11. Yang, Y., Wu, L., Lin, Q., **Yuan, M.**, Xu, D., Yu, H., Hu, Y., Duan, J., Li, X., He, Z., Xue, K., van Nostrand, J., Wang, S. and Zhou, J. (2013), Responses of the functional structure of soil microbial community to livestock grazing in the Tibetan alpine grassland. ***Global Change Biology***, 19: 637–648.
12. Li, Y., He, J., He, Z., Zhou, Y., **Yuan, M.**, Xu, X., Sun, F., Liu, C., Li, J., Xie, W., Deng, Y., Qin, Y., Van Nostrand, J., Xiao L, Wu L, Zhou J, Shi W, and Zhou X. (2014) Phylogenetic and functional gene structure shifts of the oral microbiomes in periodontitis patients. ***ISME Journal***. 8: 1879–1891.

Manuscripts in preparation:

13. Shi, Z., Lin, Y., Wilcox, K., Jiang, L., Jung, C., Xu, X., **Yuan, M.**, Guo, X., Zhou, J., and Luo, Y. Species composition regulates climate sensitivity of prairie primary productivity. ***Proceedings of the National Academy of Sciences***. In review
14. **Yuan, M.**, Shi, Z., Zhou, X., Li, J., Wu, L., He, Z., Van Nostrand, D. J., Schuur, E. A. G., Luo, C., Konstantinidis, K., Cole, J., Tiedje, J., Luo, Y. and Zhou, J. Warming facilitates the interconnection of grassland soil microbial communities. In preparation

15. **Yuan, M.**, Wang, C., Feng, J., Xue, K., Wu, L., He, Z., Van Nostrand, D. J., Schuur, E., Luo, C., Konstantinidis, K., Cole, J., Tiedje, J., Luo, Y., and Zhou, J. Differential microbial sensitivity to experimental warming: a comparative metagenomic analysis of soils from two ecosystems. In preparation
16. **Yuan, M.**, Shi, Z., Zhou, X., Li, J., Wu, L., He, Z., Van Nostrand, D. J., Schuur, E. A. G., Luo, C., Konstantinidis, K., Cole, J., Tiedje, J., Luo, Y. and Zhou, J. Seasonal variation of microbial community composition enlarged by experimental warming on a temperate grassland. In preparation
17. Guo, X. Feng, J., Shi, Z., Ning, D., Zhou, X., **Yuan, M.**, Tao, X., Hale, L., Qin, Y., Wu, L., He, Z., Van Nostrand, J., Liu, X., Luo, Y., Tiedje, J., and Zhou J. Climate warming leads to divergent succession of grassland microbial communities. In preparation
18. Gao, Y., Ding, J., Gu, B., **Yuan, M.**, Shi, Z., Chiariello, N, Niboyet, A., Le Roux, X., Docherty, K., Gutknecht, J, Hungate, B., Yuan, T., Gu, Y., Field, C., Zhou, J. and Yang, Y. The effects of long-term warming on soil microbial taxonomic and functional traits in a Mediterranean-type grassland. In preparation
19. Sun, X., Yang, Y., **Yuan, M.**, Yue, H., Ding, J., Shi, Z., Xue, K., Chiariello, N., Docherty, K., Gutknecht, J., Hungate, B., Field, F. and Zhou, J. A metagenomics study revealing microbial adaptation to elevated precipitation in a California annual grassland. In preparation
20. Escalas, A., **Yuan, M.**, Kuang, J., Liu, F., Feng, J., Paula, F., Wu, L., Zhang, Y., Yang, Y., and Zhou J. Functional rarity in soil microbes: occurrence and abundance

of patterns of functional genes reveals core and satellite functions across ecosystems. In preparation

21. Ma, X., Wang1, T., Shi, Z., Chiariello, N., Docherty, K., Field, C., Gutknecht, J., Gu, Y., Hungate, B., Le Roux, X., Niboyet, A., Xue, K., Yang, S., **Yuan, M.**, Yuan, T., Zhou, J. and Yang, Y. Changes in functional microbial communities in response to long-term nitrate amendment: implications for soil C and N accumulation. In preparation
22. Guo, X., Zhou, X., Hale, L., **Yuan, M.**, Ning, D., Shi, Zhou., Qin, Y., Liu, F., Wu, L., He, Z., Van Nostrand, J., Liu, X., Luo, Y., Schuur, E., Tiedje, J. and Zhou, J. Annual removal of aboveground plant biomass alters soil microbial successional dynamics. In preparation
23. Guo, X., Zhou, X., Hale, L., **Yuan, M.**, Ning, D., Feng, J., Shi, Z., Li, Z., Feng, B., Gao, Q., Wu, L., Zhou, A., Fu, Y., Wu, L., He, Z., Van Nostrand, J., Liu, X., Yang, Y., Luo, Y., Tiedje, J. and Zhou, J. Climate warming accelerates temporal scaling of grassland soil microbial biodiversity. In preparation
24. Guo, X., **Yuan, M.**, Gao, Q., Hale, L., Zhou, X., Ning, D., Feng, J., Shi, Z., Li, Z., Feng, B., Wu, L., Zhou, A., Fu, Y., Wu, L., He, Z., Van Nostrand, J., Liu, X., Yang, Y., Luo, Y., Tiedje, J. and Zhou, J. Drought-dependent warming effect on ecosystem carbon storage. In preparation

Appendix A: Supplementary Figures

Figure S 1 to **Figure S 8** for Chapter 2: Microbial functional diversity covaries with permafrost thaw-induced environmental heterogeneity in tundra soil

Figure S 9 to **Figure S 13** for Chapter 3: Rapid microbial feedbacks reveal vulnerability of tundra soil carbon to climate warming

Figure S 14 and **Figure S 15** for Chapter 4: Differential microbial sensitivity to experimental warming: a comparative metagenomic analysis of soils from two ecosystems

Figure S 16 to **Figure S 21** for Chapter 5: Warming facilitates the interconnection of grassland soil microbial communities

Depth	Mi	Mo	Ex	Grouping of means by depth
0-15cm				b
15-25cm				ab
25-35cm				a
35-45cm				ab
45-55cm				ab
55-65cm				ab
>65cm				b
Grouping of means by site	a	a	a	

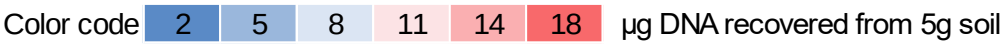

Figure S 1 DNA yield from 5g of soil along depth fractions in each site. The differences of means were tested using ANOVA followed by Fisher's LSD tests. P values were corrected based on Bonferroni methods for multiple comparisons.

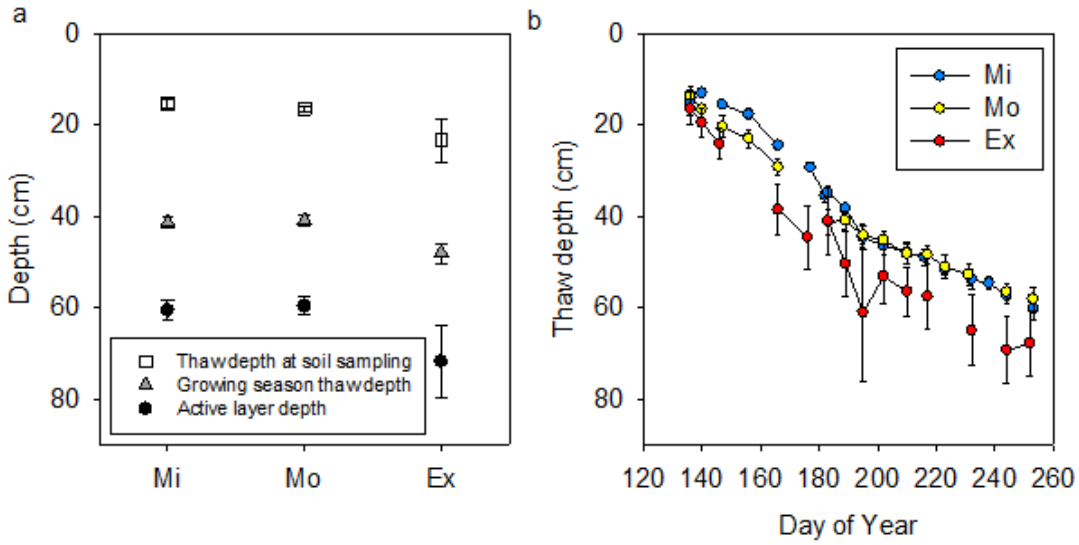

Figure S 2 (a) Thaw depth measured at sampling time, averaged during the growing season, and active layer depth in 2004. (b) Thaw depth along time in growing season. Thaw depth were determined at sampling time by measuring the unfrozen soil layer depth from the soil sample cores (n=6 for each site). Separately, thaw depth was also periodically measured during growing the season at 36 observation wells that were located differently than soil sampling cores (n=180, 161, and 146 for Mi, Mo, and Ex site, respectively, considering replicate observation wells and repeated measures on different days). The active layer depth at each observation well was estimated as the deepest thaw depth throughout the growing season (n=12 for each site). Error bar denotes standard error of the mean. Data reanalyzed from Schuur 2009.

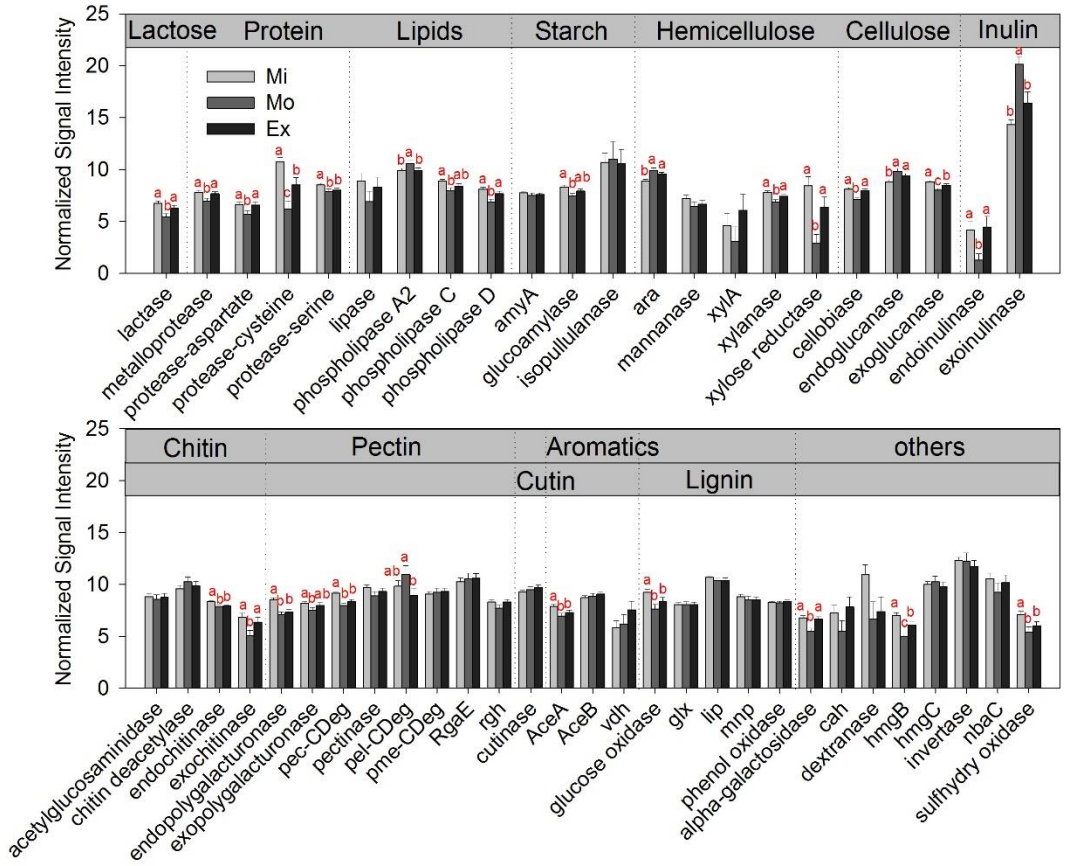

Figure S 3 Normalized relative abundance of detected fungal carbon degradation genes. The order of genes was organized based on the lability of their targeted carbon substrate. Significant differences of the means are marked by different letters.

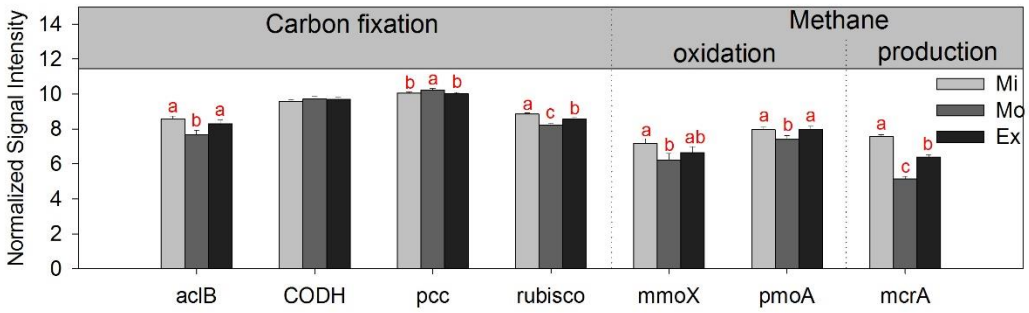

Figure S 4 Normalized relative abundance of detected carbon fixation and CH_4 genes. Significant differences of the means are marked by different letters.

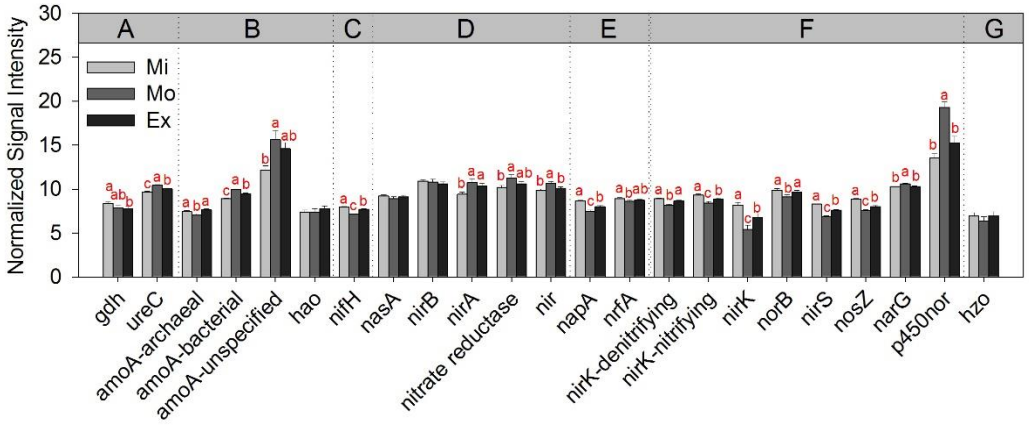

Figure S 5 Normalized relative abundance of detected nitrogen cycling genes. Significant differences of the means are marked by different letters. nitrogen cycling subcategories: A. ammonification; B. nitrification; C. nitrogen fixation; D. assimilatory nitrogen reduction; E. dissimilatory nitrogen reduction; F. denitrification; and G. anammox.

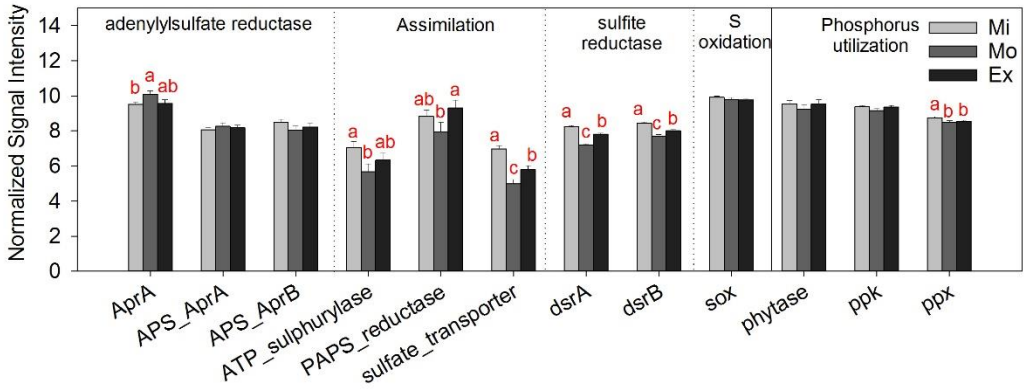

Figure S 6 Normalized relative abundance of sulfur and phosphorus cycling genes. Significant differences of the means are marked by different letters.

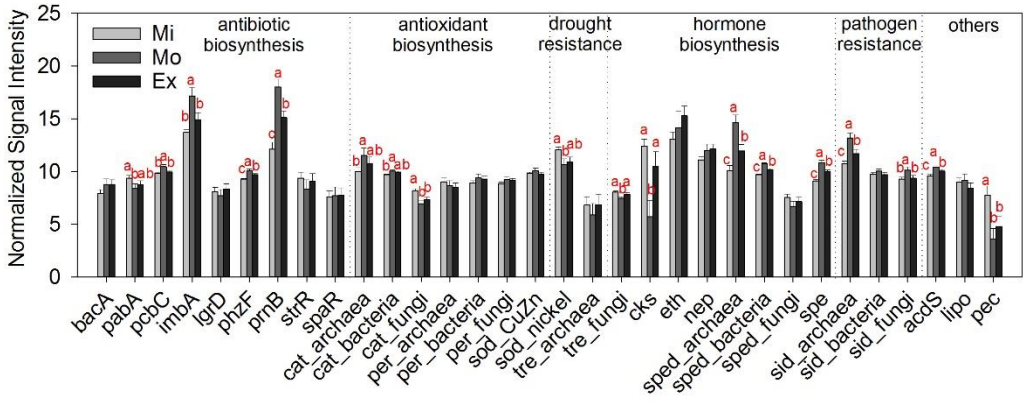

Figure S 7 Normalized relative abundance of plant benefit genes. Significant differences of the means are marked by different letters.

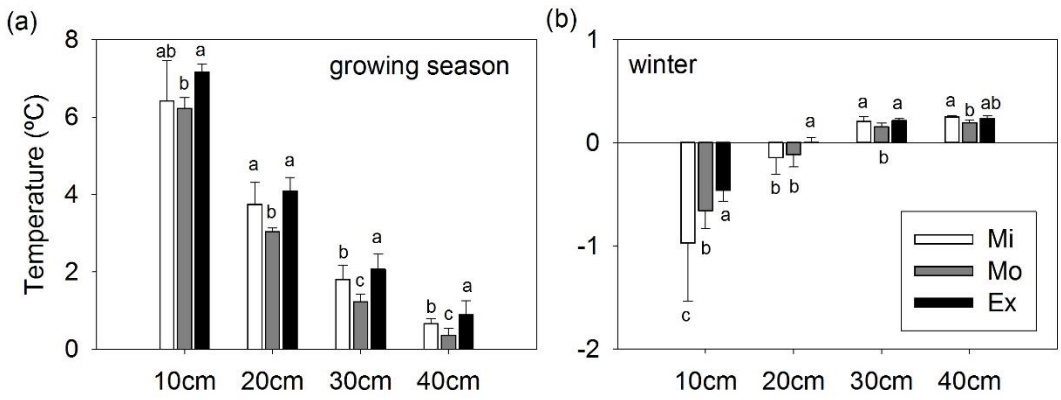

Figure S 8 Growing season (a) and winter (b) soil temperatures from four depths in the three sites. Error bars represent standard errors of the means from three replicated observation locations in each site. Different letters denote significantly difference of the means among sites, tested by one-way ANOVA considering multiple observation time points.

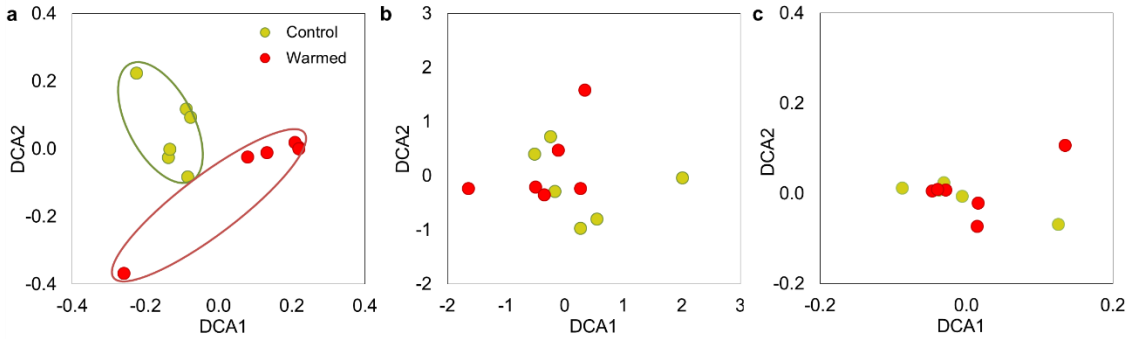

Figure S 9 Detrended correspondence analyses (DCA) for GeoChip hybridization (**a**), 16S rRNA amplicon sequences (b), and subsystems from shotgun metagenomic sequences (c). The microbial composition based on GeoChip hybridization separated clearly by treatment; while microbial composition based on 16S rRNA amplicon sequences and subsystems from shotgun metagenomic sequences did not.

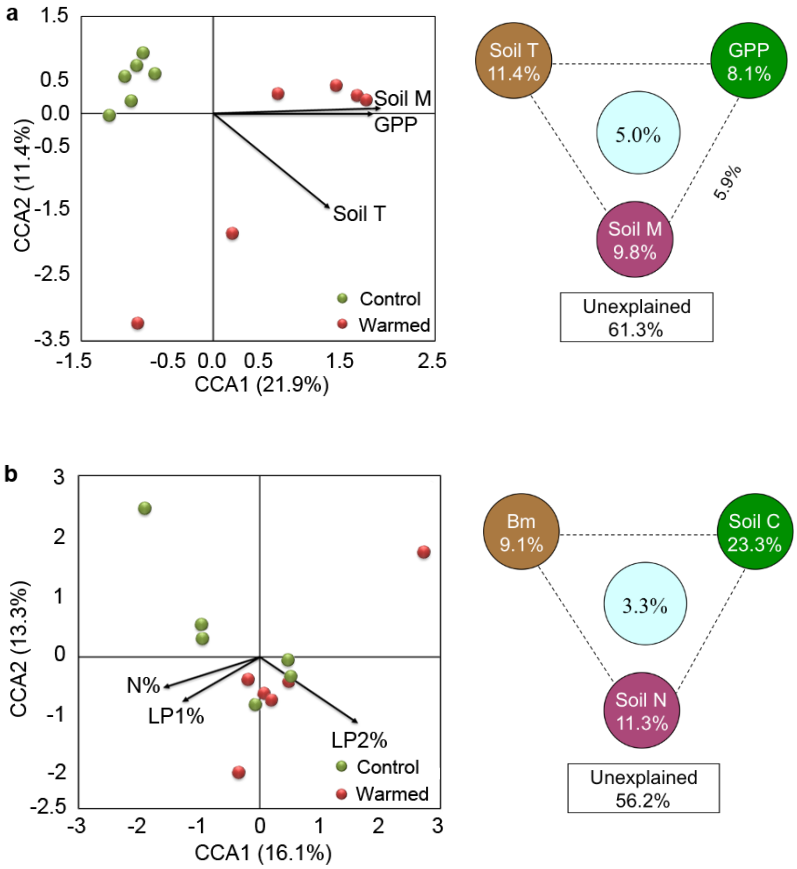

Figure S 10 Canonical correspondence analyses (CCA) based on GeoChip hybridization (a) and 16S rRNA amplicon sequences (b). The microbial composition based on GeoChip hybridization was significantly shaped by soil temperature (Soil T), soil moisture (Soil M) and gross primary productivity (GPP), which explained 38.7% of microbial composition variance. The microbial composition based on 16S rRNA amplicon sequences was significantly shaped by soil labile carbon pool 1 (LP1%), soil labile carbon pool 2 (LP2%) and soil nitrogen content (N%), which explained 43.8% of microbial composition variance.

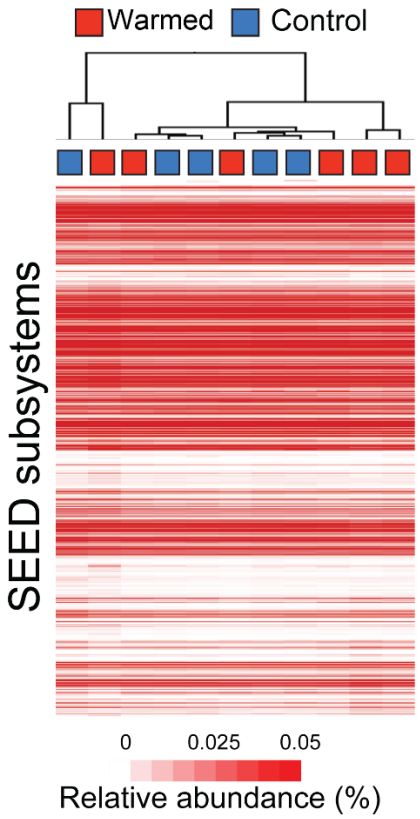

Figure S 11 The clustering of both warmed and control groups based on the normalized abundance of SEED subsystems in each sample. The trimmed reads were assigned to subsystems in the SEED database and the heatmap color-coded by subsystem relative abundance. Samples were clustered by hierarchical clustering based on Euclidean distances calculated from the SEED subsystem relative abundances.

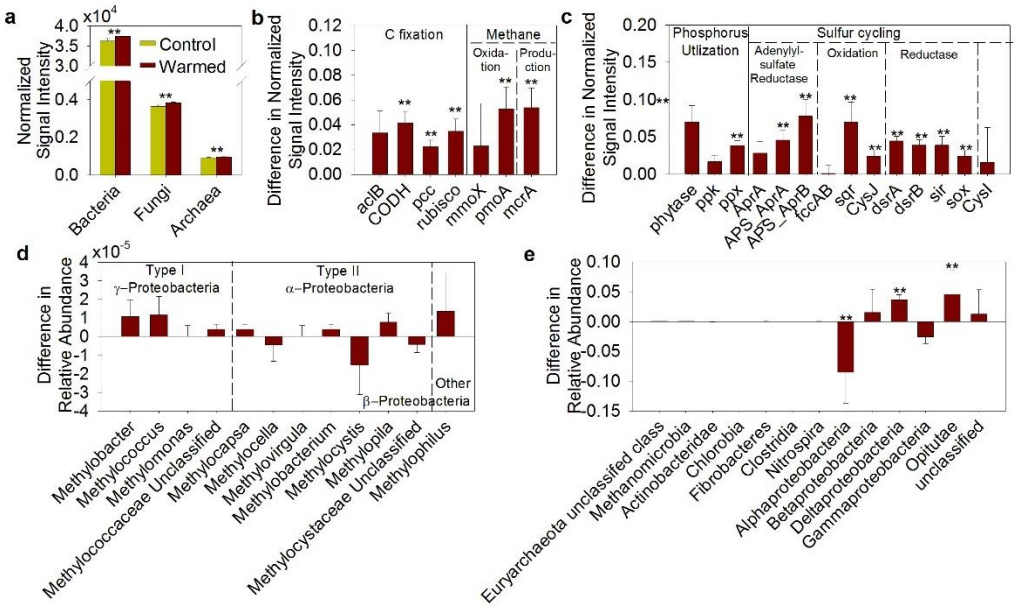

Figure S 12 Effects of warming on different components of the soil microbial communities as detected by GeoChip hybridization or amplicon sequencing. Significant differences between treatments is indicated by ** when $p<0.05$ (two-tailed paired t-test for a, and ANOVA for b-e). (a) Overall abundance of bacteria, fungi and archaea based on GeoChip hybridization. Abundance of functional genes from bacteria, fungi and archaea all tended to increase, though not significantly. (b) carbon fixation and CH_4 genes based on GeoChip hybridization. The abundances of CODH genes, *pcc*, rubisco genes (carbon fixation), *pmoA* (CH_4 oxidation), and *mcrA* (CH_4 production) were significantly stimulated by warming. (c) Phosphate and sulfur genes based on GeoChip hybridization. Warming significantly stimulated the gene encoding phytase and the *ppx* gene for phosphorus utilization, as well as *APS_AprA*, *APS_AprB*, *sqr*, *CysJ*, *dsrA*, *dsrB*, *sir* and *sox* genes in sulfur cycling. (d) Methanotrophs from 16S rRNA amplicon sequences. (e) N-fixing populations based on *nifH* amplicon sequences. Warming significantly stimulated the abundances of Deltaproteobacteria and Opitutae, but inhibited Alphaproteobacteria.

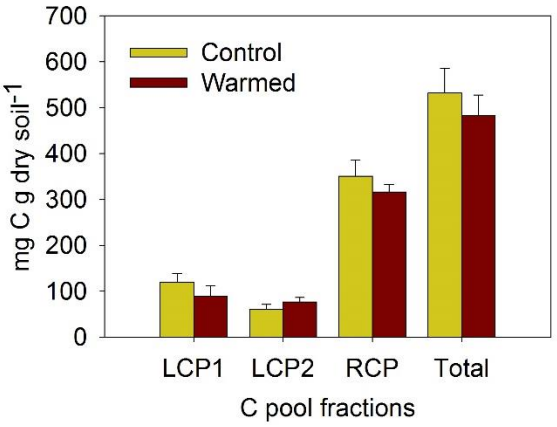

Figure S 13 Amount of carbon pool fractions, including labile carbon pool 1 (LCP1, mainly polysaccharides) and 2 (LCP2, mostly cellulose), and recalcitrant carbon pool (RCP), and total organic carbon pool sizes in control and warmed plots. None of the carbon pool fractions and total organic carbon pool significantly changed in response to warming by two-tailed t-test.

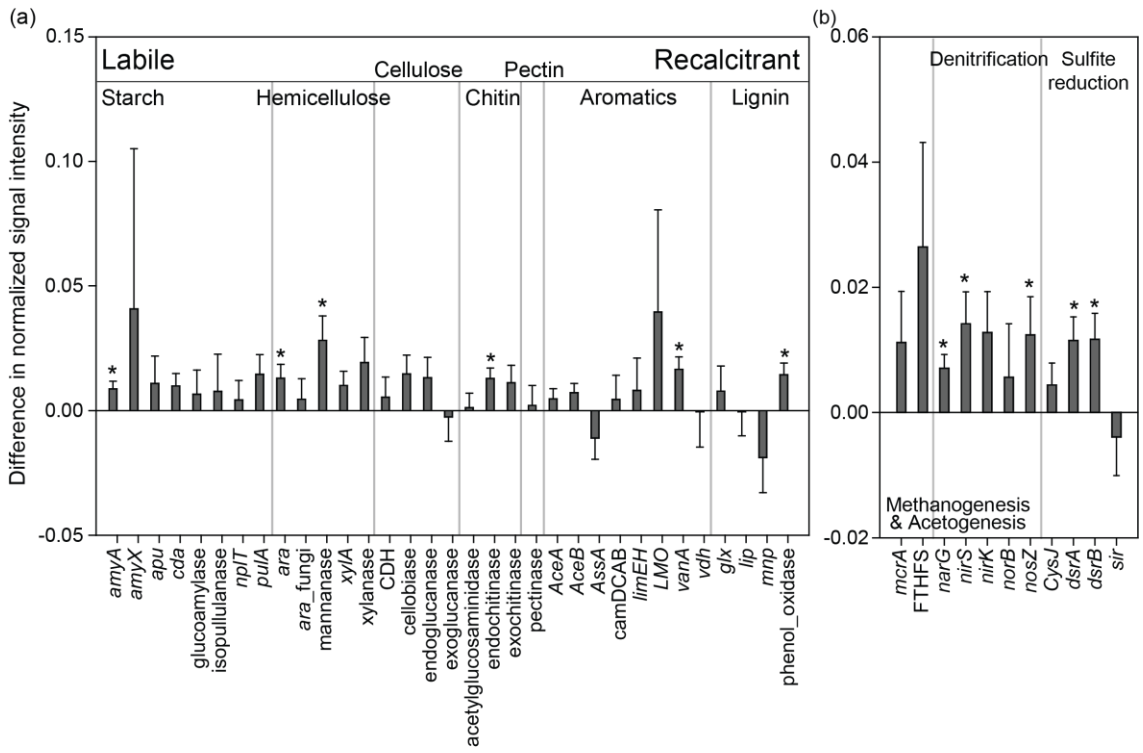

Figure S 14 The abundance of (a) carbon degradation genes and (b) anaerobic respiration genes in OK site. Asteroids indicate significant differences between the mean signals in warmed versus control plots with $p<0.05$ by ANOVA.

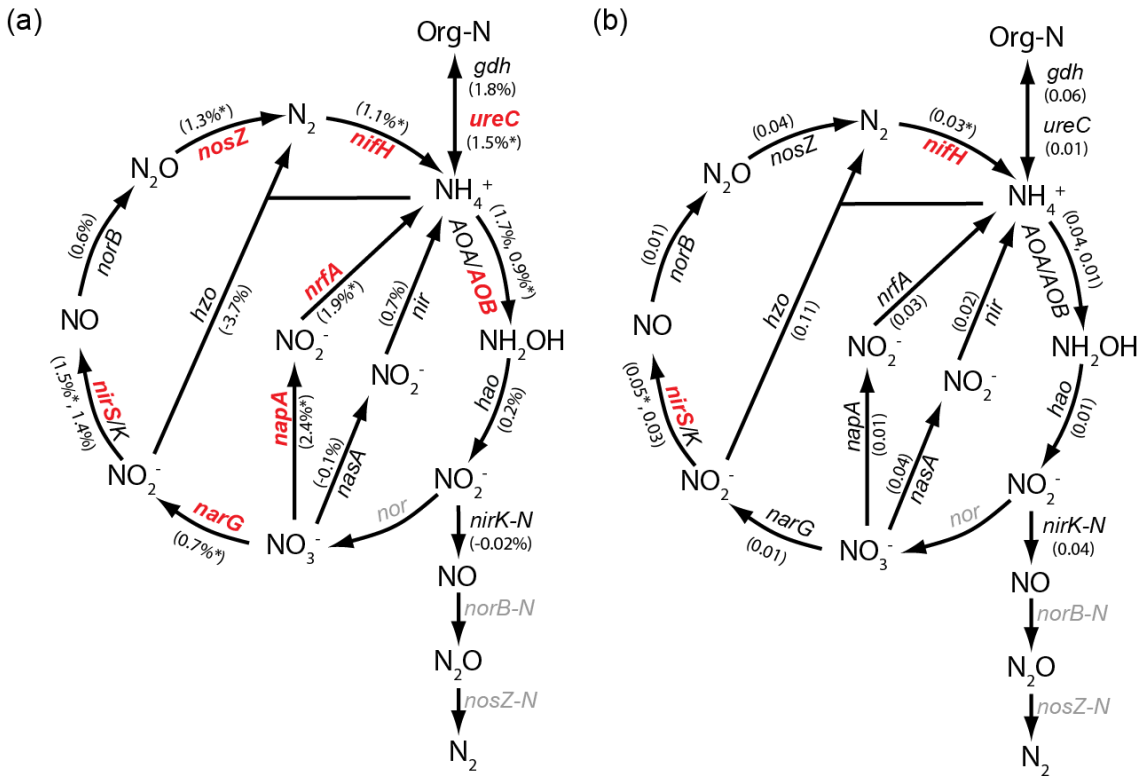

Figure S 15 (a) Percentage change of nitrogen genes to warming at the OK site and (b) the ratio of response ratios between AK and OK sites. In (a), the significance for percentage change was indicated by * and red color of gene name when $p<0.05$. In (b), the significance for ratio of response ratios was indicated by * and red color of gene name when 95% confident interval did not overlap with zero. Gray-colored genes were not targeted by the adopted version of GeoChip or not detected.

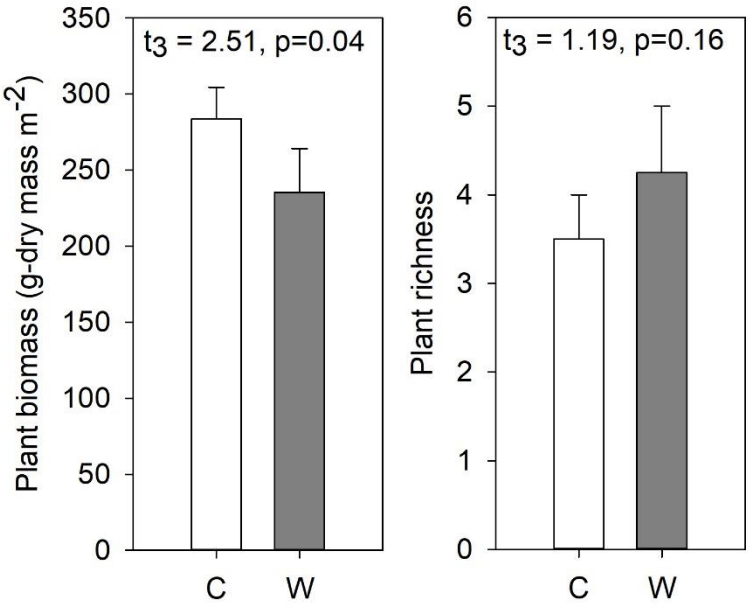

Figure S 16 Plant biomass and richness (the number of plant species) at the time of plant survey in September 2012. Differences of means between control and warming were tested by paired t-test. Error bars denote standard errors for n=4 field replicate plots.

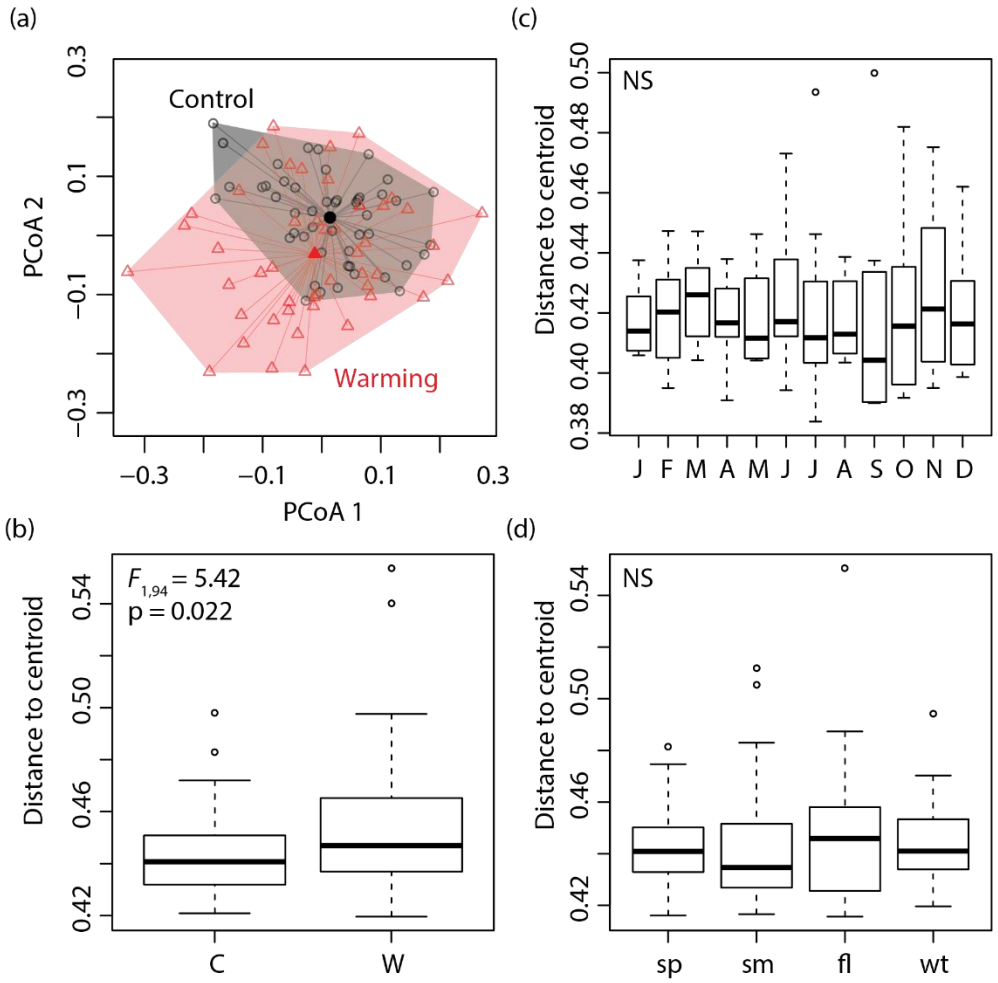

Figure S 17 Microbial community beta-diversity indicated by the multivariate homogeneity of groups variances. (a) The distribution of samples in a two-dimensional space in the Principle Coordinate Analysis (PCoA) marked differentially for control and warmed communities. Filled shapes represent theoretical locations of group centroids. (b)-(d) The distance of samples to group centroids by treatment (b), month (c) and season (d). Means of distances to centroids are significantly larger for warmed than control communities. Those among months or seasons are not significant.

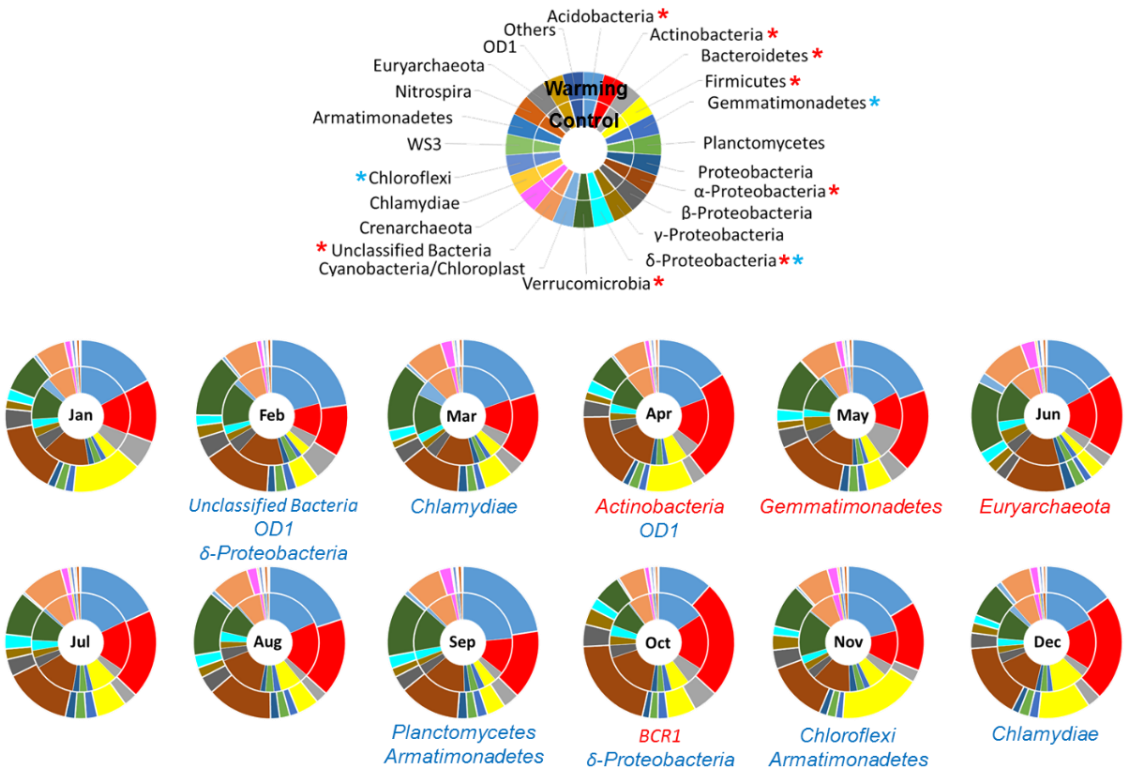

Figure S 18 Microbial taxonomic compositions (refer to the color key) in different months from control (inner circle) and warmed (outer circle) plots. On the color key, blue and red asterisks mark phyla (classes for Proteobacteria) with significantly different abundance among months in control and warmed plots, respectively. Pie fractions indicate the relative abundances of taxa in terms of retrieved sequences numbers. Below the pie chart of each month, taxa listed in red or blue are those with significantly increased or decreased abundance, respectively, in response to warming.

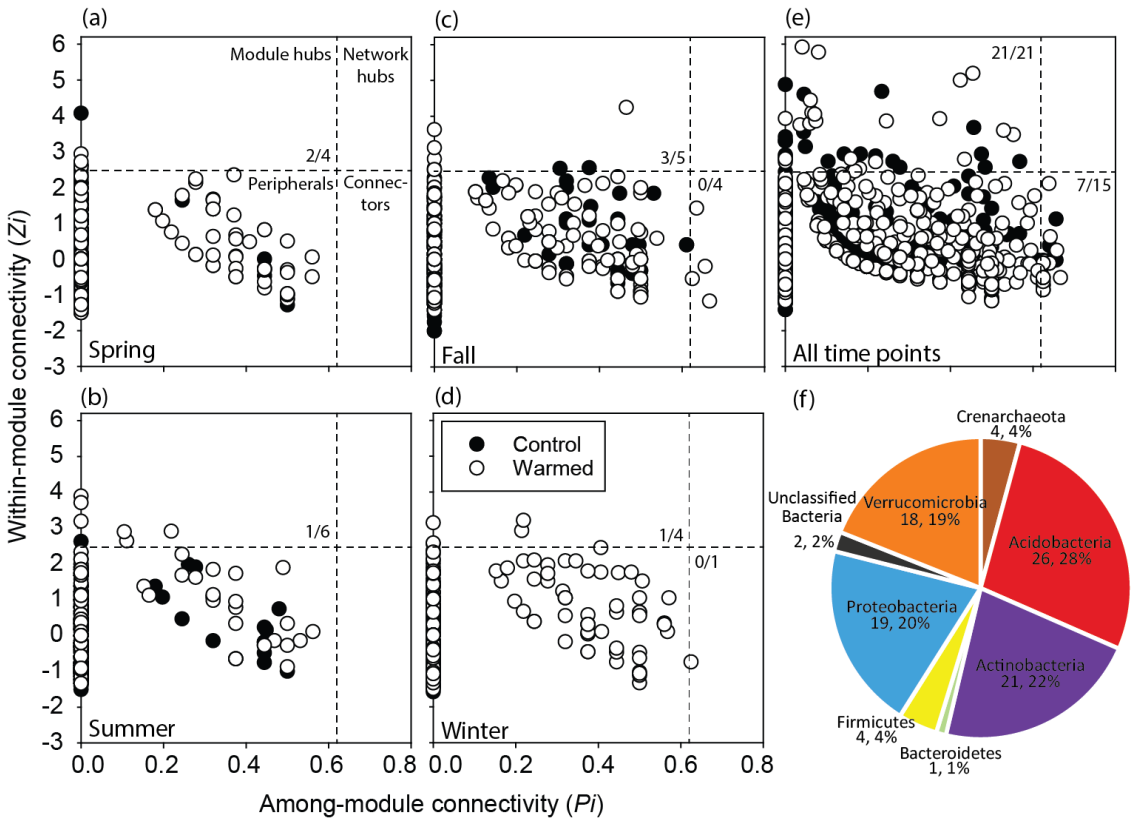

Figure S 19 (a)-(e) Z-P plots for all the networks constructed. The numbers of module hubs and connectors in control/warming networks are marked in corresponding quadrants separated by Z=2.5 and P=0.62. No network hub is present in any network. (f) The phylogenetic profile of module hub and connector OTUs identified in all networks. Numbers below phyla names are the number of OTUs and percentage in all the 95 module hubs and connectors. Their detailed taxonomic information is listed in **Table S 15**.

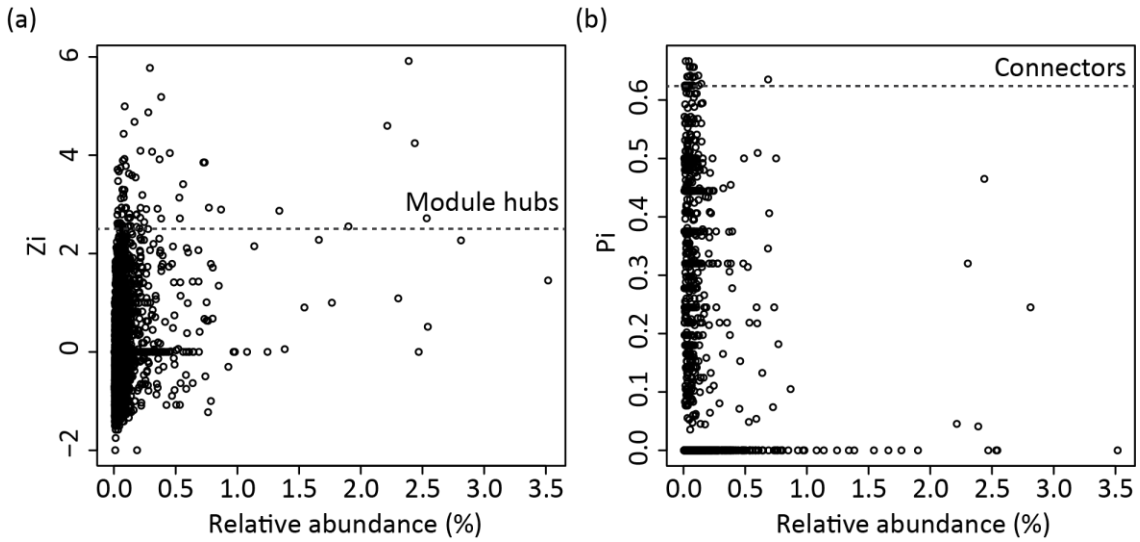

Figure S 20 The relative abundances of network module hubs and connectors in the microbial community.

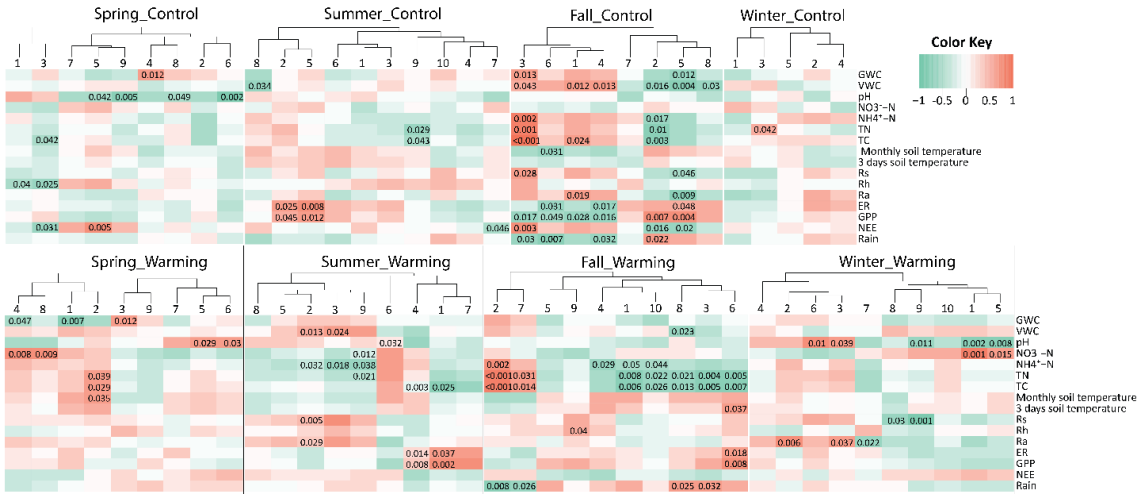

Figure S 21 Module eigengenes' correlations with environmental variables for the separate season networks. An eigengene was calculated for each module to represent all nodes within each module. Clusters show the hierarchical clustering of eigengenes for modules numbered as in **Figure 5.4**. The Pearson correlation coefficient of each eigengene-environmental variable pair is indicated by the color key. Numbers on top of the heatmap listed p values of all significant ($p<0.05$) correlations. Variables were defined as in the legend of **Figure 5.1**.

Appendix B: Supplementary Tables

Table S 1 Non-parametric multivariate dissimilarity tests of functional gene profiles among depth fractions, and among the three thaw sites within each depth fraction. MRPP, multi-response permutation procedures; Adonis, permutational multivariate analysis of variance using distance matrices; ANOSIM, analysis of similarity. Numbers in parentheses were the number of samples acquired from corresponding depth fractions. Results presented are based on distance matrices calculated with Bray-Curtis index. P values <0.1 are in bold.

		MRPP		Adonis		ANOSIM	
Compare	Sample set	δ	p	F	p	R	p
Among depths	All 107 samples	0.279	**0.052**	0.848	**0.060**	0.002	0.105
Among sites	All 107 samples	0.254	**0.001**	11.501	**0.001**	0.146	**0.001**
	Active layer (93 samples)	0.252	**0.001**	10.928	**0.001**	0.157	**0.001**
	permafrost (14 samples)	0.284	0.307	1.058	0.342	0.087	0.197
	0-15cm (18 samples)	0.278	0.595	0.934	0.436	-0.036	0.686
	15-25cm (16 samples)	0.212	**0.050**	2.334	**0.077**	0.252	**0.032**
	25-35cm (16 samples)	0.233	**0.045**	2.678	**0.032**	0.116	**0.093**
	35-45cm (17 samples)	0.267	**0.012**	3.900	**0.019**	0.236	**0.032**
	45-55cm (16 samples)	0.270	**0.025**	2.413	**0.027**	0.111	0.112
	55-65cm (11 samples)	0.263	**0.050**	2.509	**0.082**	0.204	0.120
	>65cm (13 samples)	0.311	0.652	0.503	0.779	-0.181	0.919

Table S 2 to **Table S 4** for Chapter 2: Microbial functional diversity covaries with permafrost thaw-induced environmental heterogeneity in tundra soil

Table S 5 to **Table S 11** for Chapter 3: Rapid microbial feedbacks reveal vulnerability of tundra soil carbon to climate warming

Table S 12 and **Table S 13** for Chapter 4: Differential microbial sensitivity to experimental warming: a comparative metagenomic analysis of soils from two ecosystems

Table S 14 to **Table S 16** for Chapter 5: Warming facilitates the interconnection of grassland soil microbial communities

Table S 1 Non-parametric multivariate dissimilarity tests of functional gene profiles among depth fractions, and among the three thaw sites within each depth fraction. MRPP, multi-response permutation procedures; Adonis, permutational multivariate analysis of variance using distance matrices; ANOSIM, analysis of similarity. Numbers in parentheses were the number of samples acquired from corresponding depth fractions. Results presented are based on distance matrices calculated with Bray-Curtis index. P values <0.1 are in bold.

		MRPP		Adonis		ANOSIM	
Compare	Sample set	δ	p	F	p	R	p
Among depths	All 107 samples	0.279	**0.052**	0.848	**0.060**	0.002	0.105
Among sites	All 107 samples	0.254	**0.001**	11.501	**0.001**	0.146	**0.001**
	Active layer (93 samples)	0.252	**0.001**	10.928	**0.001**	0.157	**0.001**
	permafrost (14 samples)	0.284	0.307	1.058	0.342	0.087	0.197
	0-15cm (18 samples)	0.278	0.595	0.934	0.436	-0.036	0.686
	15-25cm (16 samples)	0.212	**0.050**	2.334	**0.077**	0.252	**0.032**
	25-35cm (16 samples)	0.233	**0.045**	2.678	**0.032**	0.116	**0.093**
	35-45cm (17 samples)	0.267	**0.012**	3.900	**0.019**	0.236	**0.032**
	45-55cm (16 samples)	0.270	**0.025**	2.413	**0.027**	0.111	0.112
	55-65cm (11 samples)	0.263	**0.050**	2.509	**0.082**	0.204	0.120
	>65cm (13 samples)	0.311	0.652	0.503	0.779	-0.181	0.919

Table S 2 α-diversity indices of microbial functional genes detected by GeoChip, and microbial taxonomy revealed by 16S rRNA sequencing reported in Deng et al 2015 in the three thawing sites. Numbers presented mean ± standard error. n=23, 24, and 23 samples in GeoChip data, and n=32, 25, and 35 samples in 16S data for Mi, Mo and Ex sites, respectively. Difference of mean between each two sites was tested using permutational t-test. P-values were then adjusted based on false discovery rate for multiple comparisons. Different letters denote significant difference (adjusted $p<0.05$) of the means.

Dataset	Indices	Mi	Mo	Ex
GeoChip	#of probes	33591±1071 [a]	23394±841 [c]	28508±1262 [b]
	Shannon	10.41±0.03 [a]	10.04±0.04 [c]	10.23±0.05 [b]
	Simpson	0.999969±0.000001 [a]	0.999956±0.000002 [c]	0.999963±0.000002 [b]
	evenness	0.999745±0.000009 [b]	0.999794±0.000009 [a]	0.999766±0.000016 [ab]
16S rRNA gene sequencing*	#of OTUs	3818±207	3250±192	3710±259
	Shannon	5.78±0.14	5.50±0.13	5.79±0.13
	Simpson	0.980±0.003	0.972±0.004	0.981±0.003
	evenness	0.70±0.01	0.68±0.01	0.71±0.01

* Reanalyzed from data published in Deng et al 2015. Means were not significant in all comparisons.

Table S 3 The portion of functional gene probes in all probes shared by the three sites that were significantly different (P<0.05 by ANOVA) in abundance among sites. P values were corrected across all shared probes using false discovery rate.

Functional category	Number of shared probes among sites	Number of probes with different abundance among sites	Percentage of probes with different abundance (%)
Carbon cycling	4693	2233	47.6
Nitrogen	2793	1394	49.9
Phosphorus	514	240	46.7
Sulfur	1126	529	47.0
Fungi function	226	109	48.2
Stress	6932	3396	49.0
Antibiotic resistance	1223	608	49.7
Soil borne pathogen	446	201	45.1
Bacteria phage	193	93	48.2
Plant benefit	1302	668	51.3
Virulence	1245	633	50.8
Metal resistance	4001	1988	49.7
Organic remediation	8061	4022	49.9
Energy process	348	154	44.3
Bioleaching	225	91	40.4
Other category	689	335	48.6
Grand	34017	16694	49.1

Table S 4 Mantel and partial Mantel tests revealed correlations between plant and soil physical-chemical variables and microbial functional gene composition. ANPP, annual net primary productivity. Bold values indicate $p<0.05$.

Category	Variable			Control depth	
		r	p	r	p
Plant variable	Vascular plant biomass	0.103	**0.012**	NA	
	Graminoid	0.172	**0.001**		
	Evergreen shrub	-0.008	0.556		
	Deciduous shrub	-0.004	0.522		
	ANPP from vascular plant	0.259	**0.001**		
	Graminoid	0.172	**0.001**		
	Evergreen shrub	-0.008	0.597		
	Deciduous shrub	-0.004	0.523		
	Non-vascular plant biomass	0.004	0.405		
	ANPP from non-vascular plant	0.002	0.438		
Soil physical-chemical property	Annual temperature	0.010	0.381	0.047	0.275
	Growing season temperature	-0.008	0.522	0.013	0.439
	Winter temperature	-0.110	0.975	-0.142	0.956
	Gravimetric water content	0.104	0.109	0.099	0.117
	N content (g/m^2)	0.015	0.378	-0.019	0.598
	C content (g/m^2)	0.051	0.239	-0.052	0.767
	$\delta^{15}N$	0.000	0.478	-0.008	0.492
	$\delta^{13}C$	0.066	0.167	0.039	0.301
	Bulk Density	0.061	0.233	0.052	0.258

Table S 5 Summary of permutation tests to investigate warming effects on soil microbial community composition based on OTUs for 16S rRNA and *nifH* genes detected by amplicon sequencing, and genes or subsystems detected by metagenomic shotgun sequencing. Three dissimilarity tests were performed, including multiple response permutation procedure (MRPP), analysis of similarity (ANOSIM) and permutational multivariate analysis of variance (Adonis), based on Euclidean, Horn or Bray-Curtis distance.

Detection approaches	**Targeted genes/groups**	**Distance Method**	**MRPP**		**ANOSIM**		**Adonis**	
			δ	P	R	P	F	P
Amplicon sequencing	16S rRNA gene OTUs detected by sequencing	Euclidean	2865.01	0.23	0.03	0.21	0.99	0.35
		Horn	0.58	0.27	0.01	0.28	1.00	0.39
		Bray-Curtis	0.63	0.26	0.00	0.33	0.97	0.29
	nifH gene OTUs detected by sequencing	Euclidean	2875.46	0.72	-0.07	0.82	0.85	0.49
		Horn	0.45	0.62	-0.07	0.75	0.78	0.61
		Bray-Curtis	0.40	0.70	-0.07	0.68	0.74	0.68
Metagenomic shotgun sequencing	Functional genes relevant to GeoChip probes from shotgun sequences	Euclidean	929.61	0.52	-0.12	0.85	0.71	0.65
		Horn	0.13	0.57	-0.10	0.76	0.25	0.81
		Bray-Curtis	0.34	0.55	-0.10	0.75	0.78	0.68
	16S rRNA gene OTUs from shotgun sequences	Euclidean	14224.50	0.66	-0.06	0.58	0.55	0.62
		Horn	0.31	0.76	-0.06	0.63	0.36	0.75
		Bray-Curtis	0.44	0.47	-0.03	0.51	0.93	0.49
	Subsystems from shotgun sequences	Euclidean	16695.64	0.77	-0.12	0.97	0.32	0.77
		Horn	0.01	0.80	-0.10	0.97	-0.12	0.85
		Bray-Curtis	0.05	0.77	-0.10	0.91	0.43	0.76

Table S 6 Summary of metagenomic shotgun sequence statistics. M5NR, the M5 non-redundant protein database; SEED, the SEED project database.

	Control	Warming
Number of reads (raw, $\times 10^6$)	270.33±9.87	269.01±23.80
Number of reads (after trimming, $\times 10^6$)	232.33±8.72	124.17±24.82
Reads with M5NR hit (%)	47.83±0.65	49.00±0.97
Reads with SEED hit (%)	16.50±0.34	16.50±0.62

Table S 7 Fold change (log transformed) between warming (W) and control (C) for subsystems involved in carbon, nitrogen, phosphorous and sulfur cycling.

Subsystems	Log_2(W/C)	Direction	p
C			
Cellulosome	0.662	Increase	**<0.01**
Mannose metabolism	0.226	Increase	**<0.01**
Predicted carbohydrate hydrolases	0.257	Increase	**0.01**
Fructooligosaccharides (FOS) and raffinose utilization	0.191	Increase	**0.01**
Lactose and galactose uptake and utilization	0.132	Increase	**0.02**
L-fucose utilization	0.483	Increase	**0.02**
Xylose utilization	0.167	Increase	**0.03**
Chitin and N-acetylglucosamine utilization	0.192	Increase	**0.04**
Soluble CH_4 monooxygenase (sMMO)	0.301	Increase	0.38
Tricarballylate utilization	-0.538	Decrease	**0.05**
Isobutyryl-CoA to propionyl-CoA module	-0.205	Decrease	**0.07**
Propionate-CoA to succinate module	-0.255	Decrease	**0.09**
Lactose utilization	0.527	Increase	0.11
L-rhamnose utilization	0.112	Increase	0.13
Unknown sugar utilization (cluster yphABCDEFG)	0.200	Increase	0.16
Glycolate, glyoxylate interconversions	-0.121	Decrease	0.19
Inositol catabolism	0.085	Increase	0.20
CO_2 uptake, carboxysome	-0.104	Decrease	0.22
Sucrose utilization	0.398	Increase	0.35
D-galacturonate and D-glucuronate utilization	0.067	Increase	0.35
D-sorbitol(D-glucitol) and L-sorbose utilization	0.253	Increase	0.36
Uncharacterized sugar kinase cluster (ygc)	0.546	Increase	0.36
Dehydrogenase complexes	-0.070	Decrease	0.36
Entner-Doudoroff Pathway	0.069	Increase	0.44
Fructoselysine (Amadori product) utilization pathway	-0.489	Decrease	0.47
Butanol biosynthesis	0.375	Increase	0.48
Fructose utilization	0.066	Increase	0.49
Unknown carbohydrate utilization containing fructose-bisphosphate aldolase	0.300	Increase	0.50
Trehalose biosynthesis	-0.055	Decrease	0.53
Serine-glyoxylate cycle	-0.038	Decrease	0.59
Pentose phosphate pathway	0.050	Increase	0.61
Trehalose uptake and utilization	0.135	Increase	0.61
Acetyl-CoA fermentation to butyrate	0.139	Increase	0.67
Formaldehyde assimilation: ribulose monophosphate pathway	-0.117	Decrease	0.67
Glycerate metabolism	-0.035	Decrease	0.71
Acetone butanol ethanol synthesis	-0.068	Decrease	0.72
Methylcitrate cycle	-0.133	Decrease	0.79
D-galactarate, D-glucarate and D-glycerate catabolism	-0.013	Decrease	0.88
Propionyl-CoA to succinyl-CoA module	0.031	Increase	0.88
D-ribose utilization	0.006	Increase	0.98
Neotrehalosadiamine (NTD) biosynthesis operon	0.103	Increase	1.00
N			

Allantoin utilization	-0.046	Decrease	0.61
Nitrogen fixation	0.123	Increase	0.26
Nitrosative stress	0.021	Increase	0.65
Ammonia assimilation	-0.029	Decrease	0.89
Nitrate and nitrite ammonification	-0.077	Decrease	0.68
Cyanate hydrolysis	-0.149	Decrease	0.34
Dissimilatory nitrite reductase	-0.065	Decrease	0.62
Nitric oxide synthase	-0.236	Decrease	**0.02**
Amidase clustered with urea and nitrile hydratase functions	-0.110	Decrease	0.58
Nitrilase	0.508	Increase	0.22
Denitrification	0.162	Increase	**0.08**
P			
High affinity phosphate transporter and control of PHO regulon	0.137	Increase	0.81
Phosphoenolpyruvate phosphomutase	-0.250	Decrease	0.33
P uptake (cyanobacteria)	-0.843	Decrease	0.25
Phosphate-binding DING proteins	-0.537	Decrease	0.20
Phosphate metabolism	-0.002	Decrease	0.96
Alkylphosphonate utilization	-0.169	Decrease	0.27
Phosphonate metabolism	-0.284	Decrease	0.25
S			
Release of dimethyl sulfide (DMS) from dimethylsulfoniopropionate (DMSP)	-0.325	Decrease	0.69
L-cystine uptake and metabolism	-0.299	Decrease	0.71
Taurine utilization	-0.353	Decrease	0.14
Inorganic sulfur assimilation	-0.053	Decrease	0.54
Alkanesulfonate assimilation	-0.082	Decrease	0.30
Galactosylceramide and sulfatide metabolism	-0.053	Decrease	0.38
Sulfur oxidation	-0.234	Decrease	0.05
Sulfate reduction-associated complexes	0.018	Increase	0.69
DMSP breakdown	0.120	Increase	0.95
Utilization of glutathione as a sulfur source	-0.495	Decrease	0.03
Thioredoxin-disulfide reductase	0.052	Increase	0.66
Alkanesulfonates utilization	-0.120	Decrease	0.28

Table S 8 Fold change (log transformed) between warming (W) and control (C) for subsystems involved in anaerobic activities.

	Subsystem	log_2(W/C)	Direction	p
Acetogene-sis	Pyruvate metabolism II: acetyl-CoA, acetogenesis from pyruvate	0.064	Increase	0.57
Methano-genesis	Methanogenesis	-0.080	Decrease	0.62
	Methanogenesis from methylated compounds	0.057	Increase	0.74
	Methanogenesis strays	0.631	Increase	**0.05**
	Methanopterin biosynthesis	0.319	Increase	0.43
	Methanopterin biosynthesis2	-0.159	Decrease	0.52
	Coenzyme F420-H2 dehydrogenase	0.517	Increase	0.26
	Methanophenazine hydrogenase	0.824	Increase	0.32
N	Denitrification	0.162	Increase	**0.08**
Sulfate reduction	Sulfate reduction-associated complexes	0.018	Increase	0.69
Other	Anaerobic benzoate metabolism	-0.049	Decrease	0.66
	Threonine anaerobic catabolism gene cluster	-0.060	Decrease	0.73
	Anaerobic toluene and ethylbenzene degradation	-0.103	Decrease	0.86
	Anaerobic respiratory reductases	-0.021	Decrease	0.91
	Anaerobic oxidative degradation of L-ornithine	0.435	Increase	0.36

Table S 9 CCA between the structure of each functional gene group involved in C/N/P/S cycling and each environmental attribute. The functional community structure was determined by GeoChip hybridization. Significance is represented by ** when $p<0.05$ and * when $p<0.10$. Environmental attributes without significant correlation to any of the functional gene groups are not listed.

	Subcategory[a]	T	M	W-R_{eco}	GS-R_{eco}	GPP	Bm	Gm-Bm	LP1%	NH_4^+
C degrad-ation	Starch	**	**	**	**	**		*		
	Hemicellulose	**	**	**	**	**				
	Cellulose	**	**	**	*	**				
	Chitin	**	**	**	*	**				
	pectinase								*	*
	Others	**	**	**	**	**				
	Lignin	**	**	**	**	**				
N	Ammonification	**	**	**	**	**				
	Anammox	**	**	**		*				
	Assimilatory N reduction	**	**	**	**	**	*	**		
	Denitrification		**	**	**	**				
	Dissimilatory N reduction		**	**	**	**				
	Nitrification	**	**	**	**	**		*		
	nifH	**	**	**	**	**				
P	Phosphorus utilization	**	**	**	**	**		*		
S	Adenylylsulfate reductase	**	**	**	**	**				
	Sulfide oxidation		**	**	*	*				
	Sulfite reductase	**	**	**	**	**				
	Sulfur oxidation	**	**	**	**	**				

Environmental attributes include soil temperature (T), soil moisture (M), wintertime and growing season ecosystem respiration (W-R_{eco} and GS-R_{eco}), gross primary productivity (GPP), peak biomass of all plant species (Bm), peak biomass of graminoid (Gm-Bm), soil labile carbon pool 1 (LP1%), and ammonia (NH_4^+) contents.

Table S 10 Number of positive GeoChip probes for each gene that were significantly ($p<0.05$) or marginally significantly ($p<0.10$) correlated with the decomposition rate (mass loss % after one year by utilizing cellulose filter paper as a standard substrate) and its percentage to total detected probe number in each gene. The test was performed by Pearson correlation.

Gene category	Subcategory	Gene name	Correlated probe number	% of total probe number
C degra-dation	Starch	*amyA*	29	4.9
	Starch	*cda*	12	**6.9**
	Starch	glucoamylase	3	4.1
	Starch	*nplT*	4	4.3
	Starch	*pulA*	4	2.9
	Cellulose	CDH	1	2.0
	Cellulose	cellobiase	4	3.2
	Cellulose	endoglucanase	3	3.1
	Cellulose	exoglucanase	4	4.1
	Hemicellulose	*ara*	8	3.0
	Hemicellulose	*ara*-fungi	4	**5.0**
	Hemicellulose	*xylA*	4	2.3
	Hemicellulose	xylanase	3	3.7
	Chitin	acetylglucosaminidase	10	4.2
	Chitin	endochitinase	17	4.4
	Chitin	exochitinase	1	2.1
	Aromatics	*AceA*	14	4.6
	Aromatics	*AceB*	19	4.5
	Aromatics	*AssA*	1	**20.0**
	Aromatics	*camDCAB*	1	**33.3**
	Aromatics	*limEH*	6	**18.8**
	Aromatics	*vanA*	6	3.2
	Aromatics	*vdh*	1	2.6
	Lignin	*glx*	1	1.4
	Lignin	*lip*	3	**8.3**
	Lignin	*mnp*	3	**7.1**
	Lignin	phenol_oxidase	10	3.4
N	Ammonification	*gdh*	3	**5.9**
	Ammonification	*ureC*	16	3.6
	Anammox	*hzo*	1	**8.3**
	Assimilatory N reduction	*nasA*	4	3.8
	Assimilatory N reduction	*NiR*	2	2.6
	Assimilatory N reduction	*NirB*	2	**6.7**
	Denitrification	*narG*	22	3.1
	Denitrification	*nirS*	8	2.3
	Denitrification	*norB*	4	**6.2**

	Denitrification	*nosZ*	7	3.6
	Denitrification	*nirK*	7	2.2
	Dissimilatory N reduction	*napA*	4	2.5
	Dissimilatory N reduction	*nrfA*	4	2.6
	Nitrification	*hao*	1	4.3
	Nitrification	*amoA*	17	3.2
	Nitrogen fixation	*nifH*	32	4.5
P	Phosphorus utilization	phytase	1	2.9
	Phosphorus utilization	*ppk*	10	3.9
	Phosphorus utilization	*ppx*	23	**5.5**
S	Adenylylsulfate reductase	*AprA*	3	4.2
	Adenylylsulfate reductase	APS_*AprA*	2	1.9
	Sulfide oxidation	APS_*AprB*	3	**5.5**
	Sulfide oxidation	*fccAB*	1	1.2
	Sulfite reductase	*sqr*	10	**76.9**
	Sulfite reductase	*CysJ*	27	**8.9**
	Sulfite reductase	*dsrA*	16	2.4
	Sulfite reductase	*dsrB*	6	1.4
	Sulfur oxidation	*sir*	9	**6.7**
	Sulfur oxidation	*sox*	9	3.0

Table S 11 GenBank GI numbers of the functional gene clusters' representative sequences in **Figure 3.2**e.

Cluster name in Fig. 2e	GI number in GenBank
glucoamylase.1	321161797
ara.1	151362027
ara.2	310799506
ara.3	225792025
ara.4	264673727
ara.5	237686947
ara.6	217988056
ara.7	119947938
ara.8	177842253
ara.9	16079903
ara.10	229567653
xylA.1	116225312
xylA.2	148371493
xylA.3	157912302
xylA.4	153534
xylA.5	256800271
xylA.6	227272193
cellobiase.1	169016064
cellobiase.2	296926994
cellobiase.3	365270931
cellobiase.4	237881831
cellobiase.5	296092656
gdh.1	91203647
ureC.1	158112848
ureC.2	108770190
ureC.3	194343174
ureC.4	257045343
ureC.5	118656429
ureC.6	124895654
ureC.7	15807978
nasA.1	260217376
nasA.2	221738036
NiR.1	225793725
NiR.2	183580411

Table S 12 Summary of shotgun metagenomic sequence statistics at OK site.

Item	Control	Warming
Number of reads (after trimming, $\times 10^6$)	213.00±4.53	215.75±14.01
Reads with M5NR hit (%)	46.75±1.11	49.00±0.91
Reads with SEED hit (%)	17.00±0.41	17.00±0.41

Table S 13 Summary of α-diversity based on GeoChip, 16S rRNA, 28S rRNA, nifH sequences, GeoChip related shotgun sequences, 16S rRNA and subsystem from shotgun metagenomic sequences. The significance was tested by two-tailed t test for richness or permutation t test for diversity index, labeled with * when 0.05<p<0.10.

Data set		Richness		Shannon		Inverse Simpson		
		Control	Warming	Control	Warming	Control	Warming	
GeoChip hybridization	AK	41756.17 ±720.80	43205.83 ±1964.89	10.63 ±0.02	10.66 ±0.05	41273.04 ±705.40	42686.54 ±1927.16	
	OK	43549.50 ±573.74	44003.75 ±171.05	10.68 ±0.01	10.687 ±0.004	43113.55 ±572.09	43563.42 ±174.55	
16S amplicon sequences	AK	5462.67 ±638.29	4651.83 ±308.79	7.10 ±0.17	6.74 ±0.21	424.63 ±63.37	263.96 ±80.57	*
	OK	8152.50 ±598.95	9368.00 ±969.22	7.84 ±0.19	8.17 ±0.16	790.33 ±184.17	1242.87 ±285.32	
28S amplicon sequences	AK	256.67 ±31.68	331.83 ±51.03	3.53 ±0.19	3.01 ±0.35	16.80 ±2.71	10.53 ±2.76	*
	OK	1984.00 ±346.49	1400.00 ±535.09	5.76 ±0.12	5.29 ±0.23	102.70 ±19.40	58.46 ±9.54	
nifH amplicon sequences	AK	798.00 ±77.95	923.67 ±88.36	5.12 ±0.15	5.15 ±0.11	62.51 ±7.79	60.78 ±6.80	
	OK	918.50 ±288.86	877.75 ±335.36	4.85 ±0.51	5.20 ±0.25	60.54 ±19.06	69.45 ±6.64	
GeoChip related shotgun metagenomics sequences	AK	16967.83 ±1237.49	15946.83 ±498.06	8.72 ±0.08	8.66 ±0.04	2468.80 ±252.88	2289.30 ±105.76	
	OK	24235 ±932.13	24063 ±1303.68	9.12 ±0.05	9.10 ±0.06	3285.85 ±150.00	3166.47 ±142.04	
Subsystems from shotgun metagenomics sequences	AK	977.00 ±3.80	972.17 ±5.78	5.75 ±0.02	5.75 ±0.01	193.12 ±5.74	190.31 ±3.01	
	OK	1018.50 ±1.32	1019.25 ±3.15	5.81 ±0.01	5.81 ±0.01	213.34 ±1.15	213.17 ±1.73	

Table S 14 Data association strength cutoff (S_t) ranges for SS and AT networks detected by the improve RMT-based approach.

Network	Transition start (minimum S_t)	Transition end (maximum S_t)	Overlapping S_t range	Cutoff
spring-C	0.854	0.797	[0.852, 0.933]	0.8925
summer-C	0.933	0.781		
fall-C	0.824	0.781		
winter-C	0.828	0.784		
spring-W	0.839	0.771		
summer-W	0.930	0.776		
fall-W	0.942	0.852		
winter-W	0.943	0.805		
C	0.508	0.698	[0.563, 0.698]	0.6305
W	0.563	0.760		

Table S 15 Taxonomic information for module hubs and connectors. The superscript numbers before the OTU indicates the number of networks in which those OTUs are present as key-stone species.

OTU	network/ module	Phylum	Class	Genus
Module hubs				
[2]OTU_6318	spring-C/1	Acidobacteria	Acidobacteria_Gp4	Gp4
[2]OTU_116965	spring-C/3	Acidobacteria	Acidobacteria_Gp5	Gp5
OTU_114765	spring-W/1	Actinobacteria	Actinobacteria	Solirubrobacter
[4]OTU_70085	spring-W/3	Verrucomicrobia	Spartobacteria	Spartobacteria_genera_incertae_sedis
OTU_119760	spring-W/5	Proteobacteria	Alphaproteobacteria	Unclassified
OTU_16692	spring-W/6	Proteobacteria	Alphaproteobacteria	Unclassified
OTU_80088	summer-C/4	Verrucomicrobia	Spartobacteria	Spartobacteria_genera_incertae_sedis
OTU_89229	summer-W/1	Proteobacteria	Alphaproteobacteria	Unclassified
[2]OTU_3308	summer-W/2	Crenarchaeota	Thermoprotei	Unclassified
OTU_17125	summer-W/2	Proteobacteria	Unclassified	Unclassified
[3]OTU_132165	summer-W/3	Verrucomicrobia	Spartobacteria	Spartobacteria_genera_incertae_sedis
[2]OTU_55850	summer-W/4	Proteobacteria	Alphaproteobacteria	Unclassified
[2]OTU_1714	summer-W/6	Actinobacteria	Actinobacteria	Pseudonocardia
OTU_2778	fall-C/1	Acidobacteria	Acidobacteria_Gp6	Gp6
OTU_3667	fall-C/1	Actinobacteria	Actinobacteria	Conexibacter
[3]OTU_90925	fall-C/2	Acidobacteria	Acidobacteria_Gp1	Gp1
OTU_29290	fall-W/1	Bacteroidetes	Sphingobacteria	Unclassified
[2]OTU_1714	fall-W/2	Actinobacteria	Actinobacteria	Pseudonocardia
[4]OTU_70085	fall-W/3	Verrucomicrobia	Spartobacteria	Spartobacteria_genera_incertae_sedis
OTU_1461	fall-W/4	Proteobacteria	Alphaproteobacteria	Skermanella
OTU_1167	fall-W/5	Acidobacteria	Acidobacteria_Gp4	Gp4
[2]OTU_50262	winter-C/1	Firmicutes	Bacilli	Unclassified
OTU_107273	winter-W/1	Actinobacteria	Actinobacteria	Unclassified
OTU_2020	winter-W/2	Acidobacteria	Acidobacteria_Gp4	Gp4
OTU_764	winter-W/3	Acidobacteria	Acidobacteria_Gp4	Gp4
[2]OTU_20432	winter-W/9	Acidobacteria	Acidobacteria_Gp1	Gp1
OTU_14090	C/1	Acidobacteria	Acidobacteria_Gp4	Gp4
OTU_14558	C/1	Acidobacteria	Acidobacteria_Gp2	Gp2
OTU_3477	C/1	Acidobacteria	Acidobacteria_Gp13	Gp13
[3]OTU_90925	C/1	Acidobacteria	Acidobacteria_Gp1	Gp1
OTU_50927	C/1	Actinobacteria	Actinobacteria	Solirubrobacter
[2]OTU_13482	C/1	Proteobacteria	Gammaproteobacteria	Steroidobacter
[2]OTU_90406	C/1	Verrucomicrobia	Spartobacteria	Spartobacteria_genera_incertae_sedis
[2]OTU_115896	C/2	Verrucomicrobia	Spartobacteria	Spartobacteria_genera_incertae_sedis
[3]OTU_132165	C/2	Verrucomicrobia	Spartobacteria	Spartobacteria_genera_incertae_sedis
[4]OTU_70085	C/2	Verrucomicrobia	Spartobacteria	Spartobacteria_genera_incertae_sedis
OTU_11228	C/3	Acidobacteria	Acidobacteria_Gp4	Gp4
[2]OTU_116965	C/3	Acidobacteria	Acidobacteria_Gp5	Gp5
[2]OTU_87022	C/3	Actinobacteria	Actinobacteria	Unclassified
OTU_49878	C/3	Proteobacteria	Unclassified	Unclassified
OTU_1096	C/3	Unclassified	Unclassified	Unclassified
[2]OTU_50262	C/4	Firmicutes	Bacilli	Unclassified
OTU_120739	C/5	Crenarchaeota	Thermoprotei	Unclassified
OTU_38746	C/6	Acidobacteria	Acidobacteria_Gp16	Gp16

[2]OTU_125428	C/6	Proteobacteria	Alphaproteobacteria	Sphingosinicella
OTU_119435	C/7	Actinobacteria	Actinobacteria	Unclassified
[2]OTU_20432	C/8	Acidobacteria	Acidobacteria_Gp1	Gp1
[2]OTU_3308	W/1	Crenarchaeota	Thermoprotei	Unclassified
OTU_77723	W/1	Crenarchaeota	Thermoprotei	Unclassified
[2]OTU_115896	W/1	Verrucomicrobia	Spartobacteria	Spartobacteria_genera_incertae_sedis
[3]OTU_132165	W/1	Verrucomicrobia	Spartobacteria	Spartobacteria_genera_incertae_sedis
[2]OTU_26513	W/1	Verrucomicrobia	Spartobacteria	Spartobacteria_genera_incertae_sedis
[4]OTU_70085	W/1	Verrucomicrobia	Spartobacteria	Spartobacteria_genera_incertae_sedis
OTU_10156	W/2	Acidobacteria	Acidobacteria_Gp1	Gp1
OTU_14911	W/2	Acidobacteria	Acidobacteria_Gp1	Gp1
OTU_70836	W/2	Acidobacteria	Acidobacteria_Gp1	Gp1
OTU_80872	W/2	Acidobacteria	Acidobacteria_Gp1	Gp1
[3]OTU_90925	W/2	Acidobacteria	Acidobacteria_Gp1	Gp1
OTU_12027	W/2	Proteobacteria	Alphaproteobacteria	Rhizomicrobium
OTU_27828	W/2	Verrucomicrobia	Spartobacteria	Spartobacteria_genera_incertae_sedis
OTU_17370	W/3	Acidobacteria	Acidobacteria_Gp3	Gp3
OTU_5633	W/3	Acidobacteria	Acidobacteria_Gp4	Gp4
[2]OTU_6318	W/3	Acidobacteria	Acidobacteria_Gp4	Gp4
[2]OTU_125428	W/3	Proteobacteria	Alphaproteobacteria	Sphingosinicella
OTU_130832	W/3	Proteobacteria	Alphaproteobacteria	Pseudolabrys
OTU_3805	W/3	Proteobacteria	Betaproteobacteria	Unclassified
[2]OTU_55850	W/3	Proteobacteria	Alphaproteobacteria	Unclassified
[2]OTU_87022	W/4	Actinobacteria	Actinobacteria	Unclassified
Connectors				
[2]OTU_90406	fall-W/1	Verrucomicrobia	Spartobacteria	Spartobacteria_genera_incertae_sedis
OTU_84080	fall-W/3	Proteobacteria	Betaproteobacteria	Unclassified
[2]OTU_26513	fall-W/3	Verrucomicrobia	Spartobacteria	Spartobacteria_genera_incertae_sedis
OTU_49486	fall-W/8	Verrucomicrobia	Spartobacteria	Spartobacteria_genera_incertae_sedis
[2]OTU_86721	winter-W/1	Actinobacteria	Actinobacteria	Solirubrobacter
OTU_3265	C/3	Unclassified	Unclassified	Unclassified
OTU_91366	C/3	Verrucomicrobia	Spartobacteria	Spartobacteria_genera_incertae_sedis
OTU_56313	C/6	Actinobacteria	Actinobacteria	Solirubrobacter
OTU_4756	C/6	Proteobacteria	Deltaproteobacteria	Unclassified
OTU_28445	C/6	Verrucomicrobia	Spartobacteria	Spartobacteria_genera_incertae_sedis
OTU_8869	C/9	Proteobacteria	Alphaproteobacteria	Pseudolabrys
OTU_33220	C/NA	Acidobacteria	Acidobacteria_Gp6	Gp6
OTU_6329	W/1	Acidobacteria	Acidobacteria_Gp4	Gp4
[2]OTU_13482	W/1	Proteobacteria	Gammaproteobacteria	Steroidobacter
OTU_5850	W/3	Actinobacteria	Actinobacteria	Unclassified
[2]OTU_86721	W/3	Actinobacteria	Actinobacteria	Solirubrobacter
OTU_97401	W/3	Actinobacteria	Actinobacteria	Unclassified
OTU_98940	W/3	Actinobacteria	Actinobacteria	Thermoleophilum
OTU_80507	W/3	Proteobacteria	Betaproteobacteria	Unclassified
OTU_10516	W/4	Actinobacteria	Actinobacteria	Unclassified
OTU_135325	W/4	Actinobacteria	Actinobacteria	Thermoleophilum
OTU_143742	W/4	Actinobacteria	Actinobacteria	Unclassified
OTU_17112	W/4	Actinobacteria	Actinobacteria	Streptosporangium
OTU_18090	W/4	Actinobacteria	Actinobacteria	Solirubrobacter
OTU_27378	W/4	Actinobacteria	Actinobacteria	Solirubrobacter
OTU_146566	W/4	Firmicutes	Bacilli	Tumebacillus
OTU_20861	W/4	Firmicutes	Bacilli	Tumebacillus

Table S 16 Summary of module eigengene analysis results.

Network	Modules (≥8 nodes)	Variation explained by eigengene (Φ)
spring-C	1/2/3/4/5/6/7/8/9	61/71/72/75/65/68/81/71/74 %
summer-C	1/2/3/4/5/6/7/8/9/10	69/69/70/71/75/80/71/81/76/73 %
fall-C	1/2/3/4/5/6/7/8	65/62/67/67/78/69/70/79 %
winter-C	1/2/3/4/5	72/66/69/64/76 %
spring-W	1/2/3/4/5/6/7/8/9	62/63/68/65/64/67/78/79/77 %
summer-W	1/2/3/4/5/6/7/8/9	66/76/70/67/65/75/69/73/76 %
fall-W	1/2/3/4/5/6/7/8/9/10	65/71/62/68/66/70/73/73/73/82 %
winter-W	1/2/3/4/5/6/7/8/9/10	75/67/65/76/63/66/73/70/75/70 %
C	1/2/3/4/5/6/7/8/9/10	38/43/29/49/34/26/46/48/61/45 %
W	1/2/3/4/5	34/29/27/25/65 %

Reference

A'Bear AD, Jones TH, Kandeler E, Boddy L (2014). Interactive effects of temperature and soil moisture on fungal-mediated wood decomposition and extracellular enzyme activity. *Soil Biology and Biochemistry* **70:** 151-158.

Abbott BW, Jones JB, Schuur EAG, Chapin III FS, Bowden WB, Bret-Harte MS *et al* (2016). Biomass offsets little or none of permafrost carbon release from soils, streams, and wildfire: an expert assessment. *Environmental Research Letters* **11:** 034014.

Abram NJ, McGregor HV, Tierney JE, Evans MN, McKay NP, Kaufman DS (2016). Early onset of industrial-era warming across the oceans and continents. *Nature* **536:** 411-418.

ACIA (2004). *Impacts of a Warming Arctic-Arctic Climate Impact Assessment*. Cambridge University Press: Cambridge, UK.

Amundson R, Austin AT, Schuur EAG, Yoo K, Matzek V, Kendall C *et al* (2003). Global patterns of the isotopic composition of soil and plant nitrogen. *Global Biogeochemical Cycles* **17:** 1031.

Anders S, Huber W (2010). Differential expression analysis for sequence count data. *Genome biology* **11:** R106.

Anderson MJ (2001). A new method for non-parametric multivariate analysis of variance. *Austral Ecology* **26:** 32-46.

Anderson MJ, Ellingsen KE, McArdle BH (2006). Multivariate dispersion as a measure of beta diversity. *Ecology Letters* **9:** 683-693.

Avramidis P, Nikolaou K, Bekiari V (2015). Total organic carbon and total nitrogen in sediments and soils: A comparison of the wet oxidation – titration method with the combustion-infrared method. *Agriculture and Agricultural Science Procedia* **4:** 425-430.

Baer SE, Connelly TL, Sipler RE, Yager PL, Bronk DA (2014). Effect of temperature on rates of ammonium uptake and nitrification in the western coastal Arctic during winter, spring, and summer. *Global Biogeochemical Cycles* **28:** 1455-1466.

Bais HP, Weir TL, Perry LG, Gilroy S, Vivanco JM (2006). The role of root exudates in rhizosphere interactions with plants and other organisms. *Annual Review of Plant Biology* **57:** 233-266.

Baldrian P, Snajdr J, Merhautova V, Dobiasova P, Cajthaml T, Valaskova V (2013). Responses of the extracellular enzyme activities in hardwood forest to soil temperature and seasonality and the potential effects of climate change. *Soil Biology & Biochemistry* **56:** 60-68.

Barberan A, Bates ST, Casamayor EO, Fierer N (2012). Using network analysis to explore co-occurrence patterns in soil microbial communities. *ISME J* **6:** 343-351.

Bardgett RD, Freeman C, Ostle NJ (2008). Microbial contributions to climate change through carbon cycle feedbacks. *The ISME Journal* **2:** 805-814.

Bassler BL, Losick R (2006). Bacterially speaking. *Cell* **125:** 237-246.

Beier C, Emmett BA, Peñuelas J, Schmidt IK, Tietema A, Estiarte M *et al* (2008). Carbon and nitrogen cycles in European ecosystems respond differently to global warming. *Science of The Total Environment* **407:** 692-697.

Benjamini Y, Hochberg Y (1995). Controlling the false discovery rate: a practical and powerful approach to multiple testing. *Journal of the Royal Statistical Society Series B (Methodological)***:** 289-300.

Berry D, Widder S (2014). Deciphering microbial interactions and detecting keystone species with co-occurrence networks. *Frontiers in Microbiology* **5**.

Blasing TJ, Smith K (2006). Recent greenhouse gas concentrations. http://cdiac.ornl.gov/pns/current_ghg.html. *Updated April 2016*.

Boone RD, Nadelhoffer KJ, Canary JD, Kaye JP (1998). Roots exert a strong influence on the temperature sensitivity of soil respiration. *Nature* **396:** 570.

Bradford MA (2013). Thermal adaptation of decomposer communities in warming soils. *Front Microbiol* **4:** 333.

Bray JR, Curtis JT (1957). An ordination of the upland forest communities of southern Wisconsin. *Ecological monographs* **27:** 325-349.

Brochier-Armanet C, Forterre P (2006). Widespread distribution of archaeal reverse gyrase in thermophilic bacteria suggests a complex history of vertical inheritance and lateral gene transfers. *Archaea* **2**.

Camacho C, Coulouris G, Avagyan V, Ma N, Papadopoulos J, Bealer K *et al* (2009). BLAST+: architecture and applications. *BMC Bioinformatics* **10:** 421.

Caporaso JG, Bittinger K, Bushman FD, DeSantis TZ, Andersen GL, Knight R (2010). PyNAST: a flexible tool for aligning sequences to a template alignment. *Bioinformatics* **26:** 266-267.

Caporaso JG, Lauber CL, Walters WA, Berg-Lyons D, Lozupone CA, Turnbaugh PJ *et al* (2011). Global patterns of 16S rRNA diversity at a depth of millions of sequences per sample. *Proc Natl Acad Sci U S A* **108 Suppl 1:** 4516-4522.

Castro HF, Classen AT, Austin EE, Norby RJ, Schadt CW (2010). Soil microbial community responses to multiple experimental climate change drivers. *Applied and Environmental Microbiology* **76:** 999-1007.

Cavaleri MA, Reed SC, Smith WK, Wood TE (2015). Urgent need for warming experiments in tropical forests. *Glob Chang Biol* **21:** 2111-2121.

Chambers JM, Freeny A, Heiberger RM (1992). Analysis of variance; designed experiments. In: Chambers JM, Hastie TJ (eds). *Statistical Models in S*. Wadsworth & Brooks/Cole: Pacific Grove, California. pp 145-193.

Chapin FS, Sturm M, Serreze MC, McFadden JP, Key JR, Lloyd AH *et al* (2005). Role of land-surface changes in arctic summer warming. *Science* **310:** 657-660.

Chen H, Tian H-Q (2005). Does a general temperature-dependent Q_{10} model of soil respiration exist at biome and global scale? *Journal of Integrative Plant Biology* **47:** 1288-1302.

Chen Q, Li L, Han X, Dong Y, Wang Z, Xiong X *et al* (2003). Acclimatization of soil respiration to warming. *Acta ecologica sinica* **24:** 2649-2655.

Chou H-H, Holmes MH (2001). DNA sequence quality trimming and vector removal. *Bioinformatics* **17:** 1093-1104.

Ciais P, Sabine C, Bala G, Bopp L, Brovkin V, Canadell J *et al* (2013). Carbon and other biogeochemical cycles. In: Stocker TF, Qin D, Plattner G-K, Tignor M, Allen SK, Boschung J *et al* (eds). *Climate Change 2013: The Physical Science Basis. Contribution of Working Group I to the Fifth Assessment Report of the Intergovernmental Panel on Climate Change*: Cambridge, United Kingdom and New York, NY, USA.

Clarke KR (1993). Non-parametric multivariate analyses of changes in community structure. *Australian Journal of Ecology* **18:** 117-143.

Clymo RS (1970). The growth of sphagnum: Methods of measurement. *Journal of Ecology* **58:** 13-49.

Comiso JC, Parkinson CL, Gersten R, Stock L (2008). Accelerated decline in the Arctic sea ice cover. *Geophysical Research Letters* **35:** n/a-n/a.

Contosta AR, Frey SD, Cooper AB (2015). Soil microbial communities vary as much over time as with chronic warming and nitrogen additions. *Soil Biology and Biochemistry* **88:** 19-24.

Coolen MJL, Orsi WD (2015). The transcriptional response of microbial communities in thawing Alaskan permafrost soils. *Frontiers in Microbiology* **6**.

Crowther TW, Thomas SM, Maynard DS, Baldrian P, Covey K, Frey SD *et al* (2015). Biotic interactions mediate soil microbial feedbacks to climate change. *Proc Natl Acad Sci U S A* **112:** 7033-7038.

Das M, Royer TV, Leff LG (2007). Diversity of fungi, bacteria, and actinomycetes on leaves decomposing in a stream. *Applied and Environmental Microbiology* **73:** 756-767.

Davidson EA, Janssens IA (2006). Temperature sensitivity of soil carbon decomposition and feedbacks to climate change. *Nature* **440:** 165-173.

Davidson EA, Janssens IA, Luo Y (2006). On the variability of respiration in terrestrial ecosystems: moving beyond Q_{10}. *Global Change Biology* **12:** 154-164.

De Long JR, Dorrepaal E, Kardol P, Nilsson M-C, Teuber LM, Wardle DA (2016). Understory plant functional groups and litter species identity are stronger drivers of litter decomposition than warming along a boreal forest post-fire successional gradient. *Soil Biology and Biochemistry* **98:** 159-170.

De Mendiburu F (2014). Agricolae: statistical procedures for agricultural research. *R package version 1.2-0.*

DeMarco J, Mack MC, Bret-Harte MS (2014). Effects of arctic shrub expansion on biophysical vs. biogeochemical drivers of litter decomposition. *Ecology* **95:** 1861-1875.

Deng J, Gu Y, Zhang J, Xue K, Qin Y, Yuan M *et al* (2015). Shifts of tundra bacterial and archaeal communities along a permafrost thaw gradient in Alaska. *Molecular Ecology* **24:** 222-234.

Deng Y, Jiang Y-H, Yang Y, He Z, Luo F, Zhou J (2012). Molecular ecological network analyses. *BMC Bioinformatics* **13:** 113.

Deng Y, Zhang P, Qin Y, Tu Q, Yang Y, He Z *et al* (2016). Network succession reveals the importance of competition in response to emulsified vegetable oil amendment for uranium bioremediation. *Environmental Microbiology* **18:** 205-218.

DeSantis TZ, Hugenholtz P, Larsen N, Rojas M, Brodie EL, Keller K *et al* (2006). Greengenes, a chimera-checked 16S rRNA gene database and workbench compatible with ARB. *Applied and environmental microbiology* **72:** 5069-5072.

Docherty KM, Balser TC, Bohannan BJM, Gutknecht JLM (2012). Soil microbial responses to fire and interacting global change factors in a California annual grassland. *Biogeochemistry* **109:** 63-83.

Duarte CM, Agustí S, Wassmann P, Arrieta JM, Alcaraz M, Coello A *et al* (2012). Tipping elements in the arctic marine ecosystem. *AMBIO* **41:** 44-55.

Dufresne JL, Fairhead L, Le Treut H, Berthelot M, Bopp L, Ciais P *et al* (2002). On the magnitude of positive feedback between future climate change and the carbon cycle. *Geophysical Research Letters* **29:** 4341-4344.

Dumbrell AJ, Ashton PD, Aziz N, Feng G, Nelson M, Dytham C *et al* (2011). Distinct seasonal assemblages of arbuscular mycorrhizal fungi revealed by massively parallel pyrosequencing. *New Phytologist* **190:** 794-804.

Duran-Pinedo AE, Paster B, Teles R, Frias-Lopez J (2011). Correlation network analysis applied to complex biofilm communities. *PLOS ONE* **6:** e28438.

Eddy SR (1998). Profile hidden Markov models. *Bioinformatics* **14:** 755-763.

Edgar RC (2010). Search and clustering orders of magnitude faster than BLAST. *Bioinformatics* **26:** 2460-2461.

Edgar RC, Haas BJ, Clemente JC, Quince C, Knight R (2011). UCHIME improves sensitivity and speed of chimera detection. *Bioinformatics* **27:** 2194-2200.

Edwards KA, Jefferies RL (2013). Inter-annual and seasonal dynamics of soil microbial biomass and nutrients in wet and dry low-Arctic sedge meadows. *Soil Biology and Biochemistry* **57:** 83-90.

Euskirchen ES, McGuire AD, Kicklighter DW, Zhuang Q, Clein JS, Dargaville RJ *et al* (2006). Importance of recent shifts in soil thermal dynamics on growing season length, productivity, and carbon sequestration in terrestrial high-latitude ecosystems. *Global Change Biology* **12:** 731-750.

Faust K, Sathirapongsasuti JF, Izard J, Segata N, Gevers D, Raes J *et al* (2012). Microbial co-occurrence relationships in the human microbiome. *PLOS Computational Biology* **8:** e1002606.

Fierer N, Ladau J, Clemente JC, Leff JW, Owens SM, Pollard KS *et al* (2013). Reconstructing the microbial diversity and function of pre-agricultural tallgrass prairie soils in the United States. *Science* **342:** 621-624.

Filippidou S, Wunderlin T, Junier T, Jeanneret N, Dorador C, Molina V *et al* (2016). A combination of extreme environmental conditions favor the prevalence of endospore-forming firmicutes. *Frontiers in Microbiology* **7:** 1707.

Foster EA, Franks DW, Morrell LJ, Balcomb KC, Parsons KM, van Ginneken A *et al* (2012). Social network correlates of food availability in an endangered population of killer whales, Orcinus orca. *Animal Behaviour* **83:** 731-736.

Frank DA, McNaughton SJ (1990). Aboveground biomass estimation with the canopy intercept method: A plant growth form caveat. *Oikos* **57:** 57-60.

Friedlingstein P, Bopp L, Ciais P, Dufresne J-L, Fairhead L, LeTreut H *et al* (2001). Positive feedback between future climate change and the carbon cycle. *Geophysical Research Letters* **28:** 1543-1546.

Friedlingstein P, Cox P, Betts R, Bopp L, Von Bloh W, Brovkin V *et al* (2006). Climate-carbon cycle feedback analysis: Results from the C4MIP model intercomparison. *Journal of Climate* **19:** 3337-3353.

Fuhrman JA (2009). Microbial community structure and its functional implications. *Nature* **459:** 193-199.

Gavazov KS (2010). Dynamics of alpine plant litter decomposition in a changing climate. *Plant and Soil* **337:** 19-32.

Geer LY, Marchler-Bauer A, Geer RC, Han L, He J, He S *et al* (2010). The NCBI BioSystems database. *Nucleic Acids Research* **38:** D492-D496.

Gilbert JA, Steele JA, Caporaso JG, Steinbruck L, Reeder J, Temperton B *et al* (2012). Defining seasonal marine microbial community dynamics. *ISME J* **6:** 298-308.

Giovannoni SJ, Vergin KL (2012). Seasonality in ocean microbial communities. *Science* **335:** 671-676.

Gou X, Tan B, Wu F, Yang W, Xu Z, Li Z *et al* (2015). Seasonal dynamics of soil microbial biomass C and N along an elevational gradient on the eastern Tibetan Plateau, China. *Plos One* **10**.

Graham DE, Wallenstein MD, Vishnivetskaya TA, Waldrop MP, Phelps TJ, Pfiffner SM *et al* (2012). Microbes in thawing permafrost: the unknown variable in the climate change equation. *The ISME journal* **6:** 709-712.

Grogan P, Illeris L, Michelsen A, Jonasson S (2001). Respiration of recently-fixed plant carbon dominates mid-winter ecosystem CO_2 production in sub-Arctic heath tundra. *Climatic Change* **50:** 129-142.

Grosse G, Harden J, Turetsky M, McGuire AD, Camill P, Tarnocai C *et al* (2011). Vulnerability of high-latitude soil organic carbon in North America to disturbance. *Journal of Geophysical Research: Biogeosciences (2005–2012)* **116**.

Guimera R, Nunes Amaral LA (2005). Functional cartography of complex metabolic networks. *Nature* **433:** 895-900.

Hagerty SB, van Groenigen KJ, Allison SD, Hungate BA, Schwartz E, Koch GW *et al* (2014). Accelerated microbial turnover but constant growth efficiency with warming in soil. *Nature Climate Change* **4:** 903-906.

Hallam SJ, McCutcheon JP (2015). Microbes don't play solitaire: how cooperation trumps isolation in the microbial world. *Environmental Microbiology Reports* **7:** 26-28.

Hansen J, Sato M, Ruedy R, Lo K, Lea DW, Medina-Elizade M (2006). Global temperature change. *Proceedings of the National Academy of Sciences* **103:** 14288-14293.

Hansen J, Ruedy R, Sato M, Lo K (2010). Global surface temperature change. *Reviews of Geophysics* **48**.

Hansen J, Lacis A, Rind D, Russell G, Stone P, Fung I *et al* (2013). Climate Sensitivity: Analysis of Feedback Mechanisms. *Climate Processes and Climate Sensitivity*. American Geophysical Union. pp 130-163.

Hartley IP, Heinemeyer A, Ineson P (2007). Effects of three years of soil warming and shading on the rate of soil respiration: substrate availability and not thermal acclimation mediates observed response. *Global Change Biology* **13:** 1761-1770.

He Z, Gentry TJ, Schadt CW, Wu L, Liebich J, Chong SC *et al* (2007). GeoChip: a comprehensive microarray for investigating biogeochemical, ecological and environmental processes. *ISME J* **1:** 67-77.

Hedges LV, Gurevitch J, Curtis PS (1999). The meta-analysis of response ratios in experimental ecology. *Ecology* **80:** 1150-1156.

Heung LJ, Luberto C, Del Poeta M (2006). Role of Sphingolipids in Microbial Pathogenesis. *Infection and Immunity* **74:** 28-39.

Hicks Pries CE, Schuur EAG, Crummer KG (2012). Holocene carbon stocks and carbon accumulation rates altered in soils undergoing permafrost thaw. *Ecosystems* **15:** 162-173.

Hicks Pries CE, Schuur EAG, Crummer KG (2013a). Thawing permafrost increases old soil and autotrophic respiration in tundra: Partitioning ecosystem respiration using $\delta^{13}C$ and $\Delta^{14}C$. *Global Change Biology* **19:** 649-661.

Hicks Pries CE, Schuur EAG, Vogel JG, Natali SM (2013b). Moisture drives surface decomposition in thawing tundra. *Journal of Geophysical Research: Biogeosciences* **118:** 1133-1143.

Hieber M, Gessner MO (2002). Contribution of stream detrivores, fungi, and bacteria to leaf breakdown based on biomass estimates. *Ecology* **83:** 1026-1038.

Hill MO (1973). Diversity and evenness: A unifying notation and its consequences. *Ecology* **54:** 427-432.

Hines J, Reyes M, Mozder TJ, Gessner MO (2014). Genotypic trait variation modifies effects of climate warming and nitrogen deposition on litter mass loss and microbial respiration. *Global Change Biology* **20:** 3780-3789.

Hobbie SE (1996). Temperature and plant species control over litter decomposition in alaskan tundra. *Ecological Monographs* **66:** 503-522.

Hotelling H (1992). Relations between two sets of variates. In: Kotz S, Johnson N (eds). *Breakthroughs in Statistics*. Springer New York. pp 162-190.

Hughes L (2000). Biological consequences of global warming: is the signal already apparent? *Trends in Ecology & Evolution* **15:** 56-61.

Hultman J, Waldrop MP, Mackelprang R, David MM, McFarland J, Blazewicz SJ *et al* (2015). Multi-omics of permafrost, active layer and thermokarst bog soil microbiomes. *Nature* **521:** 208-212.

Huse SM, Huber JA, Morrison HG, Sogin ML, Welch DM (2007). Accuracy and quality of massively parallel DNA pyrosequencing. *Genome biology* **8:** R143.

Husson O (2013). Redox potential (Eh) and pH as drivers of soil/plant/microorganism systems: a transdisciplinary overview pointing to integrative opportunities for agronomy. *Plant and Soil* **362:** 389-417.

IPCC (2007). Climate change 2007: Synthesis report. Contribution of working groups i, ii and iii to the fourth assessment report of the Intergovernmental Panel on Climate Change. In: Change IPoC (ed): Geneva, Switzerland. p 104.

Janssens IA, Pilegaard KIM (2003). Large seasonal changes in Q_{10} of soil respiration in a beech forest. *Global Change Biology* **9:** 911-918.

Jansson JK, Taş N (2014). The microbial ecology of permafrost. *Nature Reviews Microbiology* **12:** 414-425.

Jassey VE, Chiapusio G, Binet P, Buttler A, Laggoun-Defarge F, Delarue F *et al* (2013). Above- and belowground linkages in Sphagnum peatland: climate warming affects plant-microbial interactions. *Global Change Biololy* **19:** 811-823.

Jassey VEJ, Chiapusio G, Gilbert D, Buttler A, Toussaint M-L, Binet P (2011). Experimental climate effect on seasonal variability of polyphenol/phenoloxidase

interplay along a narrow fen-bog ecological gradient in Sphagnum fallax. *Global Change Biology* **17:** 2945-2957.

Jonasson S, Michelsen A, Schmidt IK (1999). Coupling of nutrient cycling and carbon dynamics in the Arctic, integration of soil microbial and plant processes. *Applied Soil Ecology* **11:** 135-146.

Jones BM, Grosse G, Arp CD, Jones MC, Walter Anthony KM, Romanovsky VE (2011). Modern thermokarst lake dynamics in the continuous permafrost zone, northern Seward Peninsula, Alaska. *Journal of Geophysical Research: Biogeosciences* **116**.

Jorgenson MT, Racine CH, Walters JC, Osterkamp TE (2001). Permafrost degradation and ecological changes associated with a warming climate in central Alaska. *Climatic Change* **48:** 551-579.

Jorgenson MT, Romanovsky V, Harden J, Shur Y, O'Donnell J, Schuur EAG *et al* (2010). Resilience and vulnerability of permafrost to climate change. *Canadian Journal of Forest Research* **40:** 1219-1236.

Keller L, Surette MG (2006). Communication in bacteria: an ecological and evolutionary perspective. *Nat Rev Micro* **4:** 249-258.

Kent WJ (2002). BLAT--the BLAST-like alignment tool. *Genome research* **12:** 656-664.

Kirschbaum MUF (2000). Will changes in soil organic carbon act as a positive or negative feedback on global warming? *Biogeochemistry* **48:** 21-51.

Kirschbaum MUF (2004). Soil respiration under prolonged soil warming: are rate reductions caused by acclimation or substrate loss? *Global Change Biology* **10:** 1870-1877.

Kong Y (2011). Btrim: A fast, lightweight adapter and quality trimming program for next-generation sequencing technologies. *Genomics* **98:** 152-153.

Konopka A (2009). What is microbial community ecology? *ISME J* **3:** 1223-1230.

Körner C, Basler D (2010). Phenology Under Global Warming. *Science* **327:** 1461-1462.

Kortsch S, Primicerio R, Beuchel F, Renaud PE, Rodrigues J, Lønne OJ *et al* (2012). Climate-driven regime shifts in Arctic marine benthos. *Proceedings of the National Academy of Sciences* **109:** 14052-14057.

Kuffner M, Hai B, Rattei T, Melodelima C, Schloter M, Zechmeister-Boltenstern S *et al* (2012). Effects of season and experimental warming on the bacterial community in a temperate mountain forest soil assessed by 16S rRNA gene pyrosequencing. *Fems Microbiology Ecology* **82:** 551-562.

Lara E, Mitchell EAD, Moreira D, Garcia PL (2011). Highly diverse and seasonally dynamic protist community in a pristine peat bog. *Protist* **162:** 14-32.

Larkin MA, Blackshields G, Brown NP, Chenna R, McGettigan PA, McWilliam H *et al* (2007). Clustal W and Clustal X version 2.0. *Bioinformatics* **23:** 2947-2948.

Lau MCY, Stackhouse BT, Layton AC, Chauhan A, Vishnivetskaya TA, Chourey K *et al* (2015). An active atmospheric methane sink in high Arctic mineral cryosols. *ISME J*.

Lawrence DM, Slater AG (2005). A projection of severe near-surface permafrost degradation during the 21st century. *Geophysical Research Letters* **32:** L24401.

Lawrence DM, Slater AG, Swenson SC (2012). Simulation of present-day and future permafrost and seasonally frozen ground conditions in CCSM4. *Journal of Climate* **25:** 2207-2225.

Lee H, Schuur EAG, Vogel JG (2010). Soil CO_2 production in upland tundra where permafrost is thawing. *Journal of Geophysical Research: Biogeosciences* **115**.

Lee H, Schuur EAG, Inglett KS, Lavoie M, Chanton JP (2012). The rate of permafrost carbon release under aerobic and anaerobic conditions and its potential effects on climate. *Global Change Biology* **18:** 515-527.

Legendre P, Legendre LF (2012). *Numerical ecology*, vol. 24. Elsevier.

Lennon JT, Jones SE (2011). Microbial seed banks: the ecological and evolutionary implications of dormancy. *Nature Reviews Microbiology* **9:** 119-130.

Lenton TM, Held H, Kriegler E, Hall JW, Lucht W, Rahmstorf S *et al* (2008). Tipping elements in the Earth's climate system. *Proceedings of the National Academy of Sciences* **105:** 1786-1793.

Lenton TM (2011). Early warning of climate tipping points. *Nature Climate Change* **1:** 201-209.

Lenton TM (2012). Arctic climate tipping points. *AMBIO* **41:** 10-22.

Li D, Zhou X, Wu L, Zhou J, Luo Y (2013). Contrasting responses of heterotrophic and autotrophic respiration to experimental warming in a winter annual-dominated prairie. *Global Change Biology* **19:** 3553-3564.

Li W, Godzik A (2006). Cd-hit: a fast program for clustering and comparing large sets of protein or nucleotide sequences. *Bioinformatics* **22:** 1658-1659.

Liebner S, Wagner D (2007). Abundance, distribution and potential activity of methane oxidizing bacteria in permafrost soils from the Lena Delta, Siberia. *Environmental Microbiology* **9:** 107-117.

Lima-Mendez G, Faust K, Henry N, Decelle J, Colin S, Carcillo F *et al* (2015). Determinants of community structure in the global plankton interactome. *Science* **348**.

Lipson DA, Monson RK (1998). Plant-microbe competition for soil amino acids in the alpine tundra: effects of freeze-thaw and dry-rewet events. *Oecologia* **113:** 406-414.

Lipson DA, Raab TK, Parker M, Kelley ST, Brislawn CJ, Jansson J (2015). Changes in microbial communities along redox gradients in polygonized Arctic wet tundra soils. *Environmental Microbiology Reports* **7:** 649-657.

Liu S, Wang F, Xue K, Sun B, Zhang Y, He Z *et al* (2015). The interactive effects of soil transplant into colder regions and cropping on soil microbiology and biogeochemistry. *Environmental Microbiology* **17:** 566-576.

Liu W, Allison SD, Xia J, Liu L, Wan S (2016). Precipitation regime drives warming responses of microbial biomass and activity in temperate steppe soils. *Biology and Fertility of Soils***:** 1-9.

Lu M, Zhou X, Yang Q, Li H, Luo Y, Fang C *et al* (2013). Responses of ecosystem carbon cycle to experimental warming: a meta-analysis. *Ecology* **94:** 726-738.

Luo C, Tsementzi D, Kyrpides NC, Konstantinidis KT (2011). Individual genome assembly from complex community short-read metagenomic datasets. *ISME J.*

Luo C, Rodriguez RL, Konstantinidis KT (2013a). A user's guide to quantitative and comparative analysis of metagenomic datasets. *Methods in enzymology* **531:** 525-547.

Luo GJ, Kiese R, Wolf B, Butterbach-Bahl K (2013b). Effects of soil temperature and moisture on methane uptake and nitrous oxide emissions across three different ecosystem types. *Biogeosciences* **10:** 3205-3219.

Luo Y, Wan S, Hui D, Wallace LL (2001). Acclimatization of soil respiration to warming in a tall grass prairie. *Nature* **413:** 622-625.

Luo Y, Hui D, Zhang D (2006). Elevated CO_2 stimulates net accumulations of carbon and nitrogen in land ecosystems: a meta-analysis. *Ecology* **87:** 53-63.

Luo Y (2007). Terrestrial carbon–cycle feedback to climate warming. *Annu Rev Ecol Evol Syst* **38:** 683-712.

Luo Y, Sherry R, Zhou X, Wan S (2009). Terrestrial carbon-cycle feedback to climate warming: experimental evidence on plant regulation and impacts of biofuel feedstock harvest. *GCB Bioenergy* **1:** 62-74.

Lupatini M, Suleiman AKA, Jacques RJS, Antoniolli ZI, de Siqueira Ferreira A, Kuramae EE *et al* (2014). Network topology reveals high connectance levels and few key microbial genera within soils. *Frontiers in Environmental Science* **2**.

Lv H, Yang J, Liu L, Yu X, Yu Z, Chiang P (2014). Temperature and nutrients are significant drivers of seasonal shift in phytoplankton community from a drinking water reservoir, subtropical China. *Environmental Science and Pollution Research* **21:** 5917-5928.

Mackelprang R, Waldrop MP, DeAngelis KM, David MM, Chavarria KL, Blazewicz SJ *et al* (2011). Metagenomic analysis of a permafrost microbial community reveals a rapid response to thaw. *Nature* **480:** 368-371.

Mackelprang R, Saleska SR, Jacobsen CS, Jansson JK, Taş N (2016). Permafrost Meta-Omics and Climate Change. *Annual Review of Earth and Planetary Sciences* **44:** 439-462.

Magoč T, Salzberg SL (2011). FLASH: fast length adjustment of short reads to improve genome assemblies. *Bioinformatics* **27:** 2957-2963.

Mao Y, Yannarell AC, Mackie RI (2011). Changes in N-transforming archaea and bacteria in soil during the establishment of bioenergy crops. *PLoS ONE* **6**.

Martiny JBH, Bohannan BJM, Brown JH, Colwell RK, Fuhrman JA, Green JL *et al* (2006). Microbial biogeography: putting microorganisms on the map. *Nature Reviews Microbiology* **4:** 102-112.

McMichael AJ (2003). Global climate change and health: an old story writ large. *Climate change and human health: Risks and responses Geneva, Switzerland: World Health Organization*.

Melle C, Wallenstein M, Darrouzet-Nardi A, Weintraub MN (2015). Microbial activity is not always limited by nitrogen in Arctic tundra soils. *Soil Biology and Biochemistry* **90:** 52-61.

Meyer M, Stenzel U, Hofreiter M (2008). Parallel tagged sequencing on the 454 platform. *Nature Protocols* **3:** 267-278.

Mironova E, Telesh I, Skarlato S (2012). Diversity and seasonality in structure of ciliate communities in the Neva Estuary (Baltic Sea). *Journal of Plankton Research* **34:** 208-220.

Morales SE, Cosart T, Holben WE (2010). Bacterial gene abundances as indicators of greenhouse gas emission in soils. *ISME J* **4:** 799-808.

Natali SM, Schuur EAG, Trucco C, Hicks Pries CE, Crummer KG, Baron Lopez AF (2011). Effects of experimental warming of air, soil and permafrost on carbon balance in Alaskan tundra. *Global Change Biology* **17:** 1394-1407.

Natali SM, Schuur EAG, Rubin RL (2012). Increased plant productivity in Alaskan tundra as a result of experimental warming of soil and permafrost. *Journal of Ecology* **100:** 488-498.

Natali SM, Schuur EAG, Webb EE, Hicks Pries CE, Crummer KG (2014). Permafrost degradation stimulates carbon loss from experimentally warmed tundra. *Ecology* **95:** 602-608.

Natali SM, Schuur EAG, Mauritz M, Schade JD, Celis G, Crummer KG *et al* (2015). Permafrost thaw and soil moisture driving CO_2 and CH_4 release from upland tundra. *Journal of Geophysical Research: Biogeosciences* **120:** 525-537.

Nelson FE, Anisimov OA, Shiklomanov NI (2001). Subsidence risk from thawing permafrost. *Nature* **410:** 889-890.

Newman MEJ (2006a). Modularity and community structure in networks. *Proceedings of the National Academy of Sciences* **103:** 8577-8582.

Newman MEJ (2006b). Finding community structure in networks using the eigenvectors of matrices. *Physical Review E* **74:** 036104.

Nie M, Pendall E, Bell C, Gasch CK, Raut S, Tamang S *et al* (2013). Positive climate feedbacks of soil microbial communities in a semi-arid grassland. *Ecology Letters* **16:** 234-241.

Niu S, Wu M, Han Y, Xia J, Li L, Wan S (2008). Water-mediated responses of ecosystem carbon fluxes to climatic change in a temperate steppe. *New Phytologist* **177:** 209-219.

NOAA National Centers for Environmental Information (2017). State of the Climate: Global Climate Report for Annual 2016: Online.

Oksanen J, Blanchet FG, Kindt R, Legendre P, Minchin PR, O'Hara RB *et al* (2013). vegan: Community ecology package.

Olesen JM, Bascompte J, Dupont YL, Jordano P (2006). The smallest of all worlds: Pollination networks. *Journal of Theoretical Biology* **240:** 270-276.

Olesen JM, Bascompte J, Dupont YL, Jordano P (2007). The modularity of pollination networks. *Proceedings of the National Academy of Sciences* **104:** 19891-19896.

Osterkamp TE, Romanovsky VE (1999). Evidence for warming and thawing of discontinuous permafrost in Alaska. *Permafrost and Periglacial Processes* **10:** 17-37.

Osterkamp TE (2007). Characteristics of the recent warming of permafrost in Alaska. *J Geophys Res* **112:** F02S02.

Osterkamp TE, Jorgenson MT, Schuur EAG, Shur YL, Kanevskiy MZ, Vogel JG *et al* (2009). Physical and ecological changes associated with warming permafrost and thermokarst in Interior Alaska. *Permafrost and Periglacial Processes* **20:** 235-256.

Overbeek R, Begley T, Butler RM, Choudhuri JV, Chuang HY, Cohoon M *et al* (2005). The subsystems approach to genome annotation and its use in the project to annotate 1000 genomes. *Nucleic acids research* **33:** 5691-5702.

Pachauri RK, Allen MR, Barros VR, Broome J, Cramer W, Christ R *et al* (2014). *Climate change 2014: synthesis report. Contribution of Working Groups I, II and III to the fifth assessment report of the Intergovernmental Panel on Climate Change*. IPCC.

Pailler A, Vennetier M, Torre F, Ripert C, Guiral D (2014). Forest soil microbial functional patterns and response to a drought and warming event: Key role of climate–plant–soil interactions at a regional scale. *Soil Biology and Biochemistry* **70:** 1-4.

Paine RT (1995). A conversation on refining the concept of keystone species. *Conservation Biology* **9:** 962-964.

Palmer K, Drake HL, Horn MA (2009). Genome-derived criteria for assigning environmental *narG* and *nosZ* sequences to operational taxonomic units of nitrate reducers. *Applied and Environmental Microbiology* **75:** 5170-5174.

Patz JA, Campbell-Lendrum D, Holloway T, Foley JA (2005). Impact of regional climate change on human health. *Nature* **438:** 310.

Pecl GT, Araújo MB, Bell JD, Blanchard J, Bonebrake TC, Chen I-C *et al* (2017). Biodiversity redistribution under climate change: Impacts on ecosystems and human well-being. *Science* **355**.

Peltoniemi K, Laiho R, Juottonen H, Kiikkila O, Makiranta P, Minkkinen K *et al* (2015). Microbial ecology in a future climate: effects of temperature and moisture on microbial communities of two boreal fens. *FEMS Microbiol Ecology* **91**.

Penton CR, Yang C, Wu L, Wang Q, Zhang J, Liu F *et al* (2016). *nifH*-harboring bacterial community composition across an alaskan permafrost thaw gradient. *Frontiers in Microbiology* **7**.

Peñuelas J, Gordon C, Llorens L, Nielsen T, Tietema A, Beier C *et al* (2004). Nonintrusive field experiments show different plant responses to warming and drought among sites, seasons, and species in a north–south European GRADIENT. *Ecosystems* **7:** 598-612.

Pereira e Silva MC, Schloter-Hai B, Schloter M, van Elsas JD, Salles JF (2013). Temporal dynamics of abundance and composition of nitrogen-fixing communities across agricultural soils. *PLoS ONE* **8**.

Petit JR, Jouzel J, Raynaud D, Barkov NI, Barnola JM, Basile I *et al* (1999). Climate and atmospheric history of the past 420,000 years from the Vostok ice core, Antarctica. *Nature* **399:** 429-436.

Ponnamperuma FN (1972). The chemistry of submerged soils. *Advances in Agronomy* **24:** 29-96.

Price MN, Dehal PS, Arkin AP (2010). FastTree 2 – Approximately maximum-likelihood trees for large alignments. *PLOS ONE* **5:** e9490.

Proulx SR, Promislow DEL, Phillips PC (2005). Network thinking in ecology and evolution. *Trends in Ecology & Evolution* **20:** 345-353.

Puissant J, Cecillon L, Mills RTE, Robroek BJM, Gavazov K, De Danieli S *et al* (2015). Seasonal influence of climate manipulation on microbial community structure and function in mountain soils. *Soil Biology & Biochemistry* **80:** 296-305.

Ravasz E, Somera AL, Mongru DA, Oltvai ZN, Barabási A-L (2002). Hierarchical organization of modularity in metabolic networks. *Science* **297:** 1551-1555.

Rho M, Tang H, Ye Y (2010). FragGeneScan: predicting genes in short and error-prone reads. *Nucleic Acids Research* **38:** e191.

Rivkina E, Laurinavichius K, McGrath J, Tiedje J, Shcherbakova V, Gilichinsky D (2004). Microbial life in permafrost. *Advances in Space Research* **33:** 1215-1221.

Romaní AM, Fischer H, Mille-Lindblom C, Tranvik LJ (2006). Interactions of bacteria and fungi on decomposing litter: Differential extracellular enzyme activities. *Ecology* **87:** 2559-2569.

Romanovsky VE, Smith SL, Christiansen HH (2010). Permafrost thermal state in the polar Northern Hemisphere during the international polar year 2007–2009: A synthesis. *Permafrost and Periglacial Processes* **21:** 106-116.

Ronaghi M, Uhlén M, Nyren P (1998). A sequencing method based on real-time pyrophosphate. *Science* **281:** 363-365.

Rosenberg E (2014). The Family Chitinophagaceae. In: Rosenberg E, DeLong EF, Lory S, Stackebrandt E, Thompson F (eds). *The Prokaryotes: Other Major Lineages of Bacteria and The Archaea*. Springer Berlin Heidelberg: Berlin, Heidelberg. pp 493-495.

Rousk J, Smith AR, Jones DL (2013). Investigating the long-term legacy of drought and warming on the soil microbial community across five European shrubland ecosystems. *Glob Chang Biol* **19:** 3872-3884.

Rovira P, Vallejo VR (2002). Labile and recalcitrant pools of carbon and nitrogen in organic matter decomposing at different depths in soil: an acid hydrolysis approach. *Geoderma* **107:** 109-141.

Rustad L, Campbell J, Marion G, Norby R, Mitchell M, Hartley A *et al* (2001). A meta-analysis of the response of soil respiration, net nitrogen mineralization, and aboveground plant growth to experimental ecosystem warming. *Oecologia* **126:** 543-562.

Schadt CW, Martin AP, Lipson DA, Schmidt SK (2003). Seasonal dynamics of previously unknown fungal lineages in tundra soils. *Science* **301:** 1359-1361.

Scheffer M, Brovkin V, Cox PM (2006). Positive feedback between global warming and atmospheric CO_2 concentration inferred from past climate change. *Geophysical Research Letters* **33**.

Schmidt IK, Jonasson S, Shaver GR, Michelsen A, Nordin A (2002). Mineralization and distribution of nutrients in plants and microbes in four arctic ecosystems: responses to warming. *Plant and Soil* **242:** 93-106.

Schuur EAG, Crummer KG, Vogel JG, Mack MC (2007). Plant species composition and productivity following permafrost thaw and thermokarst in alaskan tundra. *Ecosystems* **10:** 280-292.

Schuur EAG, Bockheim J, Canadell JG, Euskirchen E, Field CB, Goryachkin SV *et al* (2008). Vulnerability of permafrost carbon to climate change: Implications for the global carbon cycle. *BioScience* **58:** 701-714.

Schuur EAG, Vogel JG, Crummer KG, Lee H, Sickman JO, Osterkamp TE (2009). The effect of permafrost thaw on old carbon release and net carbon exchange from tundra. *Nature* **459:** 556-559.

Schuur EAG, Abbott B (2011). Climate change: High risk of permafrost thaw. *Nature* **480:** 32-33.

Schuur EAG, Abbott BW, Bowden WB, Brovkin V, Camill P, Canadell JG *et al* (2013). Expert assessment of vulnerability of permafrost carbon to climate change. *Climatic Change* **119:** 359-374.

Schuur EAG, McGuire AD, Schadel C, Grosse G, Harden JW, Hayes DJ *et al* (2015). Climate change and the permafrost carbon feedback. *Nature* **520:** 171-179.

Semenova TA, Morgado LN, Welker JM, Walker MD, Smets E, Geml J (2015). Long-term experimental warming alters community composition of ascomycetes in Alaskan moist and dry arctic tundra. *Mol Ecol* **24:** 424-437.

Serreze MC, Walsh JE, Chapin FS, Osterkamp T, Dyurgerov M, Romanovsky V *et al* (2000). Observational evidence of recent change in the northern high-latitude environment. *Climatic Change* **46:** 159-207.

Shaver GR, Bret-Harte MS, Jones MH, Johnstone J, Gough L, Laundre J *et al* (2001). Species composition interacts with fertilizer to control long-term change in tundra productivity. *Ecology* **82:** 3163-3181.

Sheik CS, Beasley WH, Elshahed MS, Zhou X, Luo Y, Krumholz LR (2011). Effect of warming and drought on grassland microbial communities. *ISME J* **5:** 1692-1700.

Sherry RA, Zhou X, Gu S, Arnone JA, Schimel DS, Verburg PS *et al* (2007). Divergence of reproductive phenology under climate warming. *Proceedings of the National Academy of Sciences* **104:** 198-202.

Sherry RA, Weng E, Arnone Iii JA, Johnson DW, Schimel DS, Verburg PS *et al* (2008). Lagged effects of experimental warming and doubled precipitation on annual and seasonal aboveground biomass production in a tallgrass prairie. *Global Change Biology* **14:** 2923-2936.

Shi S, Nuccio EE, Shi ZJ, He Z, Zhou J, Firestone MK (2016). The interconnected rhizosphere: High network complexity dominates rhizosphere assemblages. *Ecology Letters* **19:** 926-936.

Slaughter LC, Weintraub MN, McCulley RL (2015). Seasonal Effects Stronger than Three-Year Climate Manipulation on Grassland Soil Microbial Community. *Soil Science Society of America Journal* **79:** 1352.

Soden BJ, Held IM (2006). An Assessment of Climate Feedbacks in Coupled Ocean–Atmosphere Models. *Journal of Climate* **19:** 3354-3360.

Steduto P, Çetinkökü Ö, Albrizio R, Kanber R (2002). Automated closed-system canopy-chamber for continuous field-crop monitoring of CO_2 and H_2O fluxes. *Agricultural and Forest Meteorology* **111:** 171-186.

Steele JA, Countway PD, Xia L, Vigil PD, Beman JM, Kim DY *et al* (2011). Marine bacterial, archaeal and protistan association networks reveal ecological linkages. *ISME J* **5:** 1414-1425.

Stegen JC, Lin X, Konopka AE, Fredrickson JK (2012). Stochastic and deterministic assembly processes in subsurface microbial communities. *ISME J* **6:** 1653-1664.

Steven B, Léveillé R, Pollard W, Whyte L (2006). Microbial ecology and biodiversity in permafrost. *Extremophiles* **10:** 259-267.

Steven B, Kuske CR, Gallegos-Graves LV, Reed SC, Belnap J (2015). Climate Change and Physical Disturbance Manipulations Result in Distinct Biological Soil Crust Communities. *Appl Environ Microbiol* **81:** 7448-7459.

Stocker T (2014). *Climate change 2013: the physical science basis: Working Group I contribution to the Fifth assessment report of the Intergovernmental Panel on Climate Change*. Cambridge University Press.

Streit K, Hagedorn F, Hiltbrunner D, Portmann M, Saurer M, Buchmann N *et al* (2014). Soil warming alters microbial substrate use in alpine soils. *Glob Chang Biol* **20:** 1327-1338.

Sturm M, Racine C, Tape K (2001). Climate change: increasing shrub abundance in the Arctic. *Nature* **411:** 546-547.

Suding KN, Ashton IW, Bechtold H, Bowman WD, Mobley ML, Winkleman R (2008). Plant and microbe contribution to community resilience in a directionally changing environment. *Ecological Monographs* **78:** 313-329.

Takahashi K, Hada Y (2012). Seasonal occurrence and distribution of myxomycetes on different types of leaf litter in a warm temperate forest of western Japan. *Mycoscience* **53:** 245-255.

Tarnocai C, Canadell JG, Schuur EAG, Kuhry P, Mazhitova G, Zimov S (2009). Soil organic carbon pools in the northern circumpolar permafrost region. *Global biogeochemical cycles* **23**.

Taş N, Prestat E, McFarland JW, Wickland KP, Knight R, Berhe AA *et al* (2014). Impact of fire on active layer and permafrost microbial communities and metagenomes in an upland Alaskan boreal forest. *ISME J* **8:** 1904-1919.

Team RC (2014). R: A language and environment for statistical computing. R Foundation for Statistical Computing: Vienna, Austria.

Trivedi P, Delgado-Baquerizo M, Trivedi C, Hu H, Anderson IC, Jeffries TC *et al* (2016). Microbial regulation of the soil carbon cycle: evidence from gene-enzyme relationships. *ISME J*.

Trucco C, Schuur EAG, Natali SM, Belshe EF, Bracho R, Vogel JG (2012). Seven-year trends of CO_2 exchange in a tundra ecosystem affected by long-term permafrost thaw. *Journal of Geophysical Research: Biogeosciences* **117**.

Tu Q, Yu H, He Z, Deng Y, Wu L, Van Nostrand JD *et al* (2014). GeoChip 4: a functional gene-array-based high-throughput environmental technology for microbial community analysis. *Molecular Ecology Resources* **14:** 914-928.

Tucker CL, Bell J, Pendall E, Ogle K (2013). Does declining carbon-use efficiency explain thermal acclimation of soil respiration with warming? *Global Change Biology* **19:** 252-263.

Van Der Heijden MGA, Bardgett RD, Van Straalen NM (2008). The unseen majority: soil microbes as drivers of plant diversity and productivity in terrestrial ecosystems. *Ecology Letters* **11:** 296-310.

Van Sickle J (1997). Using mean similarity dendrograms to evaluate classifications. *Journal of Agricultural, Biological, and Environmental Statistics* **2:** 370-388.

Vilgalys R, Hester M (1990). Rapid genetic identification and mapping of enzymatically amplified ribosomal DNA from several Cryptococcus species. *Journal of Bacteriology* **172:** 4238-4246.

Vogel JG, Schuur EAG, Trucco C, Lee H (2009). Response of CO_2 exchange in a tussock tundra ecosystem to permafrost thaw and thermokarst development. *Journal of Geophysical Research: Biogeosciences* **114**.

Waldrop MP, Wickland KP, White Iii R, Berhe AA, Harden JW, Romanovsky VE (2010). Molecular investigations into a globally important carbon pool: permafrost-protected carbon in Alaskan soils. *Global Change Biology* **16:** 2543-2554.

Walker DA, Raynolds MK, Daniëls FJA, Einarsson E, Elvebakk A, Gould WA *et al* (2005). The Circumpolar Arctic vegetation map. *Journal of Vegetation Science* **16:** 267-282.

Walker MD (1996). Community baseline measurements for ITEX studies. *ITEX manual* **41**.

Walker MD, Wahren CH, Hollister RD, Henry GH, Ahlquist LE, Alatalo JM *et al* (2006). Plant community responses to experimental warming across the tundra biome. *Proceedings of the National Academy of Sciences of the United States of America* **103:** 1342-1346.

Walter J, Hein R, Beierkuhnlein C, Hammerl V, Jentsch A, Schädler M *et al* (2013). Combined effects of multifactor climate change and land-use on decomposition in temperate grassland. *Soil Biology and Biochemistry* **60:** 10-18.

Walter KM, Zimov SA, Chanton JP, Verbyla D, Chapin FS (2006). Methane bubbling from Siberian thaw lakes as a positive feedback to climate warming. *Nature* **443:** 71-75.

Wang CT, Zhao XQ, Zi HB, Hu L, Ade L, Wang GX *et al* (2017). The effect of simulated warming on root dynamics and soil microbial community in an alpine meadow of the Qinghai-Tibet Plateau. *Appl Soil Ecol* **116:** 30-41.

Wang M, Liu S, Wang F, Sun B, Zhou J, Yang Y (2015). Microbial responses to southward and northward Cambisol soil transplant. *MicrobiologyOpen* **4:** 931-940.

Wang Q, Garrity GM, Tiedje JM, Cole JR (2007). Naïve Bayesian Classifier for Rapid Assignment of rRNA Sequences into the New Bacterial Taxonomy. *Applied and Environmental Microbiology* **73:** 5261-5267.

Wang Q, Quensen JF, Fish JA, Kwon Lee T, Sun Y, Tiedje JM *et al* (2013). Ecological patterns of *nifH* genes in four terrestrial climatic zones explored with targeted metagenomics using Framebot, a new informatics tool. *mBio* **4**.

Wang X, Dong S, Gao Q, Zhou H, Liu S, Su X *et al* (2014). Effects of short-term and long-term warming on soil nutrients, microbial biomass and enzyme activities in an alpine meadow on the Qinghai-Tibet Plateau of China. *Soil Biology and Biochemistry* **76:** 140-142.

Wigley TML, Raper SCB (1990). Natural variability of the climate system and detection of the greenhouse effect. *Nature* **344:** 324.

Wilke A, Harrison T, Wilkening J, Field D, Glass EM, Kyrpides N *et al* (2012). The M5nr: a novel non-redundant database containing protein sequences and annotations from multiple sources and associated tools. *Bmc Bioinformatics* **13**.

Willerslev E, Hansen AJ, Rønn R, Brand TB, Barnes I, Wiuf C *et al* (2004). Long-term persistence of bacterial DNA. *Current Biology* **14:** R9-R10.

Wu L, Wen C, Qin Y, Yin H, Tu Q, Van Nostrand J *et al* (2015). Phasing amplicon sequencing on Illumina Miseq for robust environmental microbial community analysis. *BMC Microbiology* **15:** 125.

Xu X, Sherry RA, Niu S, Li D, Luo Y (2013). Net primary productivity and rain-use efficiency as affected by warming, altered precipitation, and clipping in a mixed-grass prairie. *Global Change Biology* **19:** 2753-2764.

Xu X, Shi Z, Chen X, Lin Y, Niu S, Jiang L *et al* (2016). Unchanged carbon balance driven by equivalent responses of production and respiration to climate change in a mixed-grass prairie. *Global Change Biology* **22:** 1857-1866.

Xue K, Yuan M, Shi Z, Qin Y, Deng Y, Cheng L *et al* (2016a). Tundra soil carbon is vulnerable to rapid microbial decomposition under climate warming. *Nature Clim Change* **6:** 595-600.

Xue K, Yuan M, Xie J, Li D, Qin Y, Hale LE *et al* (2016b). Annual removal of aboveground plant biomass alters soil microbial responses to warming. *mBio* **7**.

Yergeau E, Bokhorst S, Kang S, Zhou J, Greer CW, Aerts R *et al* (2012). Shifts in soil microorganisms in response to warming are consistent across a range of Antarctic environments. *ISME J* **6:** 692-702.

Yoshitake S, Tabei N, Mizuno Y, Yoshida H, Sekine Y, Tatsumura M *et al* (2015). Soil microbial response to experimental warming in cool temperate semi-natural grassland in Japan. *Ecological Research* **30:** 235-245.

Yu Z, Liu J, Liu J, Jin J, Liu X, Wang G (2016). Responses of ammonia-oxidizing bacterial communities to land-use and seasonal changes in Mollisols of Northeast China. *European Journal of Soil Biology* **74:** 121-127.

Zapala MA, Schork NJ (2006). Multivariate regression analysis of distance matrices for testing associations between gene expression patterns and related variables. *Proceedings of the National Academy of Sciences* **103:** 19430-19435.

Zehr JP, Jenkins BD, Short SM, Steward GF (2003). Nitrogenase gene diversity and microbial community structure: a cross-system comparison. *Environmental Microbiology* **5:** 539-554.

Zhang N, Liu W, Yang H, Yu X, Gutknecht JM, Zhang Z *et al* (2013). Soil microbial responses to warming and increased precipitation and their implications for ecosystem C cycling. *Oecologia* **173:** 1125-1142.

Zhang W, Parker KM, Luo Y, Wan S, Wallace LL, Hu S (2005). Soil microbial responses to experimental warming and clipping in a tallgrass prairie. *Global Change Biology* **11:** 266-277.

Zhao M, Xue K, Wang F, Liu S, Bai S, Sun B *et al* (2014). Microbial mediation of biogeochemical cycles revealed by simulation of global changes with soil transplant and cropping. *ISME J* **8:** 2045-2055.

Zhou J, Bruns MA, Tiedje JM (1996). DNA recovery from soils of diverse composition. *Applied and Environmental Microbiology* **62:** 316-322.

Zhou J, Deng Y, Luo F, He Z, Tu Q, Zhi X (2010). Functional Molecular Ecological Networks. *mBio* **1**.

Zhou J, Deng Y, Luo F, He Z, Yang Y (2011). Phylogenetic molecular ecological network of soil microbial communities in response to elevated CO_2. *mBio* **2**.

Zhou J, Xue K, Xie J, Deng Y, Wu L, Cheng X *et al* (2012). Microbial mediation of carbon-cycle feedbacks to climate warming. *Nature Climate Change* **2:** 106-110.

Zhou J, Liu W, Deng Y, Jiang Y-H, Xue K, He Z *et al* (2013). Stochastic assembly leads to alternative communities with distinct functions in a bioreactor microbial community. *mBio* **4**.

Zhou J, Deng Y, Zhang P, Xue K, Liang Y, Van Nostrand JD *et al* (2014). Stochasticity, succession, and environmental perturbations in a fluidic ecosystem. *Proceedings of the National Academy of Sciences* **111:** E836-E845.

Zhou J, He Z, Yang Y, Deng Y, Tringe SG, Alvarez-Cohen L (2015). High-throughput metagenomic technologies for complex microbial community analysis: Open and closed formats. *mBio* **6**.

Zhou T, Shi P, Hui D, Luo Y (2009). Global pattern of temperature sensitivity of soil heterotrophic respiration (Q_{10}) and its implications for carbon-climate feedback. *Journal of Geophysical Research: Biogeosciences* **114**.

Zhou X, Wan S, Luo Y (2007). Source components and interannual variability of soil CO2 efflux under experimental warming and clipping in a grassland ecosystem. *Global Change Biology* **13:** 761-775.

Ziegler SE, Billings SA, Lane CS, Li J, Fogel ML (2013). Warming alters routing of labile and slower-turnover carbon through distinct microbial groups in boreal forest organic soils. *Soil Biology and Biochemistry* **60:** 23-32.